Metabolic Engineering 67 (2021) 164–172

Contents lists available at ScienceDirect

Metabolic Engineering

journal homepage: www.elsevier.com/locate/meteng

Metabolic engineering of *Escherichia coli* for quinolinic acid production by assembling L-aspartate oxidase and quinolinate synthase as an enzyme complex

Fayin Zhu [a,1], Matthew Peña [a], George N. Bennett [a,b,*]

[a] Department of BioSciences, Rice University, Houston, TX, 77005, USA
[b] Department of Chemical and Biomolecular Engineering, Rice University, Houston, TX, 77005, USA

ARTICLE INFO

Keywords:
Quinolinic acid
Peptide-peptide interaction
Enzyme complex
Metabolon
Metabolite channeling
Metabolic engineering

ABSTRACT

Quinolinic acid (QA) is a key intermediate of nicotinic acid (Niacin) which is an essential human nutrient and widely used in food and pharmaceutical industries. In this study, a quinolinic acid producer was constructed by employing comprehensive engineering strategies. Firstly, the quinolinic acid production was improved by deactivation of NadC (to block the consumption pathway), NadR (to eliminate the repression of L-aspartate oxidase and quinolinate synthase), and PtsG (to slow the glucose utilization rate and achieve a more balanced metabolism, and also to increase the availability of the precursor phosphoenolpyruvate). Further modifications to enhance quinolinic acid production were investigated by increasing the oxaloacetate pool through over-production of phosphoenolpyruvate carboxylase and deactivation of acetate-producing pathway enzymes. Moreover, quinolinic acid production was accelerated by assembling NadB and NadA as an enzyme complex with the help of peptide-peptide interaction peptides RIAD and RIDD, which resulted in up to 3.7 g/L quinolinic acid being produced from 40 g/L glucose in shake-flask cultures. A quinolinic acid producer was constructed in this study, and these results lay a foundation for further engineering of microbial cell factories to efficiently produce quinolinic acid and subsequently convert this product to nicotinic acid for industrial applications.

1. Introduction

Quinolinic acid (QA), known as pyridine-2,3-dicarboxylic acid, is a dicarboxylic acid with a pyridine backbone, and it is a key precursor to nicotinic acid and nicotine in nature (Andreoli et al., 1963). Nicotinic acid, also known as niacin or vitamin B_3, is one of the water-soluble B complex vitamins, and it commonly exists in living cells. In general, nicotinic acid is present mainly in the form of nicotinic acid amide co-enzyme [Nicotinamide Adenine Dinucleotide (NAD^+) or Nicotinamide Adenine Dinucleotide Phosphate ($NADP^+$)] *in vivo* and it acts as a cofactor for a large and diverse number of cellular oxidative-reductive reactions. Nicotinic acid is an essential human nutrient as deficiency of nicotinic acid may cause the disease pellagra and neuropathies (Crook, 2014; Hammond et al., 2013). Consequently, nicotinic acid is widely used in the food and pharmaceutical industries. Nicotinic acid has been mainly produced by chemical synthesis through oxidation of β-picoline (Andrushkevich and Ovchinnikova, 2012; Shishido et al., 2003); however, these processes result in considerable amounts of toxic wastes, which require significant expense for proper disposal. Moreover, these methods use petroleum-based non-renewable chemicals as the precursor, which is affected by concerns about climate change and unpredictable oil refining prices. To overcome these concerns, production of fuels, pharmaceuticals, or bulk and fine chemicals from renewable feedstocks using microorganisms has arisen as an attractive alternative (Keasling, 2010; Lee et al., 2012; Woolston et al., 2013), especially given advancements in metabolic engineering, however, there is little published literature directed to the over-production of nicotinic acid or even quinolinic acid in microorganisms (Kim et al., 2016).

Early work on the enzymes and genes related to quinolinic acid formation from aspartate has been described (Chandler and Gholson, 1972; Flachmann et al., 1988; Griffith et al., 1975). Quinolinic acid, NAD^+, Coenzyme A, and commercially important amino acids such as threonine and lysine (Becker et al., 2011; Ning et al., 2016; Park and Lee, 2010; Zhao et al., 2020) are generated via aspartate as a key precursor.

* Corresponding author. Department of BioSciences, Rice University, Houston, TX, 77005, USA.
E-mail address: gbennett@rice.edu (G.N. Bennett).
[1] Present address: Department of Chemical, Biological, and Materials Engineering, University of South Florida, Tampa, FL, 33620, USA

https://doi.org/10.1016/j.ymben.2021.06.007
Received 7 January 2021; Received in revised form 23 April 2021; Accepted 21 June 2021
Available online 27 June 2021

Metabolic engineering at the oxaloacetate and aspartate nodes is important to give a high level of these key intermediates (Sauer and Eikmanns, 2005), as well as to provide high and specific conversion of aspartate to quinolinic acid. We have previously engineered cells to produce compounds derived from the oxaloacetate branch of the TCA cycle and have developed useful designs for metabolic networks to product compounds around this node (Cox et al., 2006; Martinez et al., 2018; Sánchez et al., 2005; Zhu et al., 2020). Likewise, we have investigated computational methods for finding novel pathways to relevant OAA derived compounds (Heath et al., 2010; Kim et al., 2020). There are two major NAD *de novo* biosynthetic pathways used for quinolinate production *in vivo*: NAD *de novo* biosynthesis I (from aspartate) in most prokaryotes and NAD *de novo* biosynthesis II (from tryptophan), also known as the kynurenine pathway, in eukaryotes (Begley et al., 2001; Panozzo et al., 2002). These two pathways converge at quinolinic acid, a key intermediate of NAD biosynthetic pathways, and subsequently use three common steps to synthesize NAD. Five enzymes are involved in the conversion of tryptophan to quinolinate in the kynurenine pathway. In comparison, only two enzymes, L-aspartate oxidase (NadB) and quinolinate synthase (NadA), are needed for quinolinate production aerobically from aspartate (Magni et al., 1999). L-aspartate oxidase (NadB), is a monomer of a 60 kDa flavoenzyme containing 1 mol of non-covalently bound FAD/mol protein, and it catalyzes the conversion of L-aspartate to 2-iminosuccinate (Mortarino et al., 1996; Nasu et al., 1982). Quinolinate synthase (NadA), which appears mainly as a dimeric protein of 80 kDa (Ollagnier-de Choudens et al., 2005), contains an oxygen-sensitive [4Fe–4S] cluster required to catalyze the condensation of 2-iminosuccinate with dihydroxyacetone phosphate (DHAP) to produce quinolinate (Ceciliani et al., 2000; Cicchillo et al., 2005; Ollagnier-de Choudens et al., 2005). We know that the concentration of NAD(H) and NADP(H) *in vivo* remains relatively stable, and the pool is maintained by a combination of gene expression regulation, feedback inhibition, and cofactor degradation [The NAD(P) recycling and salvage pathways] (Begley et al., 2001). The expression of NadB and NadA was reported to be repressed by a DNA binding transcriptional repressor NadR (Begley et al., 2001; Tritz and Chandler, 1973). Moreover, inhibition of aspartate oxidase activity was reported by the substrate aspartate, the product 2-iminosuccinate and also NAD^+ (Mortarino et al., 1996; Seifert et al., 1990).

In this study, comprehensive engineering strategies were applied to *E. coli* K12 MG1655 to increase quinolinate production through the NAD *de novo* biosynthesis I (from aspartate) pathway. The approach included: blocking the consumption pathway, eliminating the transcriptional repression of NadA and NadB, decreasing the glucose consumption rate

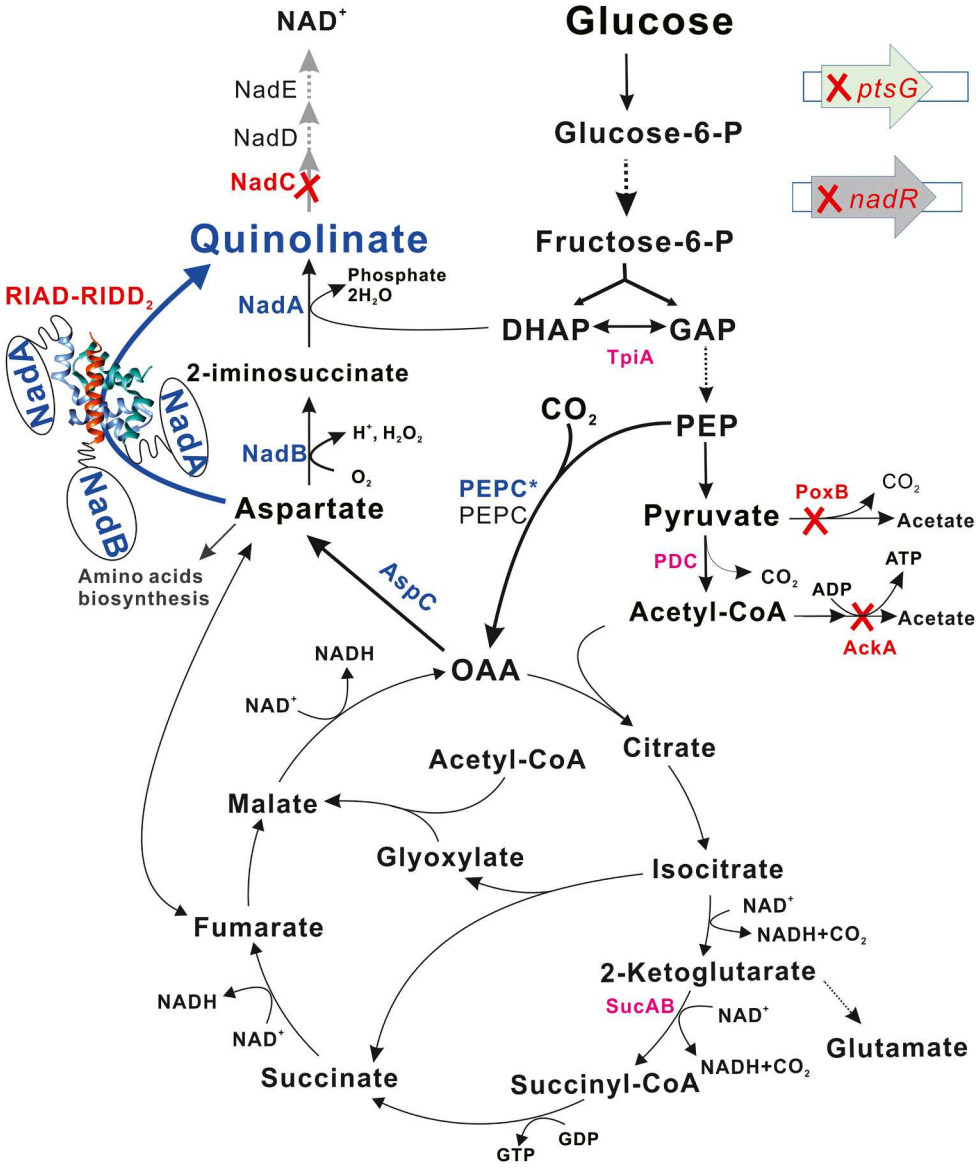

Fig. 1. Metabolic engineering of *E. coli* MG1655 for quinolinic acid production. Quinolinic acid production was enabled by deactivation of *nadC* (to block the consumption pathway), *nadR* (to eliminate the repression of L-aspartate oxidase NadB and quinolinate synthase NadA), and *ptsG* (to slow the glucose consumption rate and achieve a more balanced metabolism, and to increase the availability of phosphoenolpyruvate). Quinolinic acid production was enhanced by increasing the oxaloacetate (OAA) pool through overexpression of phosphoenolpyruvate carboxylase (PEPC) and deactivation of the acetate-producing pathways (*poxB*, *ackA*). Quinolinic acid production was accelerated by assembling NadB and NadA as a enzyme complex with the help of peptide-peptide interaction peptides RIAD and RIDD (Carlson et al., 2006; Gold et al., 2006). PtsG: glucose specific PTS enzyme II subunit BC; NadR: DNA-binding transcriptional repressor; DHAP: dihydroxyacetone phosphate; GAP: glyceraldehyde 3-phosphate; TpiA: triose-phosphate isomerase; PDC: pyruvate dehydrogenase complex; poxB: pyruvate oxidase; AckA, acetate kinase; SucAB: 2-oxoglutarate dehydrogenase multi-enzyme complex subunit AB; AspC: aspartate aminotransferase; NadC: quinolinate phosphoribosyltransferase; NadD: nicotinate-mononucleotide adenylyltransferase; NadE: NAD synthetase; RIAD, an 18 amino acids peptide from the A kinase-anchoring proteins; $RIDD_2$: RIDD dimer which contains 50 N-terminal residues of cAMP-dependent protein kinase for each peptide.

and increasing the availability of phosphoenolpyruvate, PEP followed by increasing the oxaloacetate, OAA pool for aspartate synthesis, and blocking the by-product acetate producing pathways, as well as improving the enzymatic efficiency by assembling NadA and NadB as an enzyme complex (Fig. 1). Finally, up to 3.7 g/L quinolinate was produced from 40 g/L glucose in shake-flask cultures of the improved strain. The results lay a foundation for further engineering of the strain for highly efficient production of quinolinate for industrial applications.

2. Materials and methods

2.1. Plasmids and strains

Plasmids and strains used in this study are listed in Table S1 and a brief description of the construction procedure is provided below.

The traditional digestion and ligation method was used for plasmid construction. *Nde*I-*Hin*dIII digested DNA fragment including lacI, pTrc promoter and multiple cloning sites (MCS) from pFZGNB16 (pTrc99a with a *Bgl*II site 193 bp upstream of the pTrc promoter) was ligated with a DNA fragment containing the kanamycin resistance gene and the origin of replication from pHL413Km (Thakker et al., 2011) to give pFZGNB33 (*Bgl*II-pTrc-MCS-Km-ori-lacI). Native genes, *nadA*, *nadB* and *aspC* were each individually amplified from *E. coli* MG1655 genomic DNA and inserted into pFZGNB33 to give pFZGNB34, pFZGNB35 and pFZGNB36, respectively. *AspC*, *nadB* and *nadA* gene fragments with ribosome binding sites (RBS) were combined in different orders to give pFZGNB37 to pFZGNB42 (Table S1). *nadA* from *Bacillus subtilis* (Bs*nadA*) was amplified from *Bacillus subtilis* CB10 with an extra DNA fragment coding a HisTag at the C-terminal (BsnadA-HisTag) and inserted into pFZ33 to give pFZGNB43, and pTrc-*nadB* from pFZGNB35 was inserted into pFZGNB43 to give pFZGNB207. L-aspartate oxidase from *Sulfolobus tokodaii* (St*nadB*, GenBank: KC333624.1) was synthesized and sub-cloned into pTrc99a by Genscript (pTrc99a- St*nadB*). pTrc-St*nadB* was then inserted into pFZGNB34 to give pFZGNB189. The *Spe*I-*Hin*dIII digested pTrc-*nadB* PCR product from pFZGNB35 was inserted into *Xba*I-*Hin*dIII digested pFZGNB34 to give pFZGNB190. *NadB* from *Pseudomonas putida* KT2440 (Pp*nadB*) was amplified from genomic DNA and inserted into pFZGNB33 to give pFZGNB183. pTrc-Pp*nadB* from pFZGNB183 was inserted into pFZGNB34 to give pFZGNB193 (Table S1).

For NadA-NadB fusion protein constructions, DNA fragments encoding peptide linkers $(GS)_3$, $(GS)_6$ and $(G_4S)_2$ were introduced at the end of *nadA* or *nadB* without stop codon through PCR and combined with *nadB* or *nadA* to give pFZGNB153 to pFZGNB157 (Table S1). DNA fragments encoding peptides RIAD and RIDD with a linker $(G_4S)_2G_4CG$ were codon-optimized and synthesized by Synbio Technologies (Table S2). Overlap Extension PCR (OE-PCR) was then applied to combine the peptide encoding DNA fragment with *nadA* or *nadB* to give pFZGNB228 to pFZGNB231. pTrc-nadB-RIAD from pFZGNB229 and pTrc-RIAD-nadB from pFZGNB230 were inserted into pFZ228 and pFZGNB231 individually to give pFZGNB232 to pFZGNB235, respectively (Table S1).

N_{20} of pTargetF (Jiang et al., 2015) was replaced by a *ptsG* specific N_{20} (GTATCCGTACTGCCTATCGC) through inverse PCR to give pFZGNB44. The upstream and downstream homologous arms of *ptsG* were amplified from *E. coli* MG1655 genomic DNA and inserted between the *Eco*RI and *Hin*dIII sites of pFZGNB44 with an *Xba*I site between the two homologous arms to give pFZGNB46, which can be used for *ptsG* deletion. The same method was used to construct plasmids pFZGNB63, pFZGNB65, pFZGNB74, pFZGNB75 and pFZGNB76 for deactivation of *tpiA, sucAB, lpd, ackA,* and *pta-ackA*. pTrc-pepc was amplified from pKK313 (Wang et al., 1992) and inserted into pFZGNB46, pFZGNB75, and pFZGNB76 to give pFZGNB50, pFZGNB117, and pFZGNB118, which can be used to replace *ptsG, ackA, pta-ackA* with pTrc-*pepc* fragment individually (Table S1).

E. coli K12 MG1655 was used as the parent strain in this study. Genes *nadC* and *nadR* were deleted using the lambda red recombination method (Datsenko and Wanner, 2000), and the CRISPR/Cas9 method was employed for deletion/replacement of the other selected genes (Jiang et al., 2015).

2.2. Fermentation of quinolinic acid from glucose

Freshly transformed strains were used for every batch fermentation. Ten single colonies were inoculated into 5 mL LB or quinolinic acid-producing medium with 50 mg/L kanamycin and cultured at 37 °C to form the inoculum seed culture. Fermentation was performed in 250-mL conical flasks that contain 1.5 g $CaCO_3$. Fifty milliliters of quinolinic acid-producing medium supplemented with 50 mg/L kanamycin was added into each flask, and IPTG was added to a final concentration of 0.1 mM for induction. One percent of an overnight cell culture was inoculated into the fermentation medium. The cells were grown at 37 °C with shaking at 350 rpm unless otherwise stated. A sample of 1-mL of culture broth was withdrawn at designated intervals for product and metabolite analysis by HPLC. The previous reported medium (Kim et al., 2016) with a higher concentration of Fe^{2+}, Mn^{2+}, and Zn^{2+} (increased from 5 mg/L to 10 mg/L) was used for fermentation. This culture media contains 70 g/L of glucose, 17 g/L of $(NH_4)_2SO_4$, 1 g/L of KH_2PO_4, 0.5 g/L of $MgSO_4{\cdot}7\,H_2O$, 2 g/L of yeast extract, 150 mg/L of methionine, 10 mg/L of $FeSO_4{\cdot}7H_2O$, 10 mg/L of $MnSO_4{\cdot}8H_2O$, and 10 mg/L of $ZnSO_4$, unless otherwise specified.

2.3. SDS-PAGE analysis of soluble protein

To check the protein expression level of the targeted proteins, cells from 3 mL cell culture was harvested and stocked at −80 °C until further analysis. The cells were melted on ice and suspended in 0.8 mL of 50 mM Tris-Cl (pH 8.0), and 0.6 g glass beads was added. The cells were disrupted by disruptor Genie (2500 rpm) for 3 min. Lysed cells were then centrifuged at 13,000 rpm for 10 min and the supernatants were used for SDS-PAGE analysis.

2.4. Analytical methods

For analyzing the fermentation products and residual sugars and other metabolites, the samples were centrifuged at 13,000×*g* for 2 min and then the supernatant was filtered through a 0.2 μm syringe filter. The glucose, acetate, and quinolinate were quantified using the same method as previously described (Zhu et al., 2018). In brief, an HPLC system was equipped with a cation-exchange column Aminex HPX-87H (Bio-Rad, USA) and a differential refractive index detector RID-10A (Shimadzu, Japan) and UV detector at 210 nm. 2.5 mM H_2SO_4 served as the mobile phase running at 0.5 mL/min, and the column temperature was maintained at 55 °C. Authentic quinolinic acid (Sigma, St. Louis, MO) was used to generate a standard curve from 10 mg/L to 5 g/L, less than 10 mg/L is considered as not detectable (nd) under tested conditions.

3. Results and discussion

3.1. Engineering of E. coli MG1655 for quinolinic acid production

Quinolinic acid is an intermediate of the NAD^+ *de novo* biosynthetic pathway under aerobic conditions (Fig. 1). The gene *nadC* of MG1655 was disrupted to block the consumption pathway and allow strain FZ700 to accumulate quinolinic acid. To increase expression of the NAD^+ biosynthetic genes, the DNA-binding transcriptional repressor *nadR* (of *nadA* and *nadB*) was deactivated in FZ700 to give FZ703. Plasmid pFZGNB42 (pTrc-*aspC-nadB-nadA*) was introduced into the engineered strains to check their performance. The quinolinic acid accumulated in parent strain *E. coli* MG1655 is less than 43 mg/L under tested conditions, which is likely due to it being further converted to NAD^+. 138 mg/

L of quinolinic acid was accumulated in FZ700, and QA titer goes up to 544 mg/L in FZ703.

In experiments we noticed more than 37 g/L acetate was accumulated in these strains, which was a really high level of byproduct from the feedstock, glucose. Deactivation of the glucose specific transporter, PtsG, was reported to be able to reduce acetate secretion significantly by slowing the glucose consumption rate which results in a more balanced and efficient metabolism (De Anda et al., 2006; Gosset, 2005; Wong et al., 2008), and also more PEP can be conserved and available for other metabolic pathways by decoupling glucose transport from PEP-dependent phosphorylation (Chatterjee et al., 2001; Gosset, 2005; Liang et al., 2015; Lin et al., 2005). Moreover, the *E. coli* EMP pathway was reported to potentially form an entire substrate channeling module that prevent PEP from being used by other pathways (Shearer et al., 2005). PtsG is thought to be the anchoring point of the EMP channeling and disrupting it will weaken the EMP channeling and improve the efficiency of the engineered pathway to hijack intermediate metabolites from the native pathway (Abernathy et al., 2019). So, the glucose specific transporter PtsG was deactivated in FZ703 to give FZ723. Meanwhile, the S8D mutant of sorghum phosphoenolpyruvate carboxylase (PEPC) (Wang et al., 1992) was also introduced to increase the OAA pool. This modification was accomplished by the replacement of *ptsG* with pTrc-*pepc* fragment in FZ703 to give FZ734 (Table S1). After 1-day fermentation, up to 450 mg/L quinolinic acid was accumulated in FZ703, while only 283 mg/L and 360 mg/L quinolinic acid were produced in FZ723 and FZ734, respectively. After 3-day fermentation, strains FZ723 and FZ734 attained a comparable performance to strain FZ703. Finally, 627 mg/L and 740 mg/L quinolinic acid were accumulated in FZ723 and FZ734 respectively after a 7-day fermentation period, while, only 544 mg/L quinolinic acid accumulated in FZ703 (Table 1). However, a very high concentration of acetate still accumulated in FZ734 (Table S2). The experiment clearly indicates that blocking the consumption pathway is necessary for quinolinic acid production, and deactivation of PtsG and introducing PEPC are helpful for quinolinic acid production. Strain FZ734 was used for further experiments.

Plasmid pFZGNB42 (pTrc-*aspC-nadB-nadA*) was introduced into the tested strains to examine their performance, aerobic cultures were performed at 37 °C, 350 rpm. The numbers indicate quinolinate concentration (mg/L, average of three replicates with error bars indicating standard deviation).

3.2. Effect of varying the gene order of aspC, nadB, and nadA in expression constructs on quinolinic acid production

Plasmids containing the three genes for quinolinic acid production from OAA in different arrangements were constructed to give plasmids pFZGNB37 to pFZGNB42 (Fig. 2) and their performance on quinolinic acid production in the host FZ734 was evaluated. After 4 days of fermentation, more than 48 g/L of glucose was consumed in all tested strains. The culture of the strain where only *aspC* was overexpressed produced the lowest quinolinic acid titer (123 mg/L) compared to the results observed when *nadA* or *nadB* was overexpressed (Fig. 2). When all three genes were co-overexpressed in different gene orders on a plasmid, the quinolinic acid production was slightly improved with plasmid pFZGNB37 (pTrc-*nadA-nadB-aspC*), and the quinolinic acid titer increased to 404 mg/L with plasmid pFZGNB42 (pTrc-*aspC-nadB-nadA*). Unexpectedly, a higher quinolinic acid titer was observed in the strain bearing plasmid pFZGNB190, which only overexpressed *nadA* and *nadB* under control of two individual pTrc promoters (pTrc-*nadA*-pTrc-*nadB*, Table S1), where 667 mg/L quinolinic acid was accumulated (Fig. 2). This experiment suggested the level of AspC expressed from the native gene is already enough for these tested conditions.

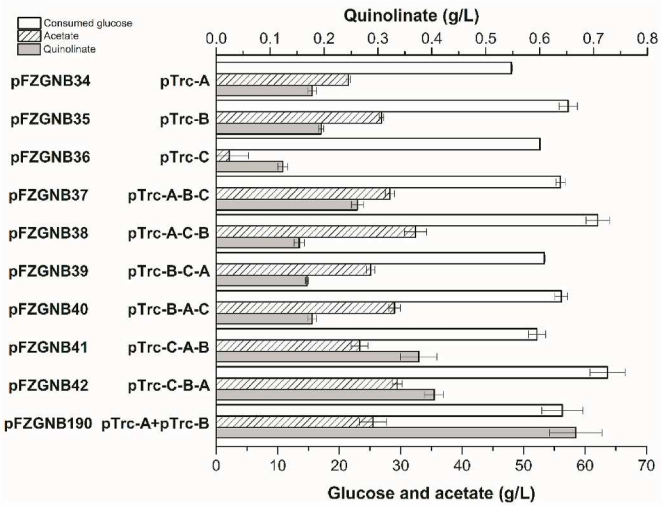

Fig. 2. Quinolinic acid production in FZ734 harboring plasmids containing various gene orders of *aspC*, *nadB*, and *nadA*. Aerobic cultures were performed at 37 °C, 350 rpm for 4 days. Values are the average of three replicates with error bars indicating standard deviation. A, B, and C indicate *nadA*, *nadB*, and *aspC* accordingly.

Table 1
Quinolinate production in engineered strains.

	MG1655	FZ700	FZ703	FZ723	FZ734
1 day	40.2 ± 1.6	97.1 ± 13.6	449.7 ± 24.3	282.6 ± 16.0	360.2 ± 29.2
3 day	42.8 ± 3.5	138.2 ± 8.3	488.5 ± 23.4	500.8 ± 28.5	594.5 ± 13.7
5 day	36.9 ± 1.8	133.8 ± 7.5	503.8 ± 26.4	544.0 ± 31.2	644.9 ± 16.4
7 day	36.8 ± 2.1	135.4 ± 6.9	544.4 ± 20.4	627.3 ± 31.6	739.7 ± 16.9
NadC	+	-	-	-	-
NadR	+	+	-	-	-
PtsG	+	+	+	-	-
pTrc-*pepc*	-	-	-	-	+

3.3. Examination of variants of nadA and nadB failed to improve quinolinate production

Although FZ734 with plasmid pFZGNB190 (pTrc-nadA + pTrc-nadB) showed the best performance as described above in section 3.2, it was reported that protein NadB displays a substrate inactivation and its activity can be inhibited by substrate aspartate and NAD, which act as competitive inhibitors (Seifert et al., 1990). NadA was also reported to form inclusion bodies when it is overproduced (Ceciliani et al., 2000), which could diminish its *in vivo* activity. Screening enzymes from diverse sources has been used as an effective strategy to increase the productivity of heterologous pathways in specific hosts. So, some NadA and NadB variants from other species were employed and tested in FZ734 for comparison.

It was reported that the activity of NadB from *Pseudomonas putida* KT2440 (Pp*nadB*) was not inhibited by aspartate when the concentration of aspartate is less than 50 mM. And the K_m, k_{cat} value of this enzyme was determined to be 2.26 mM, 10.6 s^{-1} against L-aspartate (Leese et al., 2013). NadB from *Sulfolobus tokodaii* (StNadB) was also reported to be less sensitive to NAD^+ since it can bind the FAD cofactor tightly with a different structure (Bifulco et al., 2013; Sakuraba et al., 2008); moreover, it displays some other distinctive features, e.g., stable activity over a wide range of pH (from 7 to 10), and high thermostability (with a Tm higher than 79 °C), which would make it attractive for biotechnological applications. However, evaluation of constructs expressing these alternative genes under the same conditions described in Fig. 2 revealed no improvement in quinolinic acid production (Fig. 3).

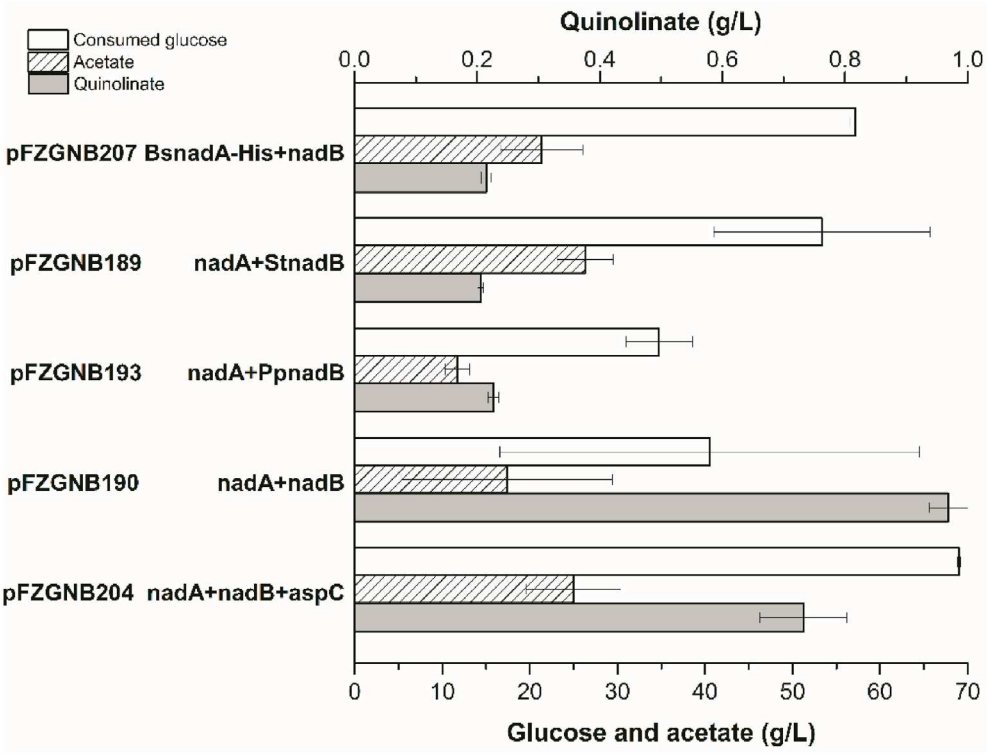

Fig. 3. The effect of nadA and nadB variants on quinolinic acid production in FZ734. Aerobic cultures were performed at 37 °C, 350 rpm for 4 days. Proteins were over-produced under the control of pTrc promoter in pFZGNB33. Values are the average of three replicates with error bars indicating standard deviation. BsnadA-HisTag indicates *nadA* from *Bacillus subtilis* with a His_6-Tag at the C-terminal, StnadB indicates *nadB* from *Sulfolobus tokodaii*, and PpnadB indicates *nadB* from *Pseudomonas putida* KT2440.

This may be due to the poor protein expression of these NadB variants (Fig. S1), especially StNadB comes from an extremophile. Another possible reason is these enzymes having a lower affinity for aspartate, the K_m value for L-aspartate of StNadB and PpNadB is 1.3 and 2.26 mM as reported (Bifulco et al., 2013; Leese et al., 2013), which is much higher than the K_m value of *E. coli* NadB (0.048 mM).

The gene encoding NadA from *Bacillus subtilis* (BsNadA) had been successfully overexpressed with a His_6 tag at its C-terminal (BsNadA-HisTag) in *E. coli* with a yield of 10 mg pure protein from 1 L culture (Marinoni et al., 2008). Unexpectedly, only 215 mg/L quinolinic acid was produced when the native *nadA* in pFZGNB190 was replaced with Bs*nadA*-HisTag (Fig. 3) as no improvement on protein expression was observed in the tested conditions (Fig. S1) and low activity of the BsNadA-HisTag enzyme was reported previously (Marinoni et al., 2008).

Unfortunately, the performance of these strains with different NadA and NadB variants is not as good as the native *E. coli* enzymes NadA and NadB under the tested conditions in FZ734 (Fig. 3). The native *aspC* was also introduced into pFZGNB190 to give pFZGNB204; however, less quinolinic acid was accumulated in the strain with pFZGNB204 (Fig. 3), possibly due to the substrate inactivation of NadB, potentially caused by the overexpression of AspC.

3.4. Engineering of FZ734F to improve quinolinic acid production

Several manipulations were explored to enhance the carbon flux to quinolinate production, including increasing the substrate availability, downregulating the TCA cycle, and blocking the by-product acetate production. DHAP can be condensed with 2-iminosuccinate by NadA to form quinolinate with a K_M of 0.74 mM (Reichmann et al., 2015), while it is reported that wild type *E. coli* strains normally only have 0.37 mM DHAP (Bennett et al., 2009), so this possibility to enhance the level of DHAP was tested. Triosephosphate isomerase (TpiA), which catalyzes the isomerization between glyceraldehyde 3-phosphate and dihydroxyacetone phosphate (DHAP), was deactivated to reserve DHAP for quinolinate biosynthesis. Meanwhile, we considered that the low yield of quinolinate may be due to too much carbon going through the TCA cycle, so *sucAB* and *lpd* were deactivated to down-regulate the carbon flux through TCA cycle. SucA and SucB are two subunits of the 2-oxoglutarate dehydrogenase multi-enzyme complex (OGDHC) that catalyzes the conversion of 2-oxoglutarate (2-ketoglutarate) to succinyl-CoA and CO_2. Deactivation of *sucAB* could accumulate 2-oxoglutarate, which can be used for glutamate synthesis and will be beneficial for aspartate synthesis. Lipoamide dehydrogenase (Lpd) is the E3 component of three multicomponent enzyme complexes: pyruvate dehydrogenase, 2-oxoglutarate dehydrogenase complex, and the glycine cleavage system (Guest and Creaghan, 1972; Pettit and Reed, 1967; Steiert et al., 1990). Deactivation of *lpd* was reported to produce more pyruvate and L-glutamate under aerobic conditions (Li et al., 2006), as it affects the function of pyruvate dehydrogenase and the 2-oxoglutarate dehydrogenase complex. However, the FZ738 (FZ734 Δ*tpiA*) or FZ742 (FZ734 Δ*lpd*) strain displayed very poor cell growth and failed to produce quinolinate (Fig. 4). Although the *sucAB*$^-$ strain can grow, unfortunately, it also failed to accumulate quinolinate. This may be due to the quinolinate production being an ATP consuming process, and it requires a high level of ATP generated through the TCA cycle or other ATP producing pathway.

More than 20 g/L acetate accumulated in nearly in all tested strains, which may inhibit the cell growth and waste the substrate glucose, so the acetate producing pathways were selected as the next target for genetic modification. There are two predominant acetate producing pathways active aerobically in *E. coli*, they are the pyruvate oxidase (PoxB) and acetate kinase/phosphotransacetylase (AckA-Pta) pathways. Pyruvate oxidase (PoxB) is a peripheral membrane enzyme that catalyzes the oxidative decarboxylation of pyruvate to form acetate and mainly functions at stationary phase, whereas the AckA-Pta catalyzed pathway, which mainly functions during the exponential phase, converts acetyl-CoA to acetate (Dittrich et al., 2005). When the fermentation was performed with strains harboring plasmid pFZGNB190, no difference was observed on acetate accumulation when only the PoxB was deactivated, while much less acetate was accumulated when both PoxB and AckA were deactivated (Fig. 4). However, there is 13% decrease in quinolinate titer in FZ757/pFZGNB190 due to 40% less

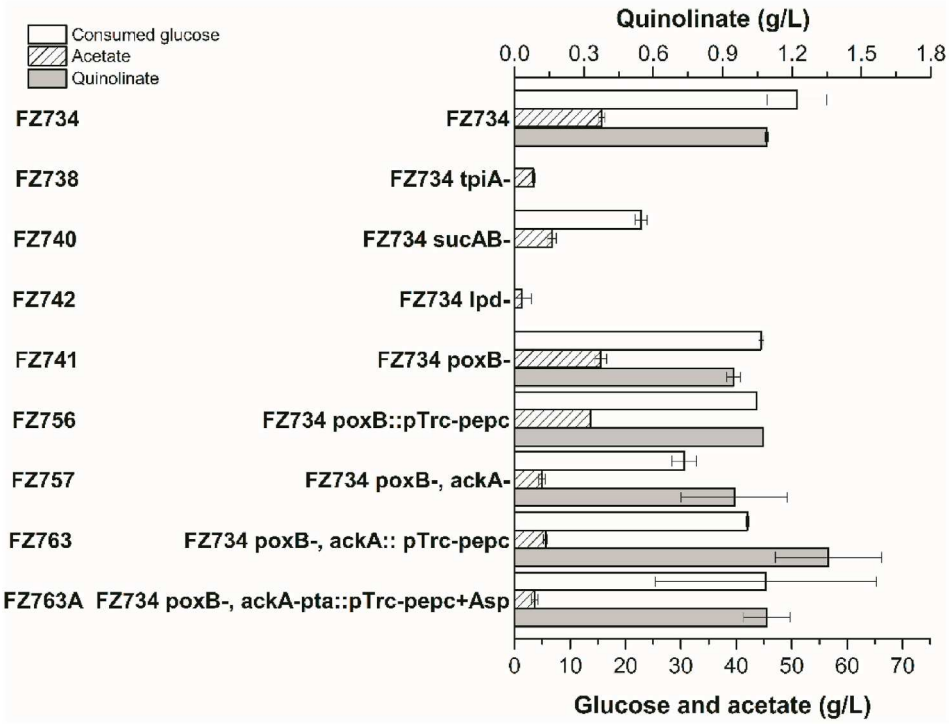

Fig. 4. Quinolinic acid production in engineered strains harboring plasmid pFZGNB190. Aerobic cultures were performed at 37 °C, 350 rpm for 4 days. FZ763A indicates 5 g/L aspartate was added into the fermentation broth (+Asp). Values are the average of three replicates with error bars indicating standard deviation.

glucose being consumed. Since this strain has two acetate producing pathways deactivated, compared with FZ734/pFZGNB190 (Fig. 4), it has a less ability to consume glucose rapidly. Interestingly, improvement was observed when an extra copy of pTrc-*pepc* was introduced into FZ757 (FZ734 *ΔpoxB*, *ΔackA*) forming strain FZ763/pFZGNB190 (Table S1). The resulting strain yielded a 24.4% increase in quinolinic acid formation compared to FZ734/pFZGNB190, with up to 1.4 g/L (32.3 mg/g consumed glucose) being accumulated while consuming 42 g/L glucose (Fig. 4), it's also worth noticing that more than 5.6 g/L acetate accumulated in FZ763/pFZGNB190 in 4-day fermentation (Fig. 4). We also examined the addition of extra aspartate and when 5 g/L aspartate was added into the fermentation broth with strain FZ763/pFZGNB190, the quinolinate titer dropped to 1.1 g/L. The decrease is consistent with the result mentioned in section 3.3 (Fig. 3) that showed quinolinate titer dropped when AspC was overproduced, indicating an imbalance in the synthesis and utilization of this intermediate, which may be due to the substrate inhibition of NadB by a high concentration of aspartate. It also indicates that the flux from aspartate to quinolinic acid is the limiting step for quinolinic acid production in our tested system.

Based on the strains' performance, the strain FZ763/pFZGNB190 was further evaluated with lower glucose concentration (40 g/L). Interestingly, strain FZ763/pFZGNB190 fermented with 40 g/L glucose has a higher quinolinate productivity based on 2-day samples, while the strain has comparable quinolinate titer after a 4-day fermentation (Fig. S2). This result may be due to the fermentation with 40 g/L glucose receiving much less metabolic stress and would be more suitable for chemicals production as the yield per glucose would be higher than in the 70 g/L cultures.

3.5. Improvement of quinolinate production by assembling NadA and NadB as an enzyme complex

The flux from aspartate to quinolinic acid has been demonstrated to be a rate-limiting factor for quinolinic acid production above by the results of experiments on overexpression of individual/combination of genes encoding AspC, NadB, and NadA (Figs. 2 and 3) and feeding extra aspartate (Fig. 4). Further increasing the flux of these steps is highly desired for quinolinic acid production; moreover, it was reported that the intermediate 2-iminosuccinate is unstable (Nasu et al., 1982), both of which brings a synthetic multiple-enzyme complex into our mind. Synthetic multi-enzyme complexes have been developed to control the flux of metabolites and to improve product yield (Conrado et al., 2008; Quin et al., 2017), not only because it improves local substrate concentration and reaction equilibrium but also prevents loss of reaction intermediates from competing pathways by diffusion, protects cells from unstable/toxic intermediates, and increases local enzyme concentration (Abernathy et al., 2017; Obata, 2020; Wheeldon et al., 2016). All these features are potentially helpful for quinolinic acid production in our system. Also, NadA easily forms an inclusion body as another complication (low protein concentration), and 2-iminosuccinate is unstable (Ceciliani et al., 2000; Nasu et al., 1982), so a synthetic multi-enzyme complex was investigated in this study.

Using a fusion protein is one of the developed strategies to form synthetic multi-enzyme complexes. Such fusions can be easily constructed by genetically fusing two or more protein domains with a peptide linker, and it is also often useful to improve the solubility of recombinant proteins. While, no improvement was observed when NadA and NadB were fused with linkers $(GS)_3$, $(GS)_6$, or $(G_4S)_2$ (Fig. S3), the performance of NadA-$(GS)_6$-NadB (FZ763/pFZGNB157) was comparable with the performance of the host-plasmid bearing separate proteins (FZ763/pFZGNB190). Possible complications could be due to the linker not being optimized, or the expression of the large fusion protein being worse than the expression of the separate proteins (Fig. S4). It also may be due to the fusion not being easily able to account for the dimer, monomer situation, and such complexes may generate an aggregate or inefficient complex as the dimeric structure is necessary for the stability of NadA (Ollagnier-de Choudens et al., 2005).

Synthetic multi-enzyme complexes can also be constructed by assembling the enzymes with a protein/peptide scaffold based on protein-protein/peptide interaction or even peptide-peptide interaction (Conrado et al., 2008; Quin et al., 2017). A dock-and-lock peptide

interacting family of peptides RIAD and RIDD have been successfully applied for lycopene overproduction (Kang et al., 2019). RIAD, an 18 amino acid peptide which is from the A kinase-anchoring proteins, specifically binds to the RIDD dimer, which contains the first 50 N-terminal residues of cAMP-dependent protein kinase. Their small size, strong binding affinity, and fixed 1:2 binding stoichiometry ratio make them a suitable pair of protein tags for multi-enzyme assembly (Kang et al., 2019). So, NadB and NadA were then assembled as an enzyme complex by adding peptides RIAD and RIDD in this study. DNA fragments encoding peptides RIAD and RIDD with a linker $(G_4S)_2G_4CG$ were codon-optimized and synthesized by Synbio Technologies and incorporated in plasmids for study (Table S3). NadA appears as a dimeric protein and the dimeric structure is essential for its stability (Ollagnier-de Choudens et al., 2005), while NadB is a monomeric protein (Mattevi et al., 1999), so RIDD was combined with *nadA* and RIAD was combined with *nadB* both at N-terminal and C-terminal by Overlap Extension PCR (OE-PCR) to give pFZGNB228 to pFZGNB231. pTrc-nadB-RIAD from pFZGNB229, and pTrc-RIAD-nadB from pFZGNB230 was inserted into pFZ228 and pFZGNB231 individually to give pFZGNB232 to pFZGNB235 (Table S1). Since no significant improvement was observed in quinolinate titer when 70 g/L glucose was used compared to 40 g/L glucose, the strains were evaluated in QA producing medium with 40 g/L glucose. The strain FZ763/pFZGNB233 [RIDD-NadA (RIDD added at the N-terminal of NadA with a $G_4SG_4SG_4CG$ linker) with RIAD-NadB] displayed poor cell growth after two days fermentation, no quinolinate was observed (Fig. 5a), and nearly no glucose was consumed (Fig. 5b). Although comparable biomass was obtained after 4 days of fermentation (cell density was not measured due to the present of $CaCO_3$), it only produced 0.7 g/L quinolinate, which is 31% less than produced in FZ763/pFZGNB190 (1.0 g/L, Fig. 5a). The other strains all exhibited better performance than FZ763/pFZGNB190 (Fig. 5). After 2 days fermentation, FZ763/pFZGNB190 had already consumed all glucose, but only produced 1.0 g/L quinolinate (25 mg/g consumed glucose, 20.8 mg/L/h). Strain FZ763/pFZGNB232 (RIDD-NadA with NadB-RIAD) shows the highest quinolinate titer (2.8 g/L) due to more glucose was consumed (37.9 g/L) than other strains (except FZ763/pFZGNB190), with a productivity of 58.3 mg/L/h which is 35 times faster than the parent strain MG1655/pFZGNB42 (Fig. 5 and Table 1). Strain FZ763/pFZGNB234 (NadA-RIDD with NadB-RIAD) produced 2.6 g/L quinolinate from 29 g/L glucose with a yield of 89.7 mg/g, and with less acetate being accumulated (Fig. 5c). 37.4 g/L glucose was consumed in FZ763/pFZGNB235 (NadA-RIDD with RIAD-NadB), and 2.4 g/L quinolinate was accumulated. After 4 days of fermentation, no significant improvement was observed in strains FZ763/pFZGNB190, FZ763/pFZGNB232 and FZ763/pFZGNB235, however most of the glucose was consumed within 2 days (Fig. 5a and b). Quinolinate titer in strain FZ763/pFZGNB234 was further increased to 3.7 g/L upon consuming the residual glucose with a yield of 92.5 mg/g. This result is 3.6-fold higher than FZ763/pFZGNB190 (Fig. 5) and more than 86.8 times higher than the parent strain MG1655/pFZGNB42 (Table 1 and Fig. 5a). The higher yield was achieved as less acetate was accumulated in these strains, except for strain FZ763/pFZGNB233, compared to strain FZ763/pFZGNB190 (Fig. 5c), which indicates a more balanced metabolism was achieved. The highest yield (92.5 mg/g) we achieved in FZ763/pFZGNB234 is 3.6-fold higher than FZ763/pFZGNB190 and 151-fold higher than the parent strain MG1655/pFZGNB42 (Table 1 and Fig. 5a). Similar amounts of protein complexes were observed through a non-reducing SDS-PAGE analysis (Fig. S5), except in FZ763/pFZGNB233. The strains were also tested in QA producing medium with 70 g/L glucose as a carbon source, and no improvement on quinolinate titer was observed among most tested strains (Fig. S6). By testing the NadA-NadB protein complex in different arrangements, it clearly shows that the activity and complex formation would depend on the position and orientation of the peptide complexes. The strains with NadA-RIDD had better performance than the strains with RIDD-NadA (Fig. 5), which is consistent with the performance of fusion proteins made in this work where NadA has been linked at the C-terminal end, such as NadA-$(GS)_6$-NadB (Fig. S3). This may be due to the C-terminal end of the NadA being closer to the active site and more flexible than N-terminal based on the available crystal structures of NadA from other species (PDB number: 4ZK6, 4P3X and 4HHE) (Cherrier et al., 2014;

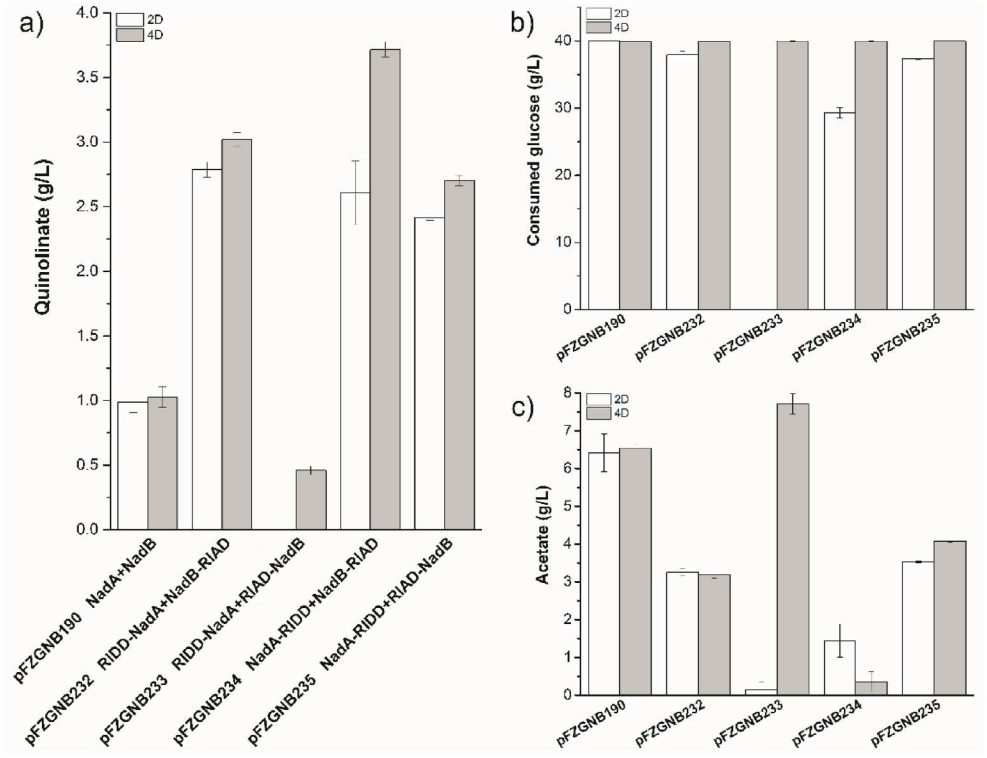

Fig. 5. The effect of NadA-NadB enzyme complex on quinolinic acid production in FZ763 with 40 g/L glucose. a) quinolinate titer, b) consumed glucose, c) accumulated acetate. Aerobic cultures were performed at 37 °C, 350 rpm, sampled at 2 days (2D) and 4 days (4D). NadA-RIDD and NadB-RIAD fusion proteins were over-expressed under the control of their pTrc promoter in pFZGNB227, NadA-NadB enzyme complex was assembled with the help of peptides, RIAD and RIDD. Values are the average of three replicates with error bars indicating standard deviation.

Esakova et al., 2016; Soriano et al., 2013), which have a similarity of greater than 55% to *E. coli* NadA, as the crystal structure of the *E. coli* native NadA is not available yet. The strains with NadB-RIAD also has better performance than the strains with RIAD-NadB (Fig. 5), which may be because the N-terminal end of NadB is the cofactor FAD-binding domain (Bossi et al., 2002), and adding a RIAD-tag to the N-terminal end affected the cofactor binding efficiency. Moreover, when the peptides were added to the N-terminal of NadA and NadB (RIDD-NadA with RIAD-NadB), the strain has the lowest quinolinate titer, which suggests it formed an non-preferred enzyme complex, perhaps inactive, and leads to a metabolic burden. In contrast, the combination with the peptides added to the C-terminal ends (NadA-RIDD with NadB-RIAD) has the highest quinolinate titer, which suggests a preferred enzyme complex being formed and stabilized in this configuration, providing an efficient and exclusive catalytic reaction series with little free diffusion of the unstable intermediate, 2-iminosuccinate (Nasu et al., 1982). Another possible reason is the RIDD: RIAD complex has a ratio of 2:1 (Kang et al., 2019), which is beneficial for NadA dimer formation and good for its activity and stability. Notably, the turnover frequency of *E. coli* NadB is only 0.267 s^{-1} (Tedeschi et al., 2010), which may limit the enzyme complex catalytic efficiency.

In conclusion, multiple engineering strategies were applied to increase the production of quinolinate. The quinolinate consumption pathway was blocked to enable the production of quinolinate by deactivation of NadC, and quinolinate production was activated by knockout the repressor gene *nadR*. Then, quinolinate production was enhanced by deactivation of glucose transporter gene *ptsG* to slow the glucose consumption rate, to achieve a more balanced metabolism, and to improve the availability of PEP. Increasing the OAA pool through overexpression of PEPC also improved quinolinate production. Moreover, the acetate-producing pathways were deactivated as acetate is a major by-product in the engineered strain FZ734/pFZGNB190. Finally, quinolinate production was accelerated by assembling NadA and NadB as an enzyme complex with the help of peptide-peptide interaction peptides, RIAD and RIDD, and up to 3.7 g/L quinolinate was accumulated in FZ763/pFZGNB234 in shake-flask cultures. These results lay a foundation for further engineering of the strains to efficiently produce quinolinic acid or even nicotinic acid for industrial applications. However, the highest yield we achieved is only 92.5 mg/g, which need to be further improved. Crystal-structural studies of the constructed protein complexes via isolation and crystallography could be employed, which would give us a better understanding of these results and lead to further optimization of the system. Further improvement may be achieved by protein engineering of NadB to eliminate the feedback inhibition and improve the enzymatic activity. Other potential enhancements may be attained through improving the expression of NadA, down-regulating the TCA cycle, optimizing the NadA-NadB enzyme complex, and assembling AspC, NadB, and NadA into a larger enzyme complex to allow more aspartate to more efficiently enter the reactions for quinolinate production.

There has been much attention to improve the efficiency of metabolic reactions through enzyme co-localization and compartmentalization. In this study, we not only built the synthetic enzyme complex (NadA-RIDD and NadB-RIAD enzyme complex) to improve quinolinate production, but also disrupted the potential native EMP channeling by deleting ptsG to release the intermediate PEP for quinolinate production. This disrupt-build strategy for metabolon engineering may be beneficial for future engineering of *in vivo* biocatalysis.

Declaration of competing interest

The authors declare no competing financial interests.

Acknowledgment

The authors thank Dr. Charles Stewart, Department of Biosciences at Rice University, for kindly sharing *Bacillus subtilis* CB10 with us, the authors thank Dr. Guoqiang Zhang at Jiangnan University (Wuxi, China) for helpful suggestions about fusion protein constructs, and Dr. Shuai Qian at Solugen (Houston, TX) for his help on protein structure analysis. This work was supported by NSF DBI-1262491, NSF EAGER: DESYN-C3 CBET-1843556, and DOE BES DE-SC0014462. M. P. was supported by a training fellowship from the Gulf Coast Consortia (NLM Grant T15 LM007093).

Appendix A. Supplementary data

Supplementary data to this article can be found online at https://doi.org/10.1016/j.ymben.2021.06.007.

References

Abernathy, M.H., et al., 2017. Channeling in native microbial pathways: implications and challenges for metabolic engineering. Biotechnol. Adv. 35, 805–814.
Abernathy, M.H., et al., 2019. Comparative studies of glycolytic pathways and channeling under in vitro and in vivo modes. AIChE J. 65, 483–490.
Andreoli, A.J., Ikeda, M., Nishizuka, Y., Hayaishi, O., 1963. Quinolinic acid: a precursor to nicotinamide adenine dinucleotide in Escherichia coli. Biochem. Biophys. Res. Commun. 12, 92.
Andrushkevich, T.V., Ovchinnikova, E.V., 2012. Gas phase catalytic oxidation of β-picoline to nicotinic acid: catalysts, mechanism and reaction kinetics. Catal. Rev. 54, 399–436.
Becker, J., Zelder, O., Häfner, S., Schröder, H., Wittmann, C., 2011. From zero to hero—design-based systems metabolic engineering of Corynebacterium glutamicum for l-lysine production. Metab. Eng. 13, 159–168.
Begley, T.P., Kinsland, C., Mehl, R.A., Osterman, A., Dorrestein, P., 2001. The biosynthesis of nicotinamide adenine dinucleotides in bacteria. Vitam. Horm. 61, 103–119.
Bennett, B.D., Kimball, E.H., Gao, M., Osterhout, R., Van Dien, S.J., Rabinowitz, J.D., 2009. Absolute metabolite concentrations and implied enzyme active site occupancy in Escherichia coli. Nat. Chem. Biol. 5, 593.
Bifulco, D., Pollegioni, L., Tessaro, D., Servi, S., Molla, G., 2013. A thermostable L-aspartate oxidase: a new tool for biotechnological applications. Appl. Microbiol. Biotechnol. 97, 7285–7295.
Bossi, R.T., et al., 2002. Structure of FAD-bound L-aspartate oxidase: insight into substrate specificity and catalysis. Biochemistry 41, 3018–3024.
Carlson, C.R., Lygren, B., Berge, T., Hoshi, N., Wong, W., Taskén, K., Scott, J.D., 2006. Delineation of type I protein kinase A-selective signaling events using an RI anchoring disruptor. J. Biol. Chem. 281, 21535–21545.
Ceciliani, F., Caramori, T., Ronchi, S., Tedeschi, G., Mortarino, M., Galizzi, A., 2000. Cloning, overexpression, and purification of Escherichia coli quinolinate synthetase. Protein Expr. Purif. 18, 64–70.
Chandler, J.L., Gholson, R., 1972. De novo biosynthesis of nicotinamide adenine dinucleotide in Escherichia coli: excretion of quinolinic acid by mutants lacking quinolinate phosphoribosyl transferase. J. Bacteriol. 111, 98–102.
Chatterjee, R., Millard, C.S., Champion, K., Clark, D.P., Donnelly, M.I., 2001. Mutation of the ptsG gene results in increased production of succinate in fermentation of glucose byEscherichia coli. Appl. Environ. Microbiol. 67, 148–154.
Cherrier, M.V., et al., 2014. The crystal structure of Fe4S4 quinolinate synthase unravels an enzymatic dehydration mechanism that uses tyrosine and a hydrolase-type triad. J. Am. Chem. Soc. 136, 5253–5256.
Cicchillo, R.M., Tu, L., Stromberg, J.A., Hoffart, L.M., Krebs, C., Booker, S.J., 2005. Escherichia coli quinolinate synthetase does indeed harbor a [4Fe-4S] cluster. J. Am. Chem. Soc. 127, 7310–7311.
Conrado, R.J., Varner, J.D., DeLisa, M.P., 2008. Engineering the spatial organization of metabolic enzymes: mimicking nature's synergy. Curr. Opin. Biotechnol. 19, 492–499.
Cox, S.J., Levanon, S.S., Sanchez, A., Lin, H., Peercy, B., Bennett, G.N., San, K.-Y., 2006. Development of a metabolic network design and optimization framework incorporating implementation constraints: a succinate production case study. Metab. Eng. 8, 46–57.
Crook, M.A., 2014. The importance of recognizing pellagra (niacin deficiency) as it still occurs. Nutrition 30, 729–730.
Datsenko, K.A., Wanner, B.L., 2000. One-step inactivation of chromosomal genes in Escherichia coli K-12 using PCR products. Proc. Natl. Acad. Sci. Unit. States Am. 97, 6640–6645.
De Anda, R., Lara, A.R., Hernández, V., Hernández-Montalvo, V., Gosset, G., Bolívar, F., Ramírez, O.T., 2006. Replacement of the glucose phosphotransferase transport system by galactose permease reduces acetate accumulation and improves process performance of Escherichia coli for recombinant protein production without impairment of growth rate. Metab. Eng. 8, 281–290.
Dittrich, C.R., Bennett, G.N., San, K.Y., 2005. Characterization of the acetate-producing pathways in Escherichia coli. Biotechnol. Prog. 21, 1062–1067.
Esakova, O.A., et al., 2016. Structure of quinolinate synthase from Pyrococcus horikoshii in the presence of its product, quinolinic acid. J. Am. Chem. Soc. 138, 7224–7227.
Flachmann, R., Kunz, N., Seifert, J., Gütlich, M., Wientjes, F.J., Läufer, A., Gassen, H.G., 1988. Molecular biology of pyridine nucleotide biosynthesis in Escherichia coli:

cloning and characterization of quinolinate synthesis genes nadA and nadB. Eur. J. Biochem. 175, 221–228.
Gold, M.G., Lygren, B., Dokurno, P., Hoshi, N., McConnachie, G., Taskén, K., Carlson, C. R., Scott, J.D., Barford, D., 2006. Molecular basis of AKAP specificity for PKA regulatory subunits. Mol. Cell. 24, 383–395.
Gosset, G., 2005. Improvement of Escherichia coli production strains by modification of the phosphoenolpyruvate: sugar phosphotransferase system. Microb. Cell Factories 4, 14.
Griffith, G.R., Chandler, J.L., Gholson, R.K., 1975. Studies on the de novo Biosynthesis of NAD in Escherichia coli: the Separation of the nadB Gene Product from the nadA Gene Product and Its Purification. Eur. J. Biochem. 54, 239–245.
Guest, J., Creaghan, I., 1972. Lipoamide dehydrogenase mutants of Escherichia coli K 12. Biochem. J. 130, 8P.
Hammond, N., Wang, Y., Dimachkie, M., Barohn, R., 2013. Nutritional neuropathies. Neurol. Clin. 31, 477–489.
Heath, A.P., Bennett, G.N., Kavraki, L.E., 2010. Finding metabolic pathways using atom tracking. Bioinformatics 26, 1548–1555.
Jiang, Y., Chen, B., Duan, C., Sun, B., Yang, J., Yang, S., 2015. Multigene editing in the Escherichia coli genome via the CRISPR-Cas9 system. Appl. Environ. Microbiol. 81, 2506–2514.
Kang, W., Ma, T., Liu, M., Qu, J., Liu, Z., Zhang, H., Shi, B., Fu, S., Ma, J., Lai, L.T.F., 2019. Modular enzyme assembly for enhanced cascade biocatalysis and metabolic flux. Nat. Commun. 10, 1–11.
Keasling, J.D., 2010. Manufacturing molecules through metabolic engineering. Science 330, 1355–1358.
Kim, S.M., Peña, M.I., Moll, M., Bennett, G.N., Kavraki, L.E., 2020. Improving the organization and interactivity of metabolic pathfinding with precomputed pathways. BMC Bioinf. 21, 1–22.
Kim, S.Y., Shin, Y.U., Heo, I.K., Kim, J.E., Son, S.K., Seo, C.I., Kim, H.A., Lee, H.J., Na, K. H., Bae, J.Y., 2016. Method for the Preparation of Nicotinic Acid. Google Patents.
Lee, J.W., Na, D., Park, J.M., Lee, J., Choi, S., Lee, S.Y., 2012. Systems metabolic engineering of microorganisms for natural and non-natural chemicals. Nat. Chem. Biol. 8, 536–546.
Leese, C., Fotheringham, I., Escalettes, F., Speight, R., Grogan, G., 2013. Cloning, expression, characterisation and mutational analysis of L-aspartate oxidase from Pseudomonas putida. J. Mol. Catal. B Enzym. 85, 17–22.
Li, M., Ho, P.Y., Yao, S., Shimizu, K., 2006. Effect of lpdA gene knockout on the metabolism in Escherichia coli based on enzyme activities, intracellular metabolite concentrations and metabolic flux analysis by 13C-labeling experiments. J. Biotechnol. 122, 254–266.
Liang, Q., Zhang, F., Li, Y., Zhang, X., Li, J., Yang, P., Qi, Q., 2015. Comparison of individual component deletions in a glucose-specific phosphotransferase system revealed their different applications. Sci. Rep. 5, 13200.
Lin, H., Bennett, G.N., San, K.-Y., 2005. Metabolic engineering of aerobic succinate production systems in Escherichia coli to improve process productivity and achieve the maximum theoretical succinate yield. Metab. Eng. 7, 116–127.
Magni, G., Amici, A., Emanuelli, M., Raffaelli, N., Ruggieri, S., 1999. Enzymology of Nad^{+} synthesis. Adv. Enzymol. Relat. Area Mol. Biol.: Mechanism of Enzyme Action, Part A. 73, 135–182.
Marinoni, I., Nonnis, S., Monteferrante, C., Heathcote, P., Härtig, E., Böttger, L.H., Trautwein, A.X., Negri, A., Albertini, A.M., Tedeschi, G., 2008. Characterization of l-aspartate oxidase and quinolinate synthase from Bacillus subtilis. FEBS J. 275, 5090–5107.
Martinez, I., Gao, H., Bennett, G.N., San, K.-Y., 2018. High yield production of four-carbon dicarboxylic acids by metabolically engineered Escherichia coli. J. Ind. Microbiol. Biotechnol. 45, 53–60.
Mattevi, A., Tedeschi, G., Bacchella, L., Coda, A., Negri, A., Ronchi, S., 1999. Structure ofL-aspartate oxidase: implications for the succinate dehydrogenase/fumarate reductase oxidoreductase family. Structure 7, 745–756.
Mortarino, M., Negri, A., Tedeschi, G., Simonic, T., Duga, S., Gassen, H.G., Ronchi, S., 1996. L-Aspartate oxidase from Escherichia coli: I. Characterization of coenzyme binding and product inhibition. Eur. J. Biochem. 239, 418–426.
Nasu, S., Wicks, F.D., Gholson, R., 1982. L-Aspartate oxidase, a newly discovered enzyme of Escherichia coli, is the B protein of quinolinate synthetase. J. Biol. Chem. 257, 626–632.
Ning, Y., Wu, X., Zhang, C., Xu, Q., Chen, N., Xie, X., 2016. Pathway construction and metabolic engineering for fermentative production of ectoine in Escherichia coli. Metab. Eng. 36, 10–18.
Ollagnier-de Choudens, S., Loiseau, L., Sanakis, Y., Barras, F., Fontecave, M., 2005. Quinolinate synthetase, an iron–sulfur enzyme in NAD biosynthesis. FEBS Lett. 579, 3737–3743.
Panozzo, C., Nawara, M., Suski, C., Kucharczyka, R., Skoneczny, M., Bécam, A.-M., Rytka, J., Herbert, C.J., 2002. Aerobic and anaerobic NAD+ metabolism in Saccharomyces cerevisiae. FEBS Lett. 517, 97–102.
Park, J.H., Lee, S.Y., 2010. Metabolic pathways and fermentative production of L-aspartate family amino acids. Biotechnol. J. 5, 560–577.
Pettit, F.H., Reed, L.J., 1967. Alpha-keto acid dehydrogenase complexes. 8. Comparison of dihydrolipoyl dehydrogenases from pyruvate and alpha-ketoglutarate dehydrogenase complexes of Escherichia coli. Proc. Natl. Acad. Sci. U. S. A 58, 1126.
Quin, M.B., Wallin, K., Zhang, G., Schmidt-Dannert, C., 2017. Spatial organization of multi-enzyme biocatalytic cascades. Org. Biomol. Chem. 15, 4260–4271.
Reichmann, D., Couté, Y., Ollagnier de Choudens, S., 2015. Dual activity of quinolinate synthase: triose phosphate isomerase and dehydration activities play together to form quinolinate. Biochemistry 54, 6443–6446.
Sakuraba, H., Yoneda, K., Asai, I., Tsuge, H., Katunuma, N., Ohshima, T., 2008. Structure of l-aspartate oxidase from the hyperthermophilic archaeon Sulfolobus tokodaii. Biochim. Biophys. Acta Protein Proteonomics 1784, 563–571.
Sánchez, A.M., Bennett, G.N., San, K.-Y., 2005. Novel pathway engineering design of the anaerobic central metabolic pathway in Escherichia coli to increase succinate yield and productivity. Metab. Eng. 7, 229–239.
Sauer, U., Eikmanns, B.J., 2005. The PEP—pyruvate—oxaloacetate node as the switch point for carbon flux distribution in bacteria: we dedicate this paper to Rudolf K. Thauer, Director of the Max-Planck-Institute for Terrestrial Microbiology in Marburg, Germany, on the occasion of his 65th birthday. FEMS Microbiol. Rev. 29, 765–794.
Seifert, J., Norbert, K., Flachmann, R., Läufer, A., Klaus-Dieter, J., Gassen, H.G., 1990. Expression of the E. coli nadB gene and characterization of the gene product L-aspartate oxidase. Biol. Chem. Hoppe-Seyler 371, 239–248.
Shearer, G., et al., 2005. Quantitative estimation of channeling from early glycolytic intermediates to CO2 in intact Escherichia coli. FEBS J. 272, 3260–3269.
Shishido, T., Song, Z., Kadowaki, E., Wang, Y., Takehira, K., 2003. Vapor-phase oxidation of 3-picoline to nicotinic acid over Cr1 − xAlxVO4 catalysts. Appl. Catal. A-Gen. 239, 287–296.
Soriano, E.V., et al., 2013. Active-site models for complexes of quinolinate synthase with substrates and intermediates. Acta Crystallogr. D69, 1685–1696.
Steiert, P., Stauffer, L., Stauffer, G., 1990. The lpd gene product functions as the L protein in the Escherichia coli glycine cleavage enzyme system. J. Bacteriol. 172, 6142–6144.
Tedeschi, G., Nonnis, S., Strumbo, B., Cruciani, G., Carosati, E., Negri, A., 2010. On the catalytic role of the active site residue E121 of E. coli L-aspartate oxidase. Biochimie 92, 1335–1342.
Thakker, C., Zhu, J., San, K.-Y., Bennett, G., 2011. Heterologous pyc gene expression under various natural and engineered promoters in Escherichia coli for improved succinate production. J. Biotechnol. 155, 236–243.
Tritz, G.J., Chandler, J.L., 1973. Recognition of a gene involved in the regulation of nicotinamide adenine dinucleotide biosynthesis. J. Bacteriol. 114, 128–136.
Wang, Y., Duff, S., Lepiniec, L., Crétin, C., Sarath, G., Condon, S.A., Vidal, J., Gadal, P., Chollet, R., 1992. Site-directed mutagenesis of the phosphorylatable serine (Ser8) in C4 phosphoenolpyruvate carboxylase from sorghum. The effect of negative charge at position 8. J. Biol. Chem. 267, 16759–16762.
Wheeldon, I., et al., 2016. Substrate channelling as an approach to cascade reactions. Nat. Chem. 8, 299.
Wong, M.S., Wu, S., Causey, T.B., Bennett, G.N., San, K.-Y., 2008. Reduction of acetate accumulation in Escherichia coli cultures for increased recombinant protein production. Metab. Eng. 10, 97–108.
Woolston, B.M., Edgar, S., Stephanopoulos, G., 2013. Metabolic engineering: past and future. Annu. Rev. Chem. Biomol. Eng. 4, 259–288.
Zhao, L., Lu, Y., Yang, J., Fang, Y., Zhu, L., Ding, Z., Wang, C., Ma, W., Hu, X., Wang, X., 2020. Expression regulation of multiple key genes to improve l-threonine in Escherichia coli. Microb. Cell Factories 19, 1–23.
Zhu, F., San, K.Y., Bennett, G.N., 2020. Improved succinate production from galactose-rich feedstocks by engineered Escherichia coli under anaerobic conditions. Biotechnol. Bioeng. 117, 1082–1091.
Zhu, F., Wang, Y., San, K.Y., Bennett, G.N., 2018. Metabolic engineering of Escherichia coli to produce succinate from soybean hydrolysate under anaerobic conditions. Biotechnol. Bioeng. 115, 1743–1754.

Metabolic engineering of *Escherichia coli* for quinolinic acid production by assembling L-aspartate oxidase and quinolinate synthase as an enzyme complex

Fayin Zhu[a,b], Matthew Peña[a], George N. Bennett[a,c]*

a Department of BioSciences, Rice University, Houston, TX, USA, 77005

b present address: Department of Chemical, Biological, and Materials Engineering, University of South Florida, Tampa, FL 33620

c Department of Chemical and Biomolecular Engineering, Rice University, Houston, TX, USA, 77005

* Corresponding author: Department of BioSciences, Rice University, Houston, TX 77005, E-mail address: gbennett@rice.edu

Abstract

Quinolinic acid (QA) is a key intermediate of nicotinic acid (Niacin) which is an essential human nutrient and widely used in food and pharmaceutical industries. In this study, a quinolinic acid producer was constructed by employing comprehensive engineering strategies. Firstly, the quinolinic acid production was improved by deactivation of NadC (to block the consumption pathway), NadR (to eliminate the repression of L-aspartate oxidase and quinolinate synthase), and PtsG (to slow the glucose utilization rate and achieve a more balanced metabolism, and also to increase the availability of the precursor phosphoenolpyruvate). Further modifications to enhance quinolinic acid production were investigated by increasing the oxaloacetate pool through overproduction of phosphoenolpyruvate carboxylase and deactivation of acetate-producing pathway enzymes. Moreover, quinolinic acid production was accelerated by assembling NadB and NadA as an enzyme complex with the help of peptide-peptide interaction peptides RIAD and RIDD, which resulted in up to 3.7 g/L quinolinic acid being produced from 40 g/L glucose in shake-flask cultures. A quinolinic acid producer was constructed in this study, and these results lay a foundation for further engineering of microbial cell factories to efficiently produce quinolinic acid and subsequently convert this product to nicotinic acid for industrial applications.

Keywords: quinolinic acid; peptide-peptide interaction; enzyme complex; metabolon; metabolite channeling; metabolic engineering

1. Introduction

Quinolinic acid (QA), known as pyridine-2,3-dicarboxylic acid, is a dicarboxylic acid with a pyridine backbone, and it is a key precursor to nicotinic acid and nicotine in nature (Andreoli et al., 1963). Nicotinic acid, also known as niacin or vitamin B_3, is one of the water-soluble B complex vitamins, and it commonly exists in living cells. In general, nicotinic acid is present mainly in the form of nicotinic acid amide coenzyme [Nicotinamide Adenine Dinucleotide (NAD^+) or Nicotinamide Adenine Dinucleotide Phosphate ($NADP^+$)] *in vivo* and it acts as a cofactor for a large and diverse number of cellular oxidative-reductive reactions. Nicotinic acid is an essential human nutrient as deficiency of nicotinic acid may cause the disease pellagra and neuropathies (Crook, 2014; Hammond et al., 2013). Consequently, nicotinic acid is widely used in the food and pharmaceutical industries. Nicotinic acid has been mainly produced by chemical synthesis through oxidation of β-picoline (Andrushkevich and Ovchinnikova, 2012; Shishido et al., 2003); however, these processes result in considerable amounts of toxic wastes, which require significant expense for proper disposal. Moreover, these methods use petroleum-based non-renewable chemicals as the precursor, which is affected by concerns about climate change and unpredictable oil refining prices. To overcome these concerns, production of fuels, pharmaceuticals, or bulk and fine chemicals from renewable feedstocks using microorganisms has arisen as an attractive alternative (Keasling, 2010; Lee et al., 2012; Woolston et al., 2013), especially given advancements in metabolic engineering, however, there is little published literature directed to the over-production of nicotinic acid or even quinolinic acid in microorganisms (Kim et al., 2016).

Early work on the enzymes and genes related to quinolinic acid formation from aspartate has been described (Chandler and Gholson, 1972; Flachmann et al., 1988; Griffith et al., 1975).

Quinolinic acid, NAD^+, Coenzyme A, and commercially important amino acids such as threonine and lysine (Becker et al., 2011; Ning et al., 2016; Park and Lee, 2010; Zhao et al., 2020) are generated via aspartate as a key precursor. Metabolic engineering at the oxaloacetate and aspartate nodes is important to give a high level of these key intermediates (Sauer and Eikmanns, 2005), as well as to provide high and specific conversion of aspartate to quinolinic acid. We have previously engineered cells to produce compounds derived from the oxaloacetate branch of the TCA cycle and have developed useful designs for metabolic networks to product compounds around this node (Cox et al., 2006; Martinez et al., 2018; Sánchez et al., 2005; Zhu et al., 2020). Likewise, we have investigated computational methods for finding novel pathways to relevant OAA derived compounds (Heath et al., 2010; Kim et al., 2020). There are two major NAD *de novo* biosynthetic pathways used for quinolinate production *in vivo*: NAD *de novo* biosynthesis I (from aspartate) in most prokaryotes and NAD *de novo* biosynthesis II (from tryptophan), also known as the kynurenine pathway, in eukaryotes (Begley et al., 2001; Panozzo et al., 2002). These two pathways converge at quinolinic acid, a key intermediate of NAD biosynthetic pathways, and subsequently use three common steps to synthesize NAD. Five enzymes are involved in the conversion of tryptophan to quinolinate in the kynurenine pathway. In comparison, only two enzymes, L-aspartate oxidase (NadB) and quinolinate synthase (NadA), are needed for quinolinate production aerobically from aspartate (Magni et al., 1999). L-aspartate oxidase (NadB), is a monomer of a 60 kDa flavoenzyme containing 1 mol of non-covalently bound FAD/mol protein, and it catalyzes the conversion of L-aspartate to 2-iminosuccinate (Mortarino et al., 1996; Nasu et al., 1982). Quinolinate synthase (NadA), which appears mainly as a dimeric protein of 80 kDa (Ollagnier-de Choudens et al., 2005), contains an oxygen-sensitive [4Fe-4S] cluster required to catalyze the condensation of 2-iminosuccinate with

dihydroxyacetone phosphate (DHAP) to produce quinolinate (Ceciliani et al., 2000; Cicchillo et al., 2005; Ollagnier-de Choudens et al., 2005). We know that the concentration of NAD(H) and NADP(H) *in vivo* remains relatively stable, and the pool is maintained by a combination of gene expression regulation, feedback inhibition, and cofactor degradation [The NAD(P) recycling and salvage pathways] (Begley et al., 2001). The expression of NadB and NadA was reported to be repressed by a DNA binding transcriptional repressor NadR (Begley et al., 2001; Tritz and Chandler, 1973). Moreover, inhibition of aspartate oxidase activity was reported by the substrate aspartate, the product 2-iminosuccinate and also NAD^+ (Mortarino et al., 1996; Seifert et al., 1990).

In this study, comprehensive engineering strategies were applied to *E. coli* K12 MG1655 to increase quinolinate production through the NAD *de novo* biosynthesis I (from aspartate) pathway. The approach included: blocking the consumption pathway, eliminating the transcriptional repression of NadA and NadB, decreasing the glucose consumption rate and increasing the availability of phosphoenolpyruvate, PEP followed by increasing the oxaloacetate, OAA pool for aspartate synthesis, and blocking the by-product acetate producing pathways, as well as improving the enzymatic efficiency by assembling NadA and NadB as an enzyme complex (Fig. 1). Finally, up to 3.7 g/L quinolinate was produced from 40 g/L glucose in shake-flask cultures of the improved strain. The results lay a foundation for further engineering of the strain for highly efficient production of quinolinate for industrial applications.

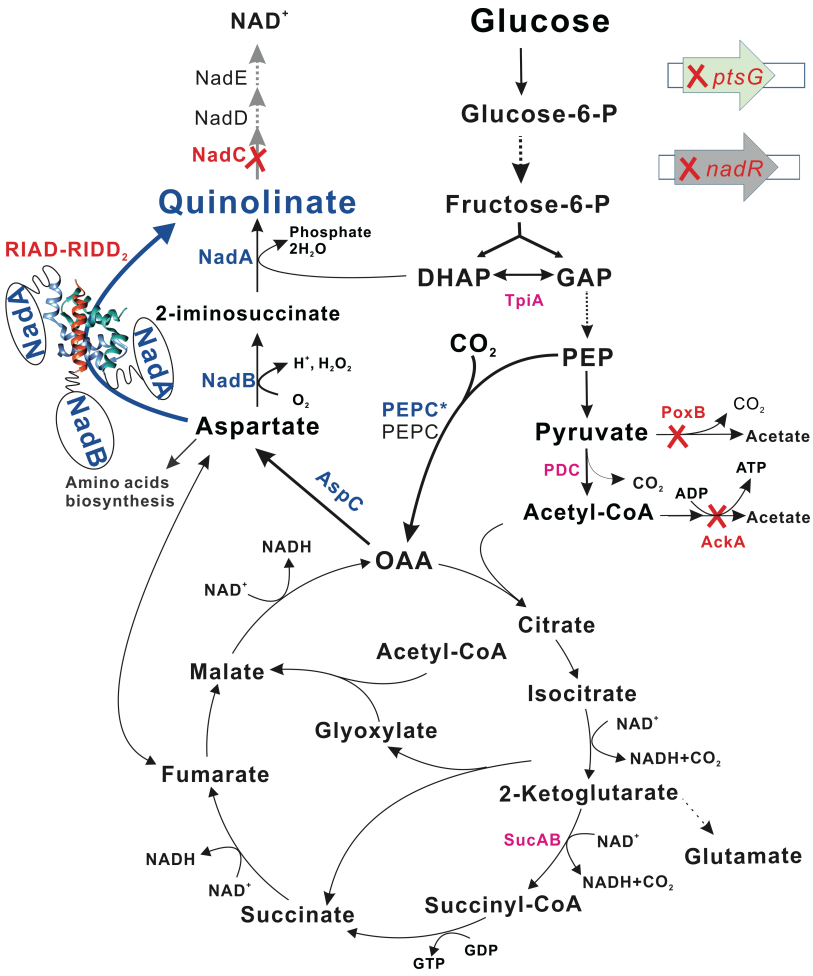

Fig. 1. Metabolic engineering of *E. coli* MG1655 for quinolinic acid production.

Quinolinic acid production was enabled by deactivation of *nadC* (to block the consumption pathway), *nadR* (to eliminate the repression of L-aspartate oxidase NadB and quinolinate synthase NadA), and *ptsG* (to slow the glucose consumption rate and achieve a more balanced metabolism, and to increase the availability of phosphoenolpyruvate). Quinolinic acid production was enhanced by increasing the oxaloacetate (OAA) pool through overexpression of phosphoenolpyruvate carboxylase (PEPC) and deactivation of the acetate-producing pathways (*poxB*, *ackA*). Quinolinic acid production was accelerated by assembling NadB and NadA as a enzyme complex with the help of peptide-peptide interaction peptides RIAD and RIDD (Carlson et al., 2006; Gold et al., 2006). PtsG: glucose specific PTS enzyme II subunit BC; NadR: DNA-

binding transcriptional repressor; DHAP: dihydroxyacetone phosphate; GAP: glyceraldehyde 3-phosphate; TpiA: triose-phosphate isomerase; PDC: pyruvate dehydrogenase complex; poxB: pyruvate oxidase; AckA, acetate kinase; SucAB: 2-oxoglutarate dehydrogenase multi-enzyme complex subunit AB; AspC: aspartate aminotransferase; NadC: quinolinate phosphoribosyltransferase; NadD: nicotinate-mononucleotide adenylyltransferase; NadE: NAD synthetase; RIAD, an 18 amino acids peptide from the A kinase-anchoring proteins; $RIDD_2$: RIDD dimer which contains 50 N-terminal residues of cAMP-dependent protein kinase for each peptide.

2. Materials and methods

2.1 Plasmids and strains

Plasmids and strains used in this study are listed in Table S1 and a brief description of the construction procedure is provided below.

The traditional digestion and ligation method was used for plasmid construction. NdeI-HindIII digested DNA fragment including lacI, pTrc promoter and multiple cloning sites (MCS) from pFZGNB16 (pTrc99a with a BglII site 193 bp upstream of the pTrc promoter) was ligated with a DNA fragment containing the kanamycin resistance gene and the origin of replication from pHL413Km (Thakker et al., 2011) to give pFZGNB33 (BglII-pTrc-MCS-Km-ori-lacI). Native genes, *nadA*, *nadB* and *aspC* were each individually amplified from *E. coli* MG1655 genomic DNA and inserted into pFZGNB33 to give pFZGNB34, pFZGNB35 and pFZGNB36, respectively. *AspC*, *nadB* and *nadA* gene fragments with ribosome binding sites (RBS) were combined in different orders to give pFZGNB37 to pFZGNB42 (Table S1). *nadA* from *Bacillus subtilis* (Bs*nadA*) was amplified from *Bacillus subtilis* CB10 with an extra DNA fragment

coding a HisTag at the C-terminal (BsnadA-HisTag) and inserted into pFZ33 to give pFZGNB43, and pTrc-*nadB* from pFZGNB35 was inserted into pFZGNB43 to give pFZGNB207. L-aspartate oxidase from *Sulfolobus tokodaii* (St*nadB*, GenBank: KC333624.1) was synthesized and sub-cloned into pTrc99a by Genscript (pTrc99a- St*nadB*). pTrc-St*nadB* was then inserted into pFZGNB34 to give pFZGNB189. The SpeI-HindIII digested pTrc-*nadB* PCR product from pFZGNB35 was inserted into XbaI-HindIII digested pFZGNB34 to give pFZGNB190. *NadB* from *Pseudomonas putida* KT2440 (Pp*nadB*) was amplified from genomic DNA and inserted into pFZGNB33 to give pFZGNB183. pTrc-Pp*nadB* from pFZGNB183 was inserted into pFZGNB34 to give pFZGNB193 (Table S1).

For NadA-NadB fusion protein constructions, DNA fragments encoding peptide linkers $(GS)_3$, $(GS)_6$ and $(G_4S)_2$ were introduced at the end of *nadA* or *nadB* without stop codon through PCR and combined with *nadB* or *nadA* to give pFZGNB153 to pFZGNB157 (Table S1). DNA fragments encoding peptides RIAD and RIDD with a linker $(G_4S)_2G_4CG$ were codon-optimized and synthesized by Synbio Technologies (Table S2). Overlap Extension PCR (OE-PCR) was then applied to combine the peptide encoding DNA fragment with *nadA* or *nadB* to give pFZGNB228 to pFZGNB231. pTrc-nadB-RIAD from pFZGNB229 and pTrc-RIAD-nadB from pFZGNB230 were inserted into pFZ228 and pFZGNB231 individually to give pFZGNB232 to pFZGNB235, respectively (Table S1).

N_{20} of pTargetF (Jiang et al., 2015) was replaced by a *ptsG* specific N_{20} (GTATCCGTACTGCCTATCGC) through inverse PCR to give pFZGNB44. The upstream and downstream homologous arms of *ptsG* were amplified from *E. coli* MG1655 genomic DNA and inserted between the EcoRI and HindIII sites of pFZGNB44 with an XbaI site between the two homologous arms to give pFZGNB46, which can be used for *ptsG* deletion. The same method

was used to construct plasmids pFZGNB63, pFZGNB65, pFZGNB74, pFZGNB75 and pFZGNB76 for deactivation of *tpiA, sucAB, lpd, ackA,* and *pta-ackA*. pTrc-pepc was amplified from pKK313 (Wang et al., 1992) and inserted into pFZGNB46, pFZGNB75, and pFZGNB76 to give pFZGNB50, pFZGNB117, and pFZGNB118, which can be used to replace *ptsG, ackA, pta-ackA* with pTrc-*pepc* fragment individually (Table S1).

E. coli K12 MG1655 was used as the parent strain in this study. Genes *nadC* and *nadR* were deleted using the lambda red recombination method (Datsenko and Wanner, 2000), and the CRISPR/Cas9 method was employed for deletion/replacement of the other selected genes (Jiang et al., 2015).

2.2 Fermentation of quinolinic acid from glucose

Freshly transformed strains were used for every batch fermentation. Ten single colonies were inoculated into 5 mL LB or quinolinic acid-producing medium with 50 mg/L kanamycin and cultured at 37 ^{o}C to form the inoculum seed culture. Fermentation was performed in 250-mL conical flasks that contain 1.5 g $CaCO_3$. Fifty milliliters of quinolinic acid-producing medium supplemented with 50 mg/L kanamycin was added into each flask, and IPTG was added to a final concentration of 0.1 mM for induction. One percent of an overnight cell culture was inoculated into the fermentation medium. The cells were grown at 37 ^{o}C with shaking at 350 rpm unless otherwise stated. A sample of 1-mL of culture broth was withdrawn at designated intervals for product and metabolite analysis by HPLC. The previous reported medium (Kim et al., 2016) with a higher concentration of Fe^{2+}, Mn^{2+}, and Zn^{2+} (increased from 5 mg/L to 10 mg/L) was used for fermentation. This culture media contains 70 g/L of glucose, 17 g/L of $(NH_4)_2SO_4$, 1 g/L of KH_2PO_4, 0.5 g/L of $MgSO_4 \cdot 7\ H_2O$, 2 g/L of yeast extract, 150 mg/L of methionine, 10 mg/L of $FeSO_4 \cdot 7H_2O$, 10 mg/L of $MnSO_4 \cdot 8H_2O$, and 10 mg/L of $ZnSO_4$, unless

otherwise specified.

2.3 SDS-PAGE analysis of soluble protein

To check the protein expression level of the targeted proteins, cells from 3mL cell culture was harvested and stocked at -80 ^{o}C until further analysis. The cells were melted on ice and suspended in 0.8 mL of 50 mM Tris-Cl (pH 8.0), and 0.6 g glass beads was added. The cells were disrupted by disruptor Genie (2500 rpm) for 3 mins. Lysed cells were then centrifuged at 13,000 rpm for 10 mins and the supernatants were used for SDS-PAGE analysis.

2.4 Analytical methods

For analyzing the fermentation products and residual sugars and other metabolites, the samples were centrifuged at 13,000× g for 2 min and then the supernatant was filtered through a 0.2 μm syringe filter. The glucose, acetate, and quinolinate were quantified using the same method as previously described (Zhu et al., 2018). In brief, an HPLC system was equipped with a cation-exchange column Aminex HPX-87H (Bio-Rad, USA) and a differential refractive index detector RID-10A (Shimadzu, Japan) and UV detector at 210 nm. 2.5 mM H_2SO_4 served as the mobile phase running at 0.5 mL/min, and the column temperature was maintained at 55 ^{o}C. Authentic quinolinic acid (Sigma, St. Louis, MO) was used to generate a standard curve from 10 mg/L to 5 g/L, less than 10 mg/L is considered as not detectable (nd) under tested conditions.

3. Results and discussion

3.1 Engineering of *E. coli* MG1655 for quinolinic acid production.

Quinolinic acid is an intermediate of the NAD^+ *de novo* biosynthetic pathway under aerobic conditions (Fig. 1). The gene *nadC* of MG1655 was disrupted to block the consumption pathway and allow strain FZ700 to accumulate quinolinic acid. To increase expression of the NAD^+

biosynthetic genes, the DNA-binding transcriptional repressor *nadR* (of *nadA* and *nadB*) was deactivated in FZ700 to give FZ703. Plasmid pFZGNB42 (pTrc-*aspC*-*nadB*-*nadA*) was introduced into the engineered strains to check their performance. The quinolinic acid accumulated in parent strain *E. coli* MG1655 is less than 43 mg/L under tested conditions, which is likely due to it being further converted to NAD^+. 138 mg/L of quinolinic acid was accumulated in FZ700, and QA titer goes up to 544 mg/L in FZ703.

In experiments we noticed more than 37 g/L acetate was accumulated in these strains, which was a really high level of byproduct from the feedstock, glucose. Deactivation of the glucose specific transporter, PtsG, was reported to be able to reduce acetate secretion significantly by slowing the glucose consumption rate which results in a more balanced and efficient metabolism (De Anda et al., 2006; Gosset, 2005; Wong et al., 2008), and also more PEP can be conserved and available for other metabolic pathways by decoupling glucose transport from PEP-dependent phosphorylation (Chatterjee et al., 2001; Gosset, 2005; Liang et al., 2015; Lin et al., 2005). Moreover, the *E. coli* EMP pathway was reported to potentially form an entire substrate channeling module that prevent PEP from being used by other pathways (Shearer et al., 2005). PtsG is thought to be the anchoring point of the EMP channeling and disrupting it will weaken the EMP channeling and improve the efficiency of the engineered pathway to hijack intermediate metabolites from the native pathway (Abernathy, 2019). So, the glucose specific transporter PtsG was deactivated in FZ703 to give FZ723. Meanwhile, the S8D mutant of sorghum phosphoenolpyruvate carboxylase (PEPC) (Wang et al., 1992) was also introduced to increase the OAA pool. This modification was accomplished by the replacement of *ptsG* with pTrc-*pepc* fragment in FZ703 to give FZ734 (Table S1). After 1-day fermentation, up to 450 mg/L quinolinic acid was accumulated in FZ703, while only 283mg/L and 360 mg/L quinolinic acid

were produced in FZ723 and FZ734, respectively. After 3-day fermentation, strains FZ723 and FZ734 attained a comparable performance to strain FZ703. Finally, 627 mg/L and 740 mg/L quinolinic acid were accumulated in FZ723 and FZ734 respectively after a 7-day fermentation period, while, only 544 mg/L quinolinic acid accumulated in FZ703 (Table 1).However, a very high concentration of acetate still accumulated in FZ734 (Table S2). The experiment clearly indicates that blocking the consumption pathway is necessary for quinolinic acid production, and deactivation of PtsG and introducing PEPC are helpful for quinolinic acid production. Strain FZ734 was used for further experiments.

Table 1 Quinolinate production in engineered strains

	MG1655	FZ700	FZ703	FZ723	FZ734
1 day	40.2 ± 1.6	97.1 ± 13.6	449.7 ± 24.3	282.6 ± 16.0	360.2 ± 29.2
3 day	42.8 ± 3.5	138.2 ± 8.3	488.5 ± 23.4	500.8 ± 28.5	594.5 ± 13.7
5 day	36.9 ± 1.8	133.8 ± 7.5	503.8 ± 26.4	544.0 ± 31.2	644.9 ± 16.4
7 day	36.8 ± 2.1	135.4 ± 6.9	544.4 ± 20.4	627.3 ± 31.6	739.7 ± 16.9
nadC	+	-	-	-	-
nadR	+	+	-	-	-
ptsG	+	+	+	-	-
pTrc-*pepc*	-	-	-	-	+

Plasmid pFZGNB42 (pTrc-*aspC*-*nadB*-*nadA*) was introduced into the tested strains to examine their performance, aerobic cultures were performed at 37 ^{o}C, 350 rpm. The numbers indicate quinolinate concentration (mg/L, average of three replicates with error bars indicating standard deviation).

3.2 Effect of varying the gene order of *aspC*, *nadB,* and *nadA* in expression constructs on quinolinic acid production

Plasmids containing the three genes for quinolinic acid production from OAA in different arrangements were constructed to give plasmids pFZGNB37 to pFZGNB42 (Fig. 2) and their

performance on quinolinic acid production in the host FZ734 was evaluated. After 4 days of fermentation, more than 48 g/L of glucose was consumed in all tested strains. The culture of the strain where only *aspC* was overexpressed produced the lowest quinolinic acid titer (123 mg/L) compared to the results observed when *nadA* or *nadB* was overexpressed (Fig. 2). When all three genes were co-overexpressed in different gene orders on a plasmid, the quinolinic acid production was slightly improved with plasmid pFZGNB37 (pTrc-*nadA*-*nadB*-*aspC*), and the quinolinic acid titer increased to 404 mg/L with plasmid pFZGNB42 (pTrc-*aspC*-*nadB*-*nadA*). Unexpectedly, a higher quinolinic acid titer was observed in the strain bearing plasmid pFZGNB190, which only overexpressed *nadA* and *nadB* under control of two individual pTrc promoters (pTrc-*nadA*-pTrc-*nadB*, Table S1), where 667 mg/L quinolinic acid was accumulated (Fig. 2). This experiment suggested the level of AspC expressed from the native gene is already enough for these tested conditions.

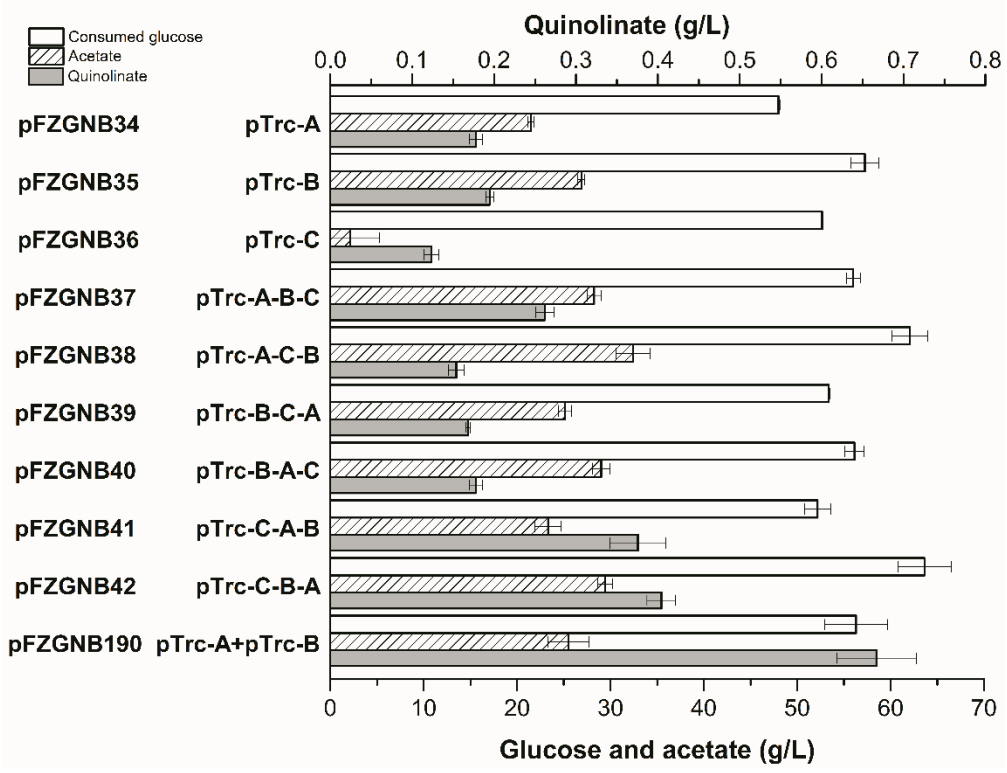

Fig. 2. Quinolinic acid production in FZ734 harboring plasmids containing various gene

orders of *aspC*, *nadB,* and *nadA*. Aerobic cultures were performed at 37 ^{o}C, 350 rpm for 4 days. Values are the average of three replicates with error bars indicating standard deviation. A, B, and C indicate *nadA*, *nadB*, and *aspC* accordingly.

3.3 Examination of variants of *nadA* and *nadB* failed to improve quinolinate production

Although FZ734 with plasmid pFZGNB190 (pTrc-nadA+ pTrc-nadB) showed the best performance as described above in section 3.2, it was reported that protein NadB displays a substrate inactivation and its activity can be inhibited by substrate aspartate and NAD, which act as competitive inhibitors (Seifert et al., 1990). NadA was also reported to form inclusion bodies when it is overproduced (Ceciliani et al., 2000), which could diminish its *in vivo* activity. Screening enzymes from diverse sources has been used as an effective strategy to increase the productivity of heterologous pathways in specific hosts. So, some NadA and NadB variants from other species were employed and tested in FZ734 for comparison.

It was reported that the activity of NadB from *Pseudomonas putida* KT2440 (Pp*nadB*) was not inhibited by aspartate when the concentration of aspartate is less than 50 mM. And the K_m, k_{cat} value of this enzyme was determined to be 2.26 mM, 10.6 s^{-1} against L-aspartate (Leese et al., 2013). NadB from *Sulfolobus tokodaii* (StNadB) was also reported to be less sensitive to NAD^+ since it can bind the FAD cofactor tightly with a different structure (Bifulco et al., 2013; Sakuraba et al., 2008); moreover, it displays some other distinctive features, e.g., stable activity over a wide range of pH (from 7 to 10), and high thermostability (with a Tm higher than 79 ^{o}C), which would make it attractive for biotechnological applications. However, evaluation of constructs expressing these alternative genes under the same conditions described in Figure 2 revealed no improvement in quinolinic acid production (Fig. 3). This may be due to the poor

protein expression of these NadB variants (Fig. S1), especially StNadB comes from an extremophile. Another possible reason is these enzymes having a lower affinity for aspartate, the K_m value for L-aspartate of StNadB and PpNadB is 1.3 and 2.26 mM as reported (Bifulco et al., 2013; Leese et al., 2013), which is much higher than the K_m value of *E. coli* NadB (0.048 mM).

The gene encoding NadA from *Bacillus subtilis* (BsNadA) had been successfully overexpressed with a His_6 tag at its C-terminal (BsNadA-HisTag) in *E. coli* with a yield of 10 mg pure protein from 1 L culture (Marinoni et al., 2008). Unexpectedly, only 215 mg/L quinolinic acid was produced when the native *nadA* in pFZGNB190 was replaced with Bs*nadA*-HisTag (Fig. 3) as no improvement on protein expression was observed in the tested conditions (Fig. S1) and low activity of the BsNadA-HisTag enzyme was reported previously (Marinoni et al., 2008).

Unfortunately, the performance of these strains with different NadA and NadB variants is not as good as the native *E. coli* enzymes NadA and NadB under the tested conditions in FZ734 (Fig. 3). The native *aspC* was also introduced into pFZGNB190 to give pFZGNB204; however, less quinolinic acid was accumulated in the strain with pFZGNB204 (Fig. 3), possibly due to the substrate inactivation of NadB, potentially caused by the overexpression of AspC.

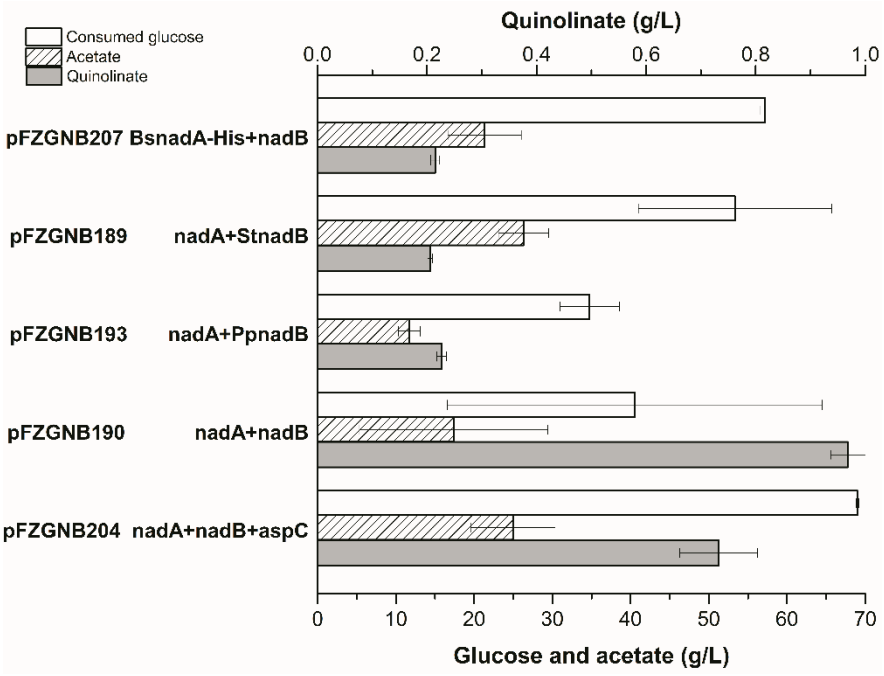

Fig. 3. The effect of nadA and nadB variants on quinolinic acid production in FZ734. Aerobic cultures were performed at 37 °C, 350 rpm for 4 days. Proteins were overproduced under the control of pTrc promoter in pFZGNB33. Values are the average of three replicates with error bars indicating standard deviation. BsnadA-HisTag indicates *nadA* from *Bacillus subtilis* with a His_6-Tag at the C-terminal, StnadB indicates *nadB* from *Sulfolobus tokodaii*, and PpnadB indicates *nadB* from *Pseudomonas putida* KT2440.

3.4 Engineering of FZ734F to improve quinolinic acid production

Several manipulations were explored to enhance the carbon flux to quinolinate production, including increasing the substrate availability, downregulating the TCA cycle, and blocking the by-product acetate production. DHAP can be condensed with 2-iminosuccinate by NadA to form quinolinate with a K_M of 0.74 mM (Reichmann et al., 2015), while it is reported that wild type *E. coli* strains normally only have 0.37 mM DHAP (Bennett et al., 2009) so this possibility to enhance the level of DHAP was tested. Triosephosphate isomerase (TpiA), which catalyzes the

317 isomerization between glyceraldehyde 3-phosphate and dihydroxyacetone phosphate (DHAP),
318 was deactivated to reserve DHAP for quinolinate biosynthesis. Meanwhile, we considered that
319 the low yield of quinolinate may be due to too much carbon going through the TCA cycle, so
320 *sucAB* and *lpd* were deactivated to down-regulate the carbon flux through TCA cycle. SucA and
321 SucB are two subunits of the 2-oxoglutarate dehydrogenase multi-enzyme complex (OGDHC)
322 that catalyzes the conversion of 2-oxoglutarate (2-ketoglutarate) to succinyl-CoA and CO_2.
323 Deactivation of *sucAB* could accumulate 2-oxoglutarate, which can be used for glutamate
324 synthesis and will be beneficial for aspartate synthesis. Lipoamide dehydrogenase (Lpd) is the
325 E3 component of three multicomponent enzyme complexes: pyruvate dehydrogenase, 2-
326 oxoglutarate dehydrogenase complex, and the glycine cleavage system (Guest and Creaghan,
327 1972; Pettit and Reed, 1967; Steiert et al., 1990). Deactivation of *lpd* was reported to produce
328 more pyruvate and L-glutamate under aerobic conditions (Li et al., 2006), as it affects the
329 function of pyruvate dehydrogenase and the 2-oxoglutarate dehydrogenase complex. However,
330 the FZ738 (FZ734 *ΔtpiA*) or FZ742 (FZ734 *Δlpd*) strain displayed very poor cell growth and
331 failed to produce quinolinate (Fig. 4). Although the *sucAB*$^-$ strain can grow, unfortunately, it also
332 failed to accumulate quinolinate. This may be due to the quinolinate production being an ATP
333 consuming process, and it requires a high level of ATP generated through the TCA cycle or other
334 ATP producing pathway.

335 More than 20 g/L acetate accumulated in nearly in all tested strains, which may inhibit the
336 cell growth and waste the substrate glucose, so the acetate producing pathways were selected as
337 the next target for genetic modification. There are two predominant acetate producing pathways
338 active aerobically in *E. coli*, they are the pyruvate oxidase (PoxB) and acetate
339 kinase/phosphotransacetylase (AckA-Pta) pathways. Pyruvate oxidase (PoxB) is a peripheral

membrane enzyme that catalyzes the oxidative decarboxylation of pyruvate to form acetate and mainly functions at stationary phase, whereas the AckA-Pta catalyzed pathway, which mainly functions during the exponential phase, converts acetyl-CoA to acetate (Dittrich et al., 2005). When the fermentation was performed with strains harboring plasmid pFZGNB190, no difference was observed on acetate accumulation when only the PoxB was deactivated, while much less acetate was accumulated when both PoxB and AckA were deactivated (Fig. 4). However, there is 13% decrease in quinolinate titer in FZ757/pFZGNB190 due to 40% less glucose being consumed. Since this strain has two acetate producing pathways deactivated, compared with FZ734/pFZGNB190 (Fig. 4), it has a less ability to consume glucose rapidly. Interestingly, improvement was observed when an extra copy of pTrc-*pepc* was introduced into FZ757 (FZ734 *ΔpoxB*, *ΔackA*) forming strain FZ763/pFZGNB190 (Table S1). The resulting strain yielded a 24.4% increase in quinolinic acid formation compared to FZ734/pFZGNB190, with up to 1.4 g/L (32.3 mg/g consumed glucose) being accumulated while consuming 42 g/L glucose (Fig. 4), it's also worth noticing that more than 5.6 g/L acetate accumulated in FZ763/pFZGNB190 in 4-day fermentation (Fig. 4). We also examined the addition of extra aspartate and when 5 g/L aspartate was added into the fermentation broth with strain FZ763/pFZGNB190, the quinolinate titer dropped to 1.1 g/L. The decrease is consistent with the result mentioned in section 3.3 (Fig. 3) that showed quinolinate titer dropped when AspC was overproduced, indicating an imbalance in the synthesis and utilization of this intermediate, which may be due to the substrate inhibition of NadB by a high concentration of aspartate. It also indicates that the flux from aspartate to quinolinic acid is the limiting step for quinolinic acid production in our tested system.

Based on the strains' performance, the strain FZ763/pFZGNB190 was further evaluated with

lower glucose concentration (40 g/L). Interestingly, strain FZ763/pFZGNB190 fermented with 40 g/L glucose has a higher quinolinate productivity based on 2-day samples, while the strain has comparable quinolinate titer after a 4-day fermentation (Fig. S2). This result may be due to the fermentation with 40 g/L glucose receiving much less metabolic stress and would be more suitable for chemicals production as the yield per glucose would be higher than in the 70 g/L cultures.

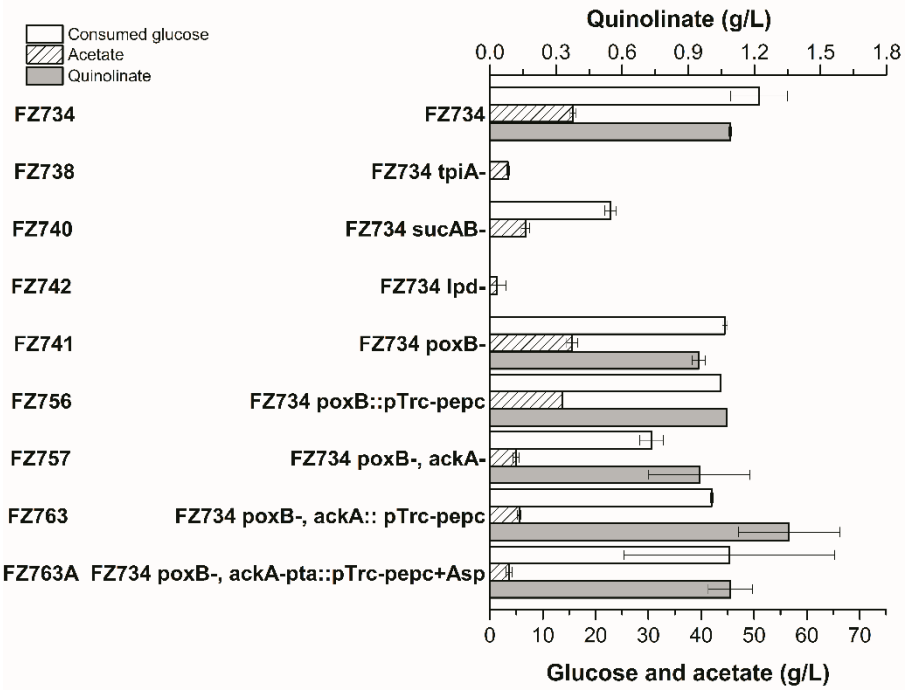

Fig. 4. Quinolinic acid production in engineered strains harboring plasmid pFZGNB190. Aerobic cultures were performed at 37 ºC, 350 rpm for 4 days. FZ763A indicates 5 g/L aspartate was added into the fermentation broth (+Asp). Values are the average of three replicates with error bars indicating standard deviation.

3.5 Improvement of quinolinate production by assembling NadA and NadB as an enzyme complex.

The flux from aspartate to quinolinic acid has been demonstrated to be a rate-limiting factor for quinolinic acid production above by the results of experiments on overexpression of

individual/combination of genes encoding AspC, NadB, and NadA (Fig. 2 and Fig. 3) and feeding extra aspartate (Fig. 4). Further increasing the flux of these steps is highly desired for quinolinic acid production; moreover, it was reported that the intermediate 2-iminosuccinate is unstable (Nasu et al., 1982), both of which brings a synthetic multiple-enzyme complex into our mind. Synthetic multi-enzyme complexes have been developed to control the flux of metabolites and to improve product yield (Conrado et al., 2008; Quin et al., 2017), not only because it improves local substrate concentration and reaction equilibrium but also prevents loss of reaction intermediates from competing pathways by diffusion, protects cells from unstable/toxic intermediates, and increases local enzyme concentration (Abernathy et al., 2017; Obata, 2020; Wheeldon et al., 2016). All these features are potentially helpful for quinolinic acid production in our system. Also, NadA easily forms an inclusion body as another complication (low protein concentration), and 2-iminosuccinate is unstable (Ceciliani et al., 2000, Nasu et al., 1982), so a synthetic multi-enzyme complex was investigated in this study.

Using a fusion protein is one of the developed strategies to form synthetic multi-enzyme complexes. Such fusions can be easily constructed by genetically fusing two or more protein domains with a peptide linker, and it is also often useful to improve the solubility of recombinant proteins. While, no improvement was observed when NadA and NadB were fused with linkers $(GS)_3$, $(GS)_6$, or $(G_4S)_2$ (Fig. S3), the performance of NadA-$(GS)_6$-NadB (FZ763/pFZGNB157) was comparable with the performance of the host-plasmid bearing separate proteins (FZ763/pFZGNB190). Possible complications could be due to the linker not being optimized, or the expression of the large fusion protein being worse than the expression of the separate proteins (Fig. S4). It also may be due to the fusion not being easily able to account for the dimer, monomer situation, and such complexes may generate an aggregate or inefficient complex as the

dimeric structure is necessary for the stability of NadA (Ollagnier-de Choudens et al., 2005).

Synthetic multi-enzyme complexes can also be constructed by assembling the enzymes with a protein/peptide scaffold based on protein-protein/peptide interaction or even peptide-peptide interaction (Conrado et al., 2008; Quin et al., 2017). A dock-and-lock peptide interacting family of peptides RIAD and RIDD have been successfully applied for lycopene overproduction (Kang et al., 2019). RIAD, an 18 amino acid peptide which is from the A kinase-anchoring proteins, specifically binds to the RIDD dimer, which contains the first 50 N-terminal residues of cAMP-dependent protein kinase. Their small size, strong binding affinity, and fixed 1:2 binding stoichiometry ratio make them a suitable pair of protein tags for multi-enzyme assembly (Kang et al., 2019). So, NadB and NadA were then assembled as an enzyme complex by adding peptides RIAD and RIDD in this study. DNA fragments encoding peptides RIAD and RIDD with a linker $(G_4S)_2G_4CG$ were codon-optimized and synthesized by Synbio Technologies and incorporated in plasmids for study (Table S3). NadA appears as a dimeric protein and the dimeric structure is essential for its stability (Ollagnier-de Choudens et al., 2005), while NadB is a monomeric protein (Mattevi et al., 1999), so RIDD was combined with *nadA* and RIAD was combined with *nadB* both at N-terminal and C-terminal by Overlap Extension PCR (OE-PCR) to give pFZGNB228 to pFZGNB231. pTrc-nadB-RIAD from pFZGNB229, and pTrc-RIAD-nadB from pFZGNB230 was inserted into pFZ228 and pFZGNB231 individually to give pFZGNB232 to pFZGNB235 (Table S1). Since no significant improvement was observed in quinolinate titer when 70 g/L glucose was used compared to 40 g/L glucose, the strains were evaluated in QA producing medium with 40 g/L glucose. The strain FZ763/pFZGNB233 [RIDD-NadA (RIDD added at the N-terminal of NadA with a $G_4SG_4SG_4CG$ linker) with RIAD-NadB] displayed poor cell growth after two days fermentation, no quinolinate was observed (Fig. 5a), and nearly no

glucose was consumed (Fig. 5b). Although comparable biomass was obtained after 4 days of fermentation (cell density was not measured due to the present of $CaCO_3$), it only produced 0.7 g/L quinolinate, which is 31% less than produced in FZ763/pFZGNB190 (1.0 g/L, Fig. 5a). The other strains all exhibited better performance than FZ763/pFZGNB190 (Fig. 5). After 2 days fermentation, FZ763/pFZGNB190 had already consumed all glucose, but only produced 1.0 g/L quinolinate (25 mg/g consumed glucose, 20.8 mg/L/h). Strain FZ763/pFZGNB232 (RIDD-NadA with NadB-RIAD) shows the highest quinolinate titer (2.8 g/L) due to more glucose was consumed (37.9 g/L) than other strains (except FZ763/pFZGNB190), with a productivity of 58.3 mg/L/h which is 35 times faster than the parent strain MG1655/pFZGNB42 (Fig. 5 and Table 1). Strain FZ763/pFZGNB234 (NadA-RIDD with NadB-RIAD) produced 2.6 g/L quinolinate from 29 g/L glucose with a yield of 89.7 mg/g, and with less acetate being accumulated (Fig. 5c). 37.4 g/L glucose was consumed in FZ763/pFZGNB235 (NadA-RIDD with RIAD-NadB), and 2.4 g/L quinolinate was accumulated. After 4 days of fermentation, no significant improvement was observed in strains FZ763/pFZGNB190, FZ763/pFZGNB232 and FZ763/pFZGNB235, however most of the glucose was consumed within 2 days (Fig. 5a and 5b). Quinolinate titer in strain FZ763/pFZGNB234 was further increased to 3.7 g/L upon consuming the residual glucose with a yield of 92.5 mg/g. This result is 3.6-fold higher than FZ763/pFZGNB190 (Fig. 5) and more than 86.8 times higher than the parent strain MG1655/pFZGNB42 (Table 1 and Fig. 5a). The higher yield was achieved as less acetate was accumulated in these strains, except for strain FZ763/pFZGNB233, compared to strain FZ763/pFZGNB190 (Fig. 5c), which indicates a more balanced metabolism was achieved. The highest yield (92.5 mg/g) we achieved in FZ763/pFZGNB234 is 3.6-fold higher than FZ763/pFZGNB190 and 151-fold higher than the parent strain MG1655/pFZGNB42 (Table 1 and Fig. 5a). Similar amounts of protein complexes

were observed through a non-reducing SDS-PAGE analysis (Fig. S5), except in FZ763/pFZGNB233. The strains were also tested in QA producing medium with 70 g/L glucose as a carbon source, and no improvement on quinolinate titer was observed among most tested strains (Fig. S6). By testing the NadA-NadB protein complex in different arrangements, it clearly shows that the activity and complex formation would depend on the position and orientation of the peptide complexes. The strains with NadA-RIDD had better performance than the strains with RIDD-NadA (Fig. 5), which is consistent with the performance of fusion proteins made in this work where NadA has been linked at the C-terminal end, such as NadA-$(GS)_6$-NadB (Fig. S3). This may be due to the C-terminal end of the NadA being closer to the active site and more flexible than N-terminal based on the available crystal structures of NadA from other species (PDB number: 4ZK6, 4P3X and 4HHE) (Cherrier et al., 2014; Esakova et al., 2016; Soriano et al., 2013), which have a similarity of greater than 55% to *E. coli* NadA, as the crystal structure of the *E. coli* native NadA is not available yet. The strains with NadB-RIAD also has better performance than the strains with RIAD-NadB (Fig. 5), which may be because the N-terminal end of NadB is the cofactor FAD-binding domain (Bossi et al., 2002), and adding a RIAD-tag to the N-terminal end affected the cofactor binding efficiency. Moreover, when the peptides were added to the N-terminal of NadA and NadB (RIDD-NadA with RIAD-NadB), the strain has the lowest quinolinate titer, which suggests it formed an non-preferred enzyme complex, perhaps inactive, and leads to a metabolic burden. In contrast, the combination with the peptides added to the C-terminal ends (NadA-RIDD with NadB-RIAD) has the highest quinolinate titer, which suggests a preferred enzyme complex being formed and stabilized in this configuration, providing an efficient and exclusive catalytic reaction series with little free diffusion of the unstable intermediate, 2-iminosuccinate (Nasu et al., 1982). Another possible reason is the

RIDD: RIAD complex has a ratio of 2:1 (Kang et al., 2019), which is beneficial for NadA dimer formation and good for its activity and stability. Notably, the turnover frequency of *E. coli* NadB is only 0.267 s^{-1} (Tedeschi et al., 2010), which may limit the enzyme complex catalytic efficiency.

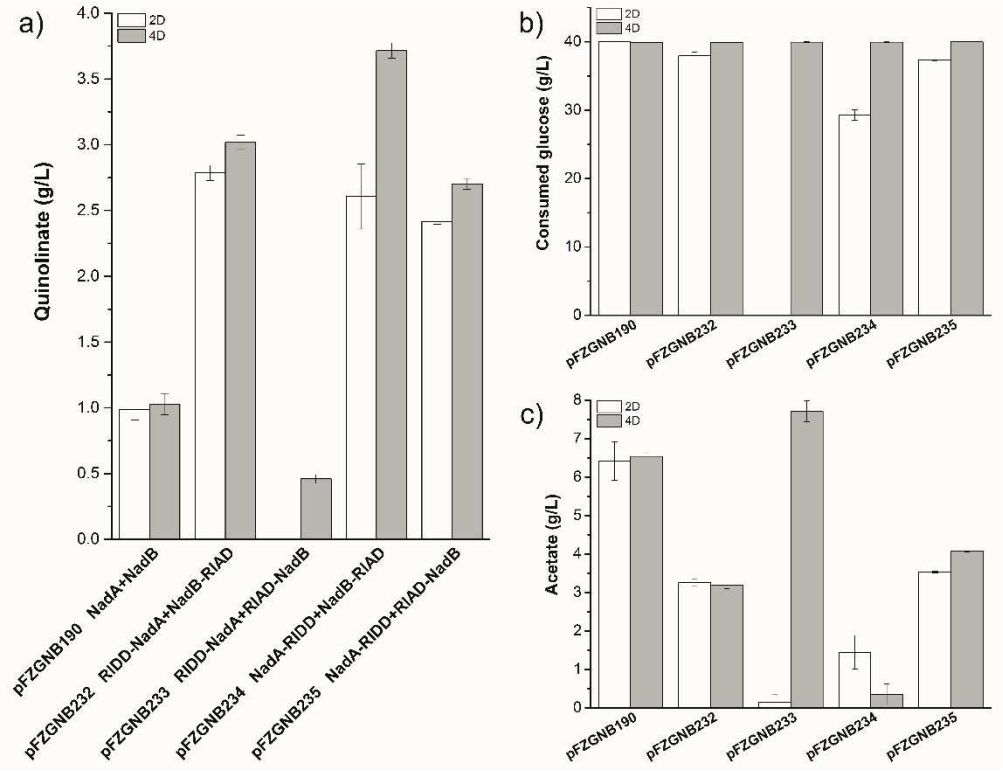

Fig. 5. The effect of NadA-NadB enzyme complex on quinolinic acid production in FZ763 with 40 g/L glucose. a) quinolinate titer, b) consumed glucose, c) accumulated acetate. Aerobic cultures were performed at 37 ºC, 350 rpm, sampled at 2 days (2D) and 4 days (4D). NadA-RIDD and NadB-RIAD fusion proteins were over-expressed under the control of their pTrc promoter in pFZGNB227, NadA-NadB enzyme complex was assembled with the help of peptides, RIAD and RIDD. Values are the average of three replicates with error bars indicating standard deviation.

In conclusion, multiple engineering strategies were applied to increase the production of quinolinate. The quinolinate consumption pathway was blocked to enable the production of

quinolinate by deactivation of NadC, and quinolinate production was activated by knockout the repressor gene *nadR*. Then, quinolinate production was enhanced by deactivation of glucose transporter gene *ptsG* to slow the glucose consumption rate, to achieve a more balanced metabolism, and to improve the availability of PEP. Increasing the OAA pool through overexpression of PEPC also improved quinolinate production. Moreover, the acetate-producing pathways were deactivated as acetate is a major by-product in the engineered strain FZ734/pFZGNB190. Finally, quinolinate production was accelerated by assembling NadA and NadB as an enzyme complex with the help of peptide-peptide interaction peptides, RIAD and RIDD, and up to 3.7 g/L quinolinate was accumulated in FZ763/pFZGNB234 in shake-flask cultures. These results lay a foundation for further engineering of the strains to efficiently produce quinolinic acid or even nicotinic acid for industrial applications. However, the highest yield we achieved is only 92.5 mg/g, which need to be further improved. Crystal-structural studies of the constructed protein complexes via isolation and crystallography could be employed, which would give us a better understanding of these results and lead to further optimization of the system. Further improvement may be achieved by protein engineering of NadB to eliminate the feedback inhibition and improve the enzymatic activity. Other potential enhancements may be attained through improving the expression of NadA, down-regulating the TCA cycle, optimizing the NadA-NadB enzyme complex, and assembling AspC, NadB, and NadA into a larger enzyme complex to allow more aspartate to more efficiently enter the reactions for quinolinate production.

There has been much attention to improve the efficiency of metabolic reactions through enzyme co-localization and compartmentalization. In this study, we not only built the synthetic enzyme complex (NadA-RIDD and NadB-RIAD enzyme complex) to improve quinolinate

production, but also disrupted the potential native EMP channeling by deleting ptsG to release the intermediate PEP for quinolinate production. This disrupt-build strategy for metabolon engineering may be beneficial for future engineering of *in vivo* biocatalysis.

Conflicts of interest

The authors declare no competing financial interests.

Acknowledgment

The authors thank Dr. Charles Stewart, Department of Biosciences at Rice University, for kindly sharing *Bacillus subtilis* CB10 with us, the authors thank Dr. Guoqiang Zhang at Jiangnan University (Wuxi, China) for helpful suggestions about fusion protein constructs, and Dr. Shuai Qian at Solugen (Houston, TX) for his help on protein structure analysis. This work was supported by NSF DBI-1262491, NSF EAGER: DESYN-C3 CBET-1843556, and DOE BES DE-SC0014462. M. P. was supported by a training fellowship from the Gulf Coast Consortia (NLM Grant T15 LM007093).

References

Abernathy, M. H., et al., 2017. Channeling in native microbial pathways: implications and challenges for metabolic engineering. Biotechnol. adv. 35, 805-814.

Abernathy, M. H., et al., 2019. Comparative studies of glycolytic pathways and channeling under in vitro and in vivo modes. AIChE J. 65, 483-490.

Andreoli, A. J., Ikeda, M., Nishizuka, Y., Hayaishi, O., 1963. Quinolinic acid: a precursor to nicotinamide adenine dinucleotide in Escherichia coli. Biochem. Biophys. Res. Commun. 12**,** 92.

Andrushkevich, T. V., Ovchinnikova, E. V., 2012. Gas Phase Catalytic Oxidation of β-Picoline to Nicotinic Acid: Catalysts, Mechanism and Reaction Kinetics. Catal. Rev. 54**,** 399-436.

Becker, J., Zelder, O., Häfner, S., Schröder, H., Wittmann, C., 2011. From zero to hero—design-based systems metabolic engineering of Corynebacterium glutamicum for l-lysine production. Metab. Eng. 13**,** 159-168.

Begley, T. P., Kinsland, C., Mehl, R. A., Osterman, A., Dorrestein, P., 2001. The biosynthesis of nicotinamide adenine dinucleotides in bacteria. Vitam. Horm. 61**,** 103-119.

Bennett, B. D., Kimball, E. H., Gao, M., Osterhout, R., Van Dien, S. J., Rabinowitz, J. D., 2009. Absolute metabolite concentrations and implied enzyme active site occupancy in Escherichia coli. Nat. Chem. Biol. 5, 593.

Bifulco, D., Pollegioni, L., Tessaro, D., Servi, S., Molla, G., 2013. A thermostable L-aspartate oxidase: a new tool for biotechnological applications. Appl. Microbiol. Biotechnol. 97**,** 7285-7295.

Bossi, R. T., et al., 2002. Structure of FAD-bound L-aspartate oxidase: insight into substrate specificity and catalysis. Biochemistry. 41, 3018-3024.

Carlson, C. R., Lygren, B., Berge, T., Hoshi, N., Wong, W., Taskén, K., Scott, J. D., 2006. Delineation of type I protein kinase A-selective signaling events using an RI anchoring disruptor. J. Biol. Chem. 281**,** 21535-21545.

Ceciliani, F., Caramori, T., Ronchi, S., Tedeschi, G., Mortarino, M., Galizzi, A., 2000. Cloning, overexpression, and purification of Escherichia coli quinolinate synthetase. Protein Expr. Purif. 18**,** 64-70.

Chandler, J. L., Gholson, R., 1972. De novo biosynthesis of nicotinamide adenine dinucleotide in Escherichia coli: excretion of quinolinic acid by mutants lacking quinolinate phosphoribosyl transferase. J. Bacteriol. 111**,** 98-102.

Chatterjee, R., Millard, C. S., Champion, K., Clark, D. P., Donnelly, M. I., 2001. Mutation of the ptsG gene results in increased production of succinate in fermentation of glucose byEscherichia coli. Appl. Environ. Microbiol. 67**,** 148-154.

Cherrier, M. V., et al., 2014. The crystal structure of Fe4S4 quinolinate synthase unravels an enzymatic dehydration mechanism that uses tyrosine and a hydrolase-type triad. J. Am. Chem. Soc. 136, 5253-5256.

Cicchillo, R. M., Tu, L., Stromberg, J. A., Hoffart, L. M., Krebs, C., Booker, S. J., 2005. Escherichia coli quinolinate synthetase does indeed harbor a [4Fe-4S] cluster. J. Am. Chem. Soc. 127**,** 7310-7311.

Conrado, R. J., Varner, J. D., DeLisa, M. P., 2008. Engineering the spatial organization of metabolic enzymes: mimicking nature's synergy. Curr. Opin. Biotechnol. 19**,** 492-499.

Cox, S. J., Levanon, S. S., Sanchez, A., Lin, H., Peercy, B., Bennett, G. N., San, K.-Y., 2006. Development of a metabolic network design and optimization framework incorporating implementation constraints: a succinate production case study. Metab. Eng. 8**,** 46-57.

Crook, M. A., 2014. The importance of recognizing pellagra (niacin deficiency) as it still occurs. Nutrition. 30**,** 729-730.

Datsenko, K. A., Wanner, B. L., 2000. One-step inactivation of chromosomal genes in Escherichia coli K-12 using PCR products. Proc. Natl. Acad. Sci. 97**,** 6640-6645.

De Anda, R., Lara, A. R., Hernández, V., Hernández-Montalvo, V., Gosset, G., Bolívar, F., Ramírez, O. T., 2006. Replacement of the glucose phosphotransferase transport system

by galactose permease reduces acetate accumulation and improves process performance of Escherichia coli for recombinant protein production without impairment of growth rate. Metab. Eng. 8**,** 281-290.

Dittrich, C. R., Bennett, G. N., San, K. Y., 2005. Characterization of the acetate-producing pathways in Escherichia coli. Biotechnol. Prog. 21**,** 1062-1067.

Esakova, O. A., et al., 2016. Structure of quinolinate synthase from Pyrococcus horikoshii in the presence of its product, quinolinic acid. J. Am. Chem. Soc. 138, 7224-7227.

Flachmann, R., KUNZ, N., SEIFERT, J., GÜTLICH, M., WIENTJES, F. J., LÄUFER, A., GASSEN, H. G., 1988. Molecular biology of pyridine nucleotide biosynthesis in Escherichia coli: cloning and characterization of quinolinate synthesis genes nadA and nadB. Eur. J. Biochem. 175**,** 221-228.

Gold, M. G., Lygren, B., Dokurno, P., Hoshi, N., McConnachie, G., Taskén, K., Carlson, C. R., Scott, J. D., Barford, D., 2006. Molecular basis of AKAP specificity for PKA regulatory subunits. Mol. Cell. 24**,** 383-395.

Gosset, G., 2005. Improvement of Escherichia coli production strains by modification of the phosphoenolpyruvate: sugar phosphotransferase system. Microb. Cell Fact. 4**,** 14.

Griffith, G. R., Chandler, J. L., Gholson, R. K., 1975. Studies on the de novo Biosynthesis of NAD in Escherichia coli: The Separation of the nadB Gene Product from the nadA Gene Product and Its Purification. Eur. J. Biochem. 54**,** 239-245.

Guest, J., Creaghan, I., 1972. Lipoamide dehydrogenase mutants of Escherichia coli K 12. Biochem. J. 130**,** 8P.

Hammond, N., Wang, Y., Dimachkie, M., Barohn, R., 2013. Nutritional neuropathies. Neurol. Clin. 31**,** 477-489.

Heath, A. P., Bennett, G. N., Kavraki, L. E., 2010. Finding metabolic pathways using atom tracking. Bioinformatics. 26**,** 1548-1555.

Jiang, Y., Chen, B., Duan, C., Sun, B., Yang, J., Yang, S., 2015. Multigene editing in the Escherichia coli genome via the CRISPR-Cas9 system. Appl. Environ. Microbiol. 81**,** 2506-2514.

Kang, W., Ma, T., Liu, M., Qu, J., Liu, Z., Zhang, H., Shi, B., Fu, S., Ma, J., Lai, L. T. F., 2019. Modular enzyme assembly for enhanced cascade biocatalysis and metabolic flux. Nat. Commun. 10**,** 1-11.

Keasling, J. D., 2010. Manufacturing molecules through metabolic engineering. Science. 330**,** 1355-1358.

Kim, S. M., Peña, M. I., Moll, M., Bennett, G. N., Kavraki, L. E., 2020. Improving the organization and interactivity of metabolic pathfinding with precomputed pathways. BMC Bioinformatics. 21**,** 1-22.

Kim, S. Y., Shin, Y. U., Heo, I. K., Kim, J. E., Son, S. K., Seo, C. I., Kim, H. A., Lee, H. J., Na, K. H., Bae, J. Y., Method for the preparation of nicotinic acid. Google Patents, 2016.

Lee, J. W., Na, D., Park, J. M., Lee, J., Choi, S., Lee, S. Y., 2012. Systems metabolic engineering of microorganisms for natural and non-natural chemicals. Nat. Chem. Biol. 8**,** 536-546.

Leese, C., Fotheringham, I., Escalettes, F., Speight, R., Grogan, G., 2013. Cloning, expression, characterisation and mutational analysis of L-aspartate oxidase from Pseudomonas putida. J. Mol. Catal. B Enzym. 85**,** 17-22.

Li, M., Ho, P. Y., Yao, S., Shimizu, K., 2006. Effect of lpdA gene knockout on the metabolism in Escherichia coli based on enzyme activities, intracellular metabolite concentrations and metabolic flux analysis by 13C-labeling experiments. J. Biotechnol. 122**,** 254-266.

Liang, Q., Zhang, F., Li, Y., Zhang, X., Li, J., Yang, P., Qi, Q., 2015. Comparison of individual component deletions in a glucose-specific phosphotransferase system revealed their different applications. Sci. rep. 5**,** 13200.

Lin, H., Bennett, G. N., San, K.-Y., 2005. Metabolic engineering of aerobic succinate production systems in Escherichia coli to improve process productivity and achieve the maximum theoretical succinate yield. Metab. Eng. 7**,** 116-127.

Magni, G., Amici, A., Emanuelli, M., Raffaelli, N., Ruggieri, S., 1999. Enzymology of Nad^+ Synthesis. Advances in Enzymology and Related Areas of Molecular Biology: Mechanism of Enzyme Action, Part A. 73**,** 135-182.

Marinoni, I., Nonnis, S., Monteferrante, C., Heathcote, P., Härtig, E., Böttger, L. H., Trautwein, A. X., Negri, A., Albertini, A. M., Tedeschi, G., 2008. Characterization of l-aspartate oxidase and quinolinate synthase from Bacillus subtilis. FEBS J. 275**,** 5090-5107.

Martinez, I., Gao, H., Bennett, G. N., San, K.-Y., 2018. High yield production of four-carbon dicarboxylic acids by metabolically engineered Escherichia coli. J. Ind. Microbiol. Biotechnol. 45**,** 53-60.

Mattevi, A., Tedeschi, G., Bacchella, L., Coda, A., Negri, A., Ronchi, S., 1999. Structure ofL-aspartate oxidase: implications for the succinate dehydrogenase/fumarate reductase oxidoreductase family. Structure. 7**,** 745-756.

Mortarino, M., Negri, A., Tedeschi, G., Simonic, T., Duga, S., Gassen, H. G., Ronchi, S., 1996. L-Aspartate Oxidase from Escherichia coli: I. Characterization of Coenzyme Binding and Product Inhibition. Eur. J. Biochem. 239**,** 418-426.

Nasu, S., Wicks, F. D., Gholson, R., 1982. L-Aspartate oxidase, a newly discovered enzyme of Escherichia coli, is the B protein of quinolinate synthetase. J. Biol. Chem. 257**,** 626-632.

643 Ning, Y., Wu, X., Zhang, C., Xu, Q., Chen, N., Xie, X., 2016. Pathway construction and
644 metabolic engineering for fermentative production of ectoine in Escherichia coli. Metab.
645 Eng. 36**,** 10-18.
646 Ollagnier-de Choudens, S., Loiseau, L., Sanakis, Y., Barras, F., Fontecave, M., 2005.
647 Quinolinate synthetase, an iron–sulfur enzyme in NAD biosynthesis. FEBS Lett. 579**,**
648 3737-3743.
649 Panozzo, C., Nawara, M., Suski, C., Kucharczyka, R., Skoneczny, M., Bécam, A.-M., Rytka, J.,
650 Herbert, C. J., 2002. Aerobic and anaerobic NAD+ metabolism in Saccharomyces
651 cerevisiae. FEBS Lett. 517**,** 97-102.
652 Park, J. H., Lee, S. Y., 2010. Metabolic pathways and fermentative production of L-aspartate
653 family amino acids. Biotechnol J. 5**,** 560-577.
654 Pettit, F. H., Reed, L. J., 1967. Alpha-keto acid dehydrogenase complexes. 8. Comparison of
655 dihydrolipoyl dehydrogenases from pyruvate and alpha-ketoglutarate dehydrogenase
656 complexes of Escherichia coli. Proc. Natl. Acad. Sci. U S A. 58**,** 1126.
657 Quin, M. B., Wallin, K., Zhang, G., Schmidt-Dannert, C., 2017. Spatial organization of multi-
658 enzyme biocatalytic cascades. Organic & biomolecular chemistry. 15**,** 4260-4271.
659 Reichmann, D., Couté, Y., Ollagnier de Choudens, S., 2015. Dual activity of quinolinate
660 synthase: triose phosphate isomerase and dehydration activities play together to form
661 quinolinate. Biochemistry. 54, 6443-6446.
662 Sakuraba, H., Yoneda, K., Asai, I., Tsuge, H., Katunuma, N., Ohshima, T., 2008. Structure of l-
663 aspartate oxidase from the hyperthermophilic archaeon Sulfolobus tokodaii. Biochim.
664 Biophys. Acta. Proteins Proteom. 1784**,** 563-571.

Sánchez, A. M., Bennett, G. N., San, K.-Y., 2005. Novel pathway engineering design of the anaerobic central metabolic pathway in Escherichia coli to increase succinate yield and productivity. Metab. Eng. 7**,** 229-239.

Sauer, U., Eikmanns, B. J., 2005. The PEP—pyruvate—oxaloacetate node as the switch point for carbon flux distribution in bacteria: We dedicate this paper to Rudolf K. Thauer, Director of the Max-Planck-Institute for Terrestrial Microbiology in Marburg, Germany, on the occasion of his 65th birthday. FEMS Microbiol. Rev. 29**,** 765-794.

Seifert, J., Norbert, K., FLACHMANN, R., LÄUFER, A., Klaus-Dieter, J., GASSEN, H. G., 1990. Expression of the E. coli nadB gene and characterization of the gene product L-aspartate oxidase. Biol. Chem. Hoppe-Seyler. 371**,** 239-248.

Shearer, G., et al., 2005. Quantitative estimation of channeling from early glycolytic intermediates to CO2 in intact Escherichia coli. FEBS J. 272, 3260-3269.

Shishido, T., Song, Z., Kadowaki, E., Wang, Y., Takehira, K., 2003. Vapor-phase oxidation of 3-picoline to nicotinic acid over Cr1− xAlxVO4 catalysts. Appl. Catal. A-Gen. 239**,** 287-296.

Soriano, E. V., et al., 2013. Active-site models for complexes of quinolinate synthase with substrates and intermediates. Acta Cryst. D69, 1685-1696.

Steiert, P., Stauffer, L., Stauffer, G., 1990. The lpd gene product functions as the L protein in the Escherichia coli glycine cleavage enzyme system. J. Bacteriol. 172**,** 6142-6144.

Tedeschi, G., Nonnis, S., Strumbo, B., Cruciani, G., Carosati, E., Negri, A., 2010. On the catalytic role of the active site residue E121 of E. coli L-aspartate oxidase. Biochimie. 92**,** 1335-1342.

687 Thakker, C., Zhu, J., San, K.-Y., Bennett, G., 2011. Heterologous pyc gene expression under
688 various natural and engineered promoters in Escherichia coli for improved succinate
689 production. J. Biotechnol. 155**,** 236-243.
690 Tritz, G. J., Chandler, J. L., 1973. Recognition of a gene involved in the regulation of
691 nicotinamide adenine dinucleotide biosynthesis. J. Bacteriol. 114**,** 128-136.
692 Wang, Y., Duff, S., Lepiniec, L., Crétin, C., Sarath, G., Condon, S. A., Vidal, J., Gadal, P.,
693 Chollet, R., 1992. Site-directed mutagenesis of the phosphorylatable serine (Ser8) in C4
694 phosphoenolpyruvate carboxylase from sorghum. The effect of negative charge at
695 position 8. J. Biol. Chem. 267**,** 16759-16762.
696 Wheeldon, I., et al., 2016. Substrate channelling as an approach to cascade reactions. Nat. Chem.
697 8, 299.
698 Wong, M. S., Wu, S., Causey, T. B., Bennett, G. N., San, K.-Y., 2008. Reduction of acetate
699 accumulation in Escherichia coli cultures for increased recombinant protein production.
700 Metab. Eng. 10**,** 97-108.
701 Woolston, B. M., Edgar, S., Stephanopoulos, G., 2013. Metabolic engineering: past and future.
702 Annu. Rev. Chem. Biomol. Eng. 4**,** 259-288.
703 Zhao, L., Lu, Y., Yang, J., Fang, Y., Zhu, L., Ding, Z., Wang, C., Ma, W., Hu, X., Wang, X.,
704 2020. Expression regulation of multiple key genes to improve l-threonine in Escherichia
705 coli. Microb. Cell Fact. 19**,** 1-23.
706 Zhu, F., San, K. Y., Bennett, G. N., 2020. Improved succinate production from galactose-rich
707 feedstocks by engineered Escherichia coli under anaerobic conditions. Biotechnol.
708 Bioeng. 117**,** 1082-1091

Zhu, F., Wang, Y., San, K. Y., Bennett, G. N., 2018. Metabolic engineering of Escherichia coli to produce succinate from soybean hydrolysate under anaerobic conditions. Biotechnol. Bioeng. 115**,** 1743-1754.

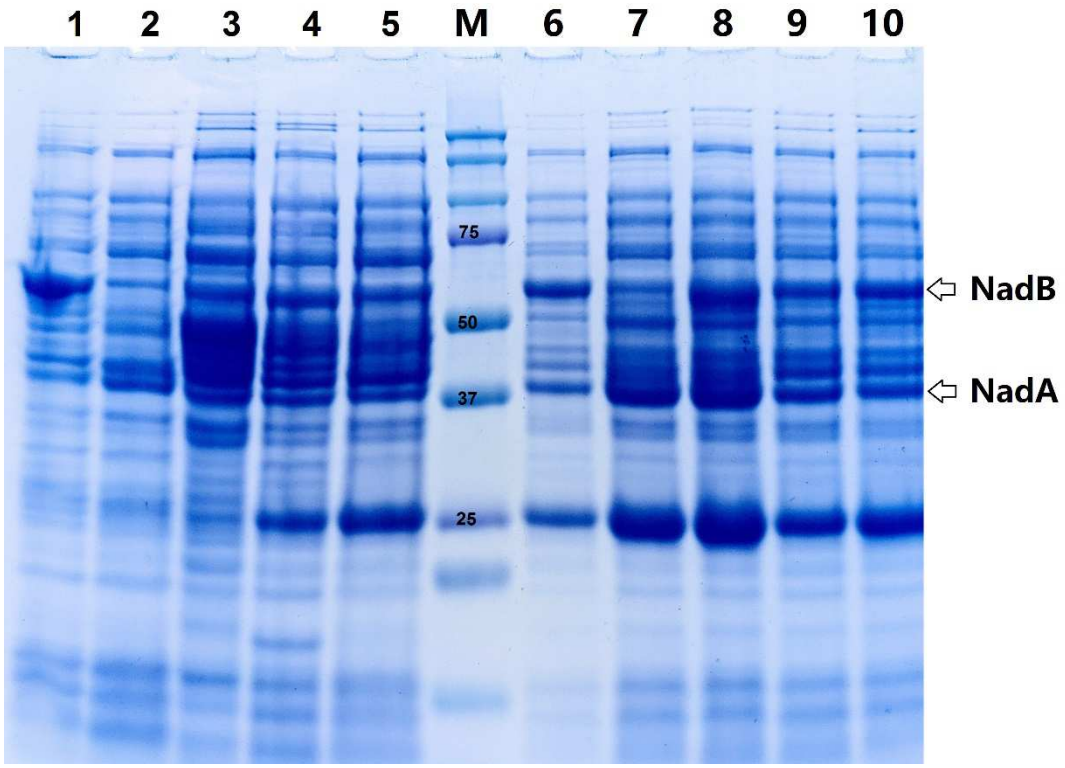

Fig. S1. SDS-PAGE analysis of soluble protein. FZ763 was used as the host strain, 12 μL sample was loaded unless otherwise specified. From left to right: 1, pFZGNB14 [*E. coli* NadB (5 μL)]; 2, pFZGNB34 (*E. coli* NadA); 3, pTrc99a- St*nadB* [*Sulfolobus tokodaii* NadB (StNadB)]; 4, pFZGNB183 [*Pseudomonas putida* KT2440 NadB (PpNadB)]; 5, pFZGNB43[*Bacillus subtilis* NadA (BsNadA)]; M: Bio-Rad dual color standards (5 μL); 6, FZ763/pFZGNB190 (7 μL); 7, FZ763/pFZGNB189; 8, FZ763/pFZGNB193; 9, FZ763/pFZGNB207; 10, FZ763/pFZGNB190. Numbers on the marker indicates the protein molecular weight (kDa)

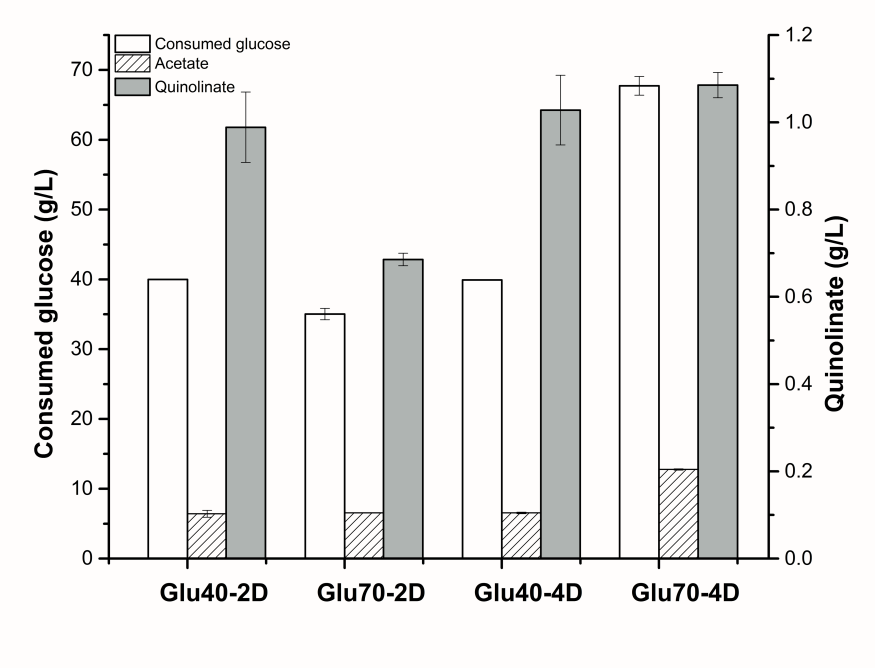

Fig. S2. The effect of glucose concentration on quinolinate production in FZ763/pFZGNB190. Aerobic cultures were performed at 37 ^{o}C, 350 rpm. Values are the average of three replicates with error bars indicating standard deviation. Glu40/70 indicates fermentation with 40 or 70 g/L glucose and the -2D or -4D indicates the culture was incubated for 2 or 4 days.

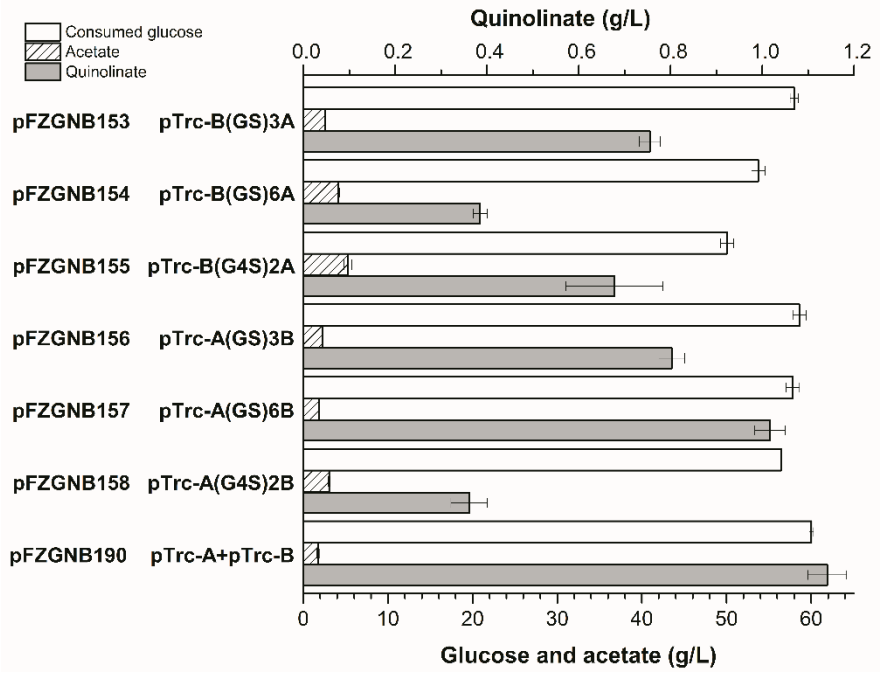

728

729 **Fig. S3. The effect of NadA-NadB fusion proteins on quinolinic acid production in FZ763.**

730 Aerobic cultures were performed at 37 °C, 350 rpm for 4 days. NadA-NadB fusion protein with

731 different linkers and different orders were over-expressed under the control of pTrc promoter in

732 pFZGNB33. Values are the average of three replicates with error bars indicating standard

733 deviation.

734

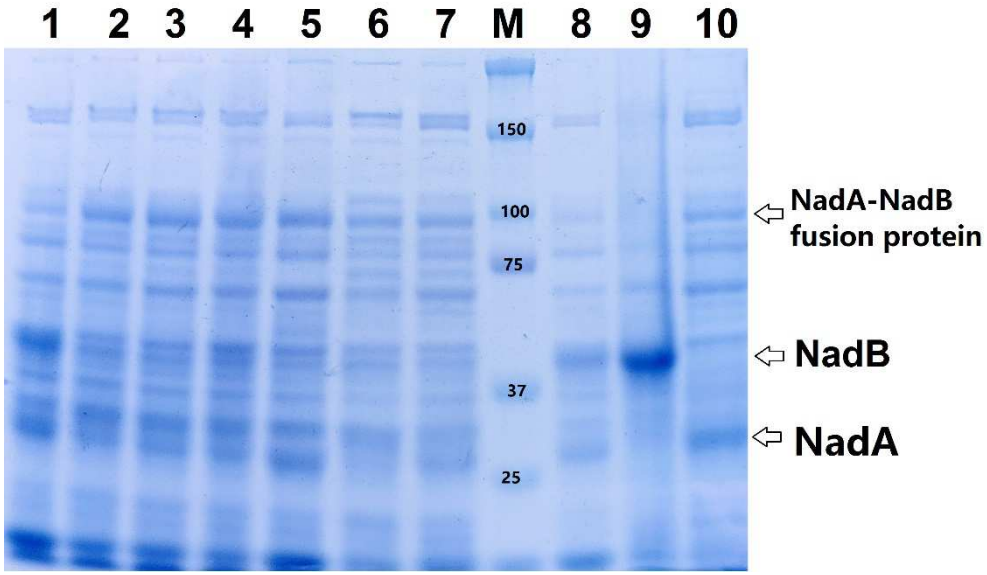

Fig. S4. SDS-PAGE analysis of soluble protein. Non-reducing SDS-PAGE analysis of soluble protein in FZ763 harboring different plasmids. 20 μL sample was loaded otherwise specified. From left to right: 1, pFZGNB190; 2, pFZGNB153; 3, pFZGNB154; 4, pFZGNB155; 5, pFZGNB156; 6, pFZGNB157; 7, pFZGNB158; M: Bio-Rad dual color standards (5 μL); 8, pFZGNB190 (7 μL); 9, pFZGNB14 [*E. coli* NadB (7 μL)]; 10, pFZGNB34 (*E. coli* NadA). Numbers on the marker indicates the protein molecular weight (kDa), the approximate protein location was also labeled based on the protein molecular weight.

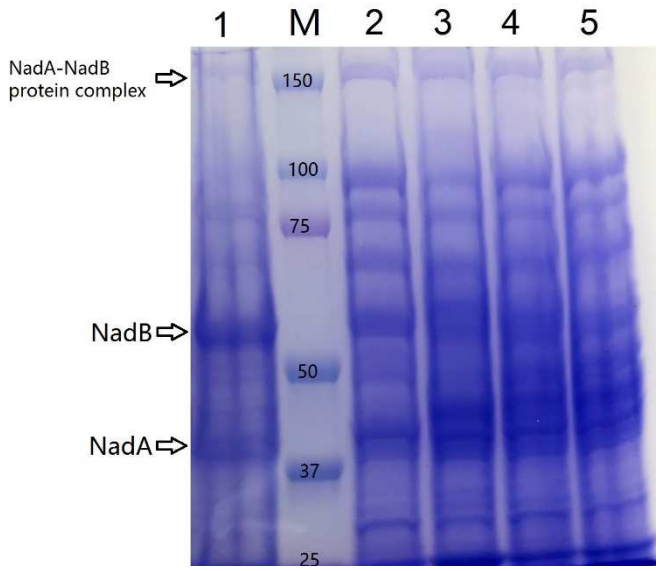

744

745 **Fig. S5: Non-reducing SDS-PAGE analysis of soluble protein in FZ763 harboring**

746 **different plasmids.** 20 μL sample was loaded otherwise specified. From left to right: 1,

747 pFZGNB190 (7 μL); M: Bio-Rad dual color standards (5 μL); 2, pFZGNB232 (15 μL); 3,

748 pFZGNB233 (25 μL); 4, pFZGNB234 (15 μL); 5, pFZGNB235 (15 μL). Numbers on the marker

749 indicates the protein molecular weight (kDa), the approximate protein location was also labeled

750 based on the protein molecular weight. Non-reducing SDS-PAGE indicates no reductant

751 (Dithiothreitol or 2-mercaptoethanol) was added to the loading buffer.

752

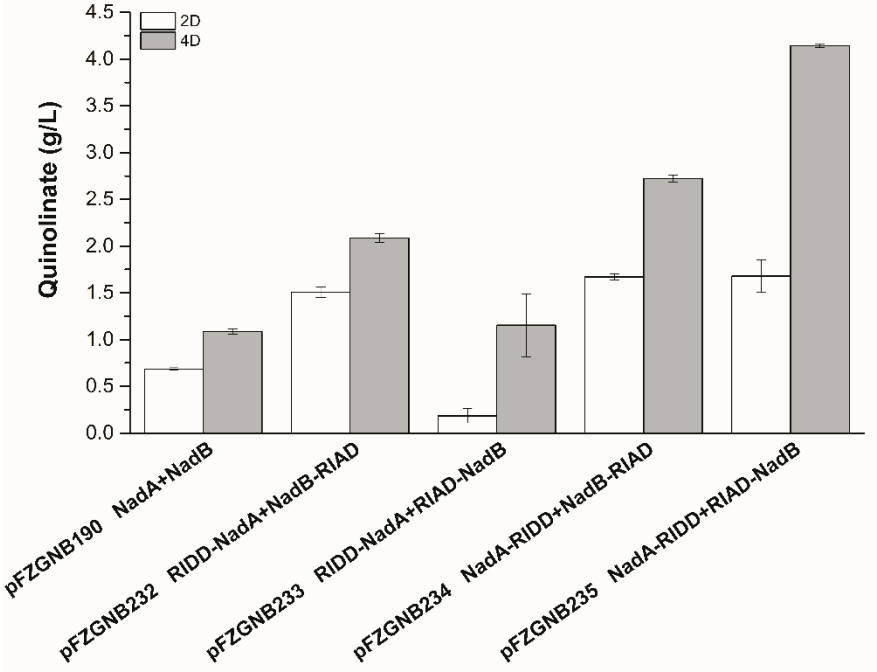

753

754 **Fig. S6. The effect of NadA-NadB enzyme complex on quinolinic acid production in FZ763**
755 **with 70 g/L glucose.** Aerobic cultures were performed at 37 ^{o}C, 350 rpm for 4 days. NadA-
756 RIDD and NadB-RIAD fusion proteins were over-expressed under the control of their pTrc
757 promoter in pFZGNB227, NadA-NadB enzyme complex was assembled with the help of
758 peptides, RIAD and RIDD. Values are the average of three replicates with error bars indicating
759 standard deviation.

760 **Table S1. Plasmids and strains used in this study.**

	Description	Source
plasmids		
pHL413K	Amp^R of pTrc99a was replaced with Km^R, and *pycA* gene	(Thakker et al., 2011)
pKK313	S8D mutant *Pepc* from *sorghum*, Amp^R	(Wang et al., 1992)
pFZGNB16	BglII was introduced 193 bp before pTrc promoter of pTrc99a, Amp^R	This study
pFZGNB33	Amp^R of pFZGNB16 was replaced by Km^R from pHL413K, Km^R	This study
pFZGNB34	*nadA* was inserted into pFZGNB33 between EcoRI and BamHI	This study
pFZGNB35	*nadB* was inserted into pFZGNB33 between NcoI and BamHI	This study
pFZGNB36	*aspC* was inserted into pFZGNB33 between EcoRI and BamHI	This study
pFZGNB37	pFZGNB33 with *nadA-nadB-aspC*	This study
pFZGNB38	pFZGNB33 with *nadA-aspC-nadB*	This study
pFZGNB39	pFZGNB33 with *nadB-aspC-nadA*	This study
pFZGNB40	pFZGNB33 with *nadB-nadA-aspC*	This study
pFZGNB41	pFZGNB33 with *aspC-nadA-nadB*	This study
pFZGNB42	pFZGNB33 with *aspC-nadB-nadA*	This study
pFZGNB43	*nadA* from *Bacillus subtilis* with an extra DNA fragment coding an HisTag at C-terminal (Bs*nadA*-HisTag) was cloned into pFZGNB33 between EcoRI and XbaI	This study

pFZGNB44	pTargetT contains N_{20} specific for *ptsG*, Sm^R	This study
pFZGNB46	Upstream and downstream homologous arms of *ptsG* were inserted into pFZGNB44, for *ptsG* deletion, Sm^R	This study
pFZGNB50	pTrc-*pepc* fragment from pKK313 was inserted into pFZGNB46 between homologous arms, for replacement of native *ptsG* with pTrc-*pepc* fragment, Sm^R	This study
pFZGNB63	pTargetT contains N_{20} specific for *tpiA*, upstream and downstream homologous arms of *tpiA*, Sm^R, for *tpiA* deletion	This study
pFZGNB65	pTargetT contains N_{20} specific for *sucA*, upstream and downstream homologous arms of suc*AB*, Sm^R, for *sucAB* deletion	This study
pFZGNB74	pTargetT contains N_{20} specific for *lpd*, upstream and downstream homologous arms of *lpd*, Sm^R, for *lpd* deletion	This study
pFZGNB75	pTargetT contains N_{20} specific for *ackA*, upstream and downstream homologous arms of *ackA*, Sm^R, for *ackA* deletion	This study
pFZGNB76	pTargetT contains N_{20} specific for *ackA*, upstream and downstream homologous arms of *pta-ackA*, Sm^R, for *pta-ackA* deletion	This study
pFZGNB117	pTrc-*pepc* from pKK313 was inserted into pFZGNB75 between homologous arms, for replacement of *ackA* with pTrc-*pepc* fragment, Sm^R	This study

pFZGNB118	pTrc-*pepc* from pKK313 was inserted into pFZGNB76 between homologous arms, for replacement of *pta-ackA* with pTrc-*pepc* fragment, Sm^R	This study
pFZGNB153	Gene encoding NadB-$(GlySer)_3$-NadA under the control of pTrc promoter in pFZGNB33	This study
pFZGNB154	Gene encoding NadB-$(GlySer)_6$-NadA under the control of pTrc promoter in pFZGNB33	This study
pFZGNB155	Gene encoding NadB-$(Gly_4Ser)_2$-NadA under the control of pTrc promoter in pFZGNB33	This study
pFZGNB156	Gene encoding NadA-$(GlySer)_3$-NadB under the control of pTrc promoter in pFZGNB33	This study
pFZGNB157	Gene encoding NadA-$(GlySer)_6$-NadB under the control of pTrc promoter in pFZGNB33	This study
pFZGNB158	Gene encoding NadA-$(Gly_4Ser)_2$-NadB under the control of pTrc promoter in pFZGNB33	This study
pFZGNB183	*nadB* from *Pseudomonas putida* KT2440 (Pp*nadB*) was inserted into pFZGNB33 between BamHI and XbaI	This study
pFZGNB33-staspO	*nadB* (StaspO) from *Sulfolobus tokodaii* (St*nadB*) was inserted into pFZGNB33 between NcoI and BamHI	This study
pFZGNB189	pFZGNB33 with pTrc-*nadA* and pTrc-St*nadB*	This study
pFZGNB190	pFZGNB33 with pTrc-*nadA* and pTrc-*nadB*	This study
pFZGNB193	pFZGNB33 with pTrc-*nadA* and pTrc-Pp*nadB*	This study
pFZGNB204	pFZGNB33 with pTrc-*nadA*, pTrc-*nadB* and pTrc-*aspC*	This study

pFZGNB207	pFZGNB33 with pTrc-Bs*nadA* and pTrc-*nadB*	This study
RIDD	DNA coding RIDD with linker was synthesized and inserted into pUC57	This study
RIAD	DNA coding RIAD with linker was synthesized and inserted into pUC57	This study
pFZGNB227	A SpeI was introduced into pFZGNB33 in front of pTrc promoter, Km^R	This study
pFZGNB228	pFZGNB227 with pTrc-*ridd-nadA*	This study
pFZGNB229	pFZGNB227 with pTrc-*nadB-riad*	This study
pFZGNB230	pFZGNB227 with pTrc-*riad-nadB*	This study
pFZGNB231	pFZGNB227 with pTrc-*nadA-ridd*	This study
pFZGNB232	pFZGNB227 with pTrc-*ridd-nadA* and pTrc-*nadB-riad*	This study
pFZGNB233	pFZGNB227 with pTrc-*ridd-nadA* and pTrc-*riad-nadB*	This study
pFZGNB234	pFZGNB227 with pTrc-*nadA-ridd* and pTrc-*nadB-riad*	This study
pFZGNB235	pFZGNB227 with pTrc-*nadA-ridd* and pTrc-*riad-nadB*	This study
Strains		
MG1655	*E. coli* K12 MG1655, F^- *lambda*$^-$ *ilvG- rfb*-50 *rph*-1	
FZ700	MG1655 Δ*nadC*	This study
FZ703	MG1655 Δ*nadC,* Δ*nadR*	This study
FZ723	MG1655 Δ*nadC,* Δ*nadR,* Δ*ptsG*	This study
FZ734	MG1655 Δ*nadC,* Δ*nadR, ptsG::pTrc-pepc*	This study
FZ738	FZ734 Δ*tpiA*	This study
FZ740	FZ734 Δ*sucAB*	This study

FZ741	FZ734 Δ*poxB*	This study
FZ742	FZ734 Δ*lpd*	This study
FZ756	FZ734 Δ*poxB::pTrc-pepc*	This study
FZ757	FZ734 Δ*poxB*, Δ*ackA*	This study
FZ763	FZ734 Δ*poxB, ackA::pTrc-pepc*	This study

Table S2. Acetate accumulated in engineered strains

	MG1655	FZ700	FZ703	FZ723	FZ734
1 day	18.0 ± 0.3	7.2 ± 0.1	14.1 ± 0.3	4.8 ± 0.5	4.6 ± 0.1
3 day	34.7 ± 0.4	30.4 ± 1.9	29.0 ± 0.5	18.8 ± 0.2	18.4 ± 0.5
5 day	38.8 ± 1.2	34.2 ± 1.1	33.9 ± 0.3	26.1 ± 0.1	25.8 ± .5
7 day	42.2 ± 0.9	36.0 ± .4	37.0 ± 0.4	32.0 ± 0.6	32.5 ± 0.5
nadC	+	-	-	-	-
nadR	+	+	-	-	-
ptsG	+	+	+	-	-
pTrc-pepc	-	-	-	-	+

Plasmid pFZGNB42 (pTrc-*aspC-nadB-nadA*) was introduced into the tested strains to check their performance, aerobic cultures were performed at 37 ºC, 350 rpm. The numbers indicate acetate concentration (g/L, average of three replicates with error bars indicating standard deviation).

Table S3. DNA sequences used in this study

>pFZGNB33 partial sequence

GCGCAACGCAATTAATGTGAGTTAGCGCGAATAGATCTGGTTTGACAGCTTATCATC
GACTGCACGGTGCACCAATGCTTCTGGCGTCAGGCAGCCATCGGAAGCTGTGGTATG

GCTGTGCAGGTCGTAAATCACTGCATAATTCGTGTCGCTCAAGGCGCACTCCCGTTC
TGGATAATGTTTTTTGCGCCGACATCATAACGGTTCTGGCAAATATTCTGAAATGAG
CTGTTGACAATTAATCATCCGGCTCGTATAATGTGTGGAATTGTGAGCGGATAACAA
TTTCACACAGGAAACAGACCATGGAATTCGAGCTCGGTACCCGGGGATCCTCTAGA
GTCGACCTGCAGGCATGCAAGCTTAGCTTGCAGTGGGCTTACATGGCGATAGCTAGA
CTGGGCGGTTTTATGGACAGCAAGCGAACCGGA

The special features are highlighted BglII, pTrc promoter, MCS

>pFZGNB227 partial sequence

GCGCAACGCAATTAATGTGAGTTAGCGCGAATAGATCTGGTTTGACAGCTTATCATC
GACTGCACGGTGCACCAATGCTTCTGGCGTCAGGCAGCCATCGGAAGCTGTGGTATG
GCTGTGCAGGTCGTAAATCACTGCATAATTCGTGTCGCTCAAGGCGCACTCCCGTTC
TGGATAATGTTTTTTGCGCCGACATCATAACGGTTCTGGCAAATATTCTGAAATGAC
TAGTGTTGACAATTAATCATCCGGCTCGTATAATGTGTGGAATTGTGAGCGGATAAC
AATTTCACACAGGAAACAGACCATGGAATTCGAGCTCGGTACCCGGGGATCCTCTA
GAGTCGACCTGCAGGCATGCAAGCTTAGCTTGCAGTGGGCTTACATGGCGATAGCTA
GACTGGGCGGTTTTATGGACAGCAAGCGAACCGGA

The special features are highlighted BglII, SpeI, pTrc promoter, MCS

> BsnadA-HisTag sequence

gaattcATGTCAATTCTTGATGTGATCAAACAATCGAATGATATGATGCCCGAAAGTTA
TAAAGAACTATCGAGAAAGGATATGGAAACGCGCGTTGCCGCCATTAAGAAAAAGT
TCGGCAGCAGGCTCTTTATACCAGGCCATCATTATCAAAAGGATGAAGTGATACAAT
TTGCTGACCAAACAGGCGACTCCCTGCAATTGGCCCAAGTAGCGGAAAAAAACAAA
GAAGCGGATTATATCGTATTTTGCGGCGTTCACTTTATGGCAGAAACCGCCGATATG
CTGACAAGCGAGCAGCAAACGGTCGTCCTGCCAGATATGAGAGCTGGATGTTCTAT
GGCTGACATGGCTGACATGCAGCAGACCAATAGGGCATGGAAGAAGCTTCAGCATA
TATTTGGAGATACGATCATACCTTTAACTTATGTGAACTCCACTGCGGAGATCAAGG
CATTCGTCGGAAAGCATGGCGGAGCAACTGTAACTTCTTCGAATGCGAAAAAAGTG
CTTGAATGGGCGTTTACACAGAAAAAAAGAATTTTATTTTTGCCTGATCAGCATTTA
GGGAGAAATACGGCTTATGATCTGGGCATTGCGCTTGAAGATATGGCTGTGTGGGAT
CCGATGAAAGATGAATTAGTAGCTGAATCCGGGCATACGAATGTGAAAGTGATTTT
GTGGAAAGGGCATTGCTCTGTTCACGAGAAATTCACCACTAAAAATATCCATGATAT
GAGAGAGCGAGACCCCGACATTCAGATCATTGTGCACCCGGAATGTTCACACGAAG
TCGTGACACTAAGCGATGATAACGGATCAACGAAATATATTATCGACACAATCAAC
CAGGCTCCGGCGGGAAGCAAGTGGGCAATCGGGACAGAAATGAATCTTGTTCAGCG
GATCATTCACGAGCATCCAGATAAACAAATCGAATCACTCAACCCTGACATGTGCCC
TTGCCTGACAATGAACCGAATTGATTTGCCGCATTTGTTGTGGTCGCTGGAACAAAT

TGAAAAAGGAGAACCTTCAGGCGTCATCAAGGTGCCAAAAGCCATTCAGGAAGATG
CACTCCTTGCCCTGAATCGAATGCTTTCGATCACGCACCACCACCACCACCactaga

>stnadB sequence

ccatggaaATGATCTATATTATCGGTAGCGGTATTGCAGGTCTGAGTGCCGGTGTTGCAC
TGCGTCGTGCAGGTAAAAAAGTTACCCTGATTAGCAAACGCATTGATGGTGGTAGC
ACCCCGATTGCAAAAGGTGGTGTTGCAGCAAGCGTTGGTAGTGATGATAGTCCGGA
ACTGCATGCACAGGATACCATTCGTGTTGGTGATGGTCTGTGTGATGTTAAAACCGT
TAATTATGTTACCAGCGAGGCCAAAAACGTGATTGAAACCTTTGAAAGCTGGGGCTT
TGAATTTGAAGAAGATCTGCGTCTGGAAGGTGGTCATACCAAACGTCGTGTTCTGCA
TCGTACCGATGAAACCGGTCGTGAAATTTTTAACTTCCTGCTGAAACTGGCACGCGA
AGAAGGTATTCCGATTATTGAAGATCGCCTGGTTGAAATTCGCGTGAAAGATGGTAA
AGTTACCGGTTTTGTGACCGAAAAACGTGGTCTGGTTGAAGATGTTGATAAACTGGT
TCTGGCAACCGGTGGTTATAGCTATCTGTATGAATATAGCAGCACCCAGAGCACCAA
TATCGGTGATGGTATGGCAATTGCATTTAAAGCAGGCACCATTCTGGCCGATATGGA
ATTTGTTCAGTTTCATCCGACCGTTACCAGCCTGGATGGTGAAGTTTTTCTGCTGACC
GAAACCCTGCGTGGTGAAGGTGCACAGATTATTAATGAAAATGGCGAACGCTTTCT
GTTTAACTATGATAAACGTGGTGAACTGGCACCGCGTGATATTCTGAGCCGTGCAAT
TTATATCGAAATGCTGAAAGGCCATAAAGTGTTTATCGACCTGAGCAAAATCGAAG
ATTTCGAACGTAAATTTCCGGTGGTTGCAAAATATCTGGCACGTCATGGCCATAACT
ATAAAGTGAAAATTCCGATTTTTCCGGCAGCCCATTTTGTGGATGGTGGTATTCGTG
TTAATATTCGTGGCGAAAGCAACATTGTGAACCTGTATGCAATTGGTGAAGTTAGCG
ATAGCGGTCTGCATGGTGCAAATCGTCTGGCAAGCAATAGCCTGCTGGAAGGTCTG
GTTTTTGGTATTAATCTGCCTCGTTATGTTGATAGCAGCTGGGAAGGTATTAGCACC
GATGATGGTATTGTTCATAGCGTTCGTATTAGCGGTAATAAAACCCTGAGCCTGAAA
GAAATTCGTCGCATTAATTGGGAAAACGTGGGCATTATTCGCAACGAAGAAAAACT
GGTGAAAGCCATTAACACCTATAGCAGCAGTACCCAGAACGAAGCAATTATTAGCT
ATCTGACCGCACTGGCAGCAGAAATTCGTAAAGAAAGCCGTGGTAATCACTTTCGTG
AGGATTATCCGTATAAAGATCCGAATTGGGAGAAACGCATTTACTTTAAACTGGTGG
TGCTCGAGTAATAAggatcc

>PpnadB sequence

ggatccATGAGCCAACAATTCCAACATGATGTCCTGGTGATCGGCAGCGGTGCCGCCGG
TCTCAGCCTGGCACTTAACCTCCCCAGCCACCTTCGCGTTGCCGTATTGAGCAAGGG
CGACCTGTCCAACGGCTCGACCTTCTGGGCCCAGGGCGGCGTCGCTGCAGTGCTGGA
CAACACCGATACTGTGCAGTCGCATGTCGAGGACACCCTCAATGCCGGCGGCGGGC
TGTGCCATGAAGACGCAGTGCGCTTTACCGTCGAGCACAGCCGCGAAGCGATCCAA
TGGCTGATCGAGCAAGGCGTGCCCTTCACCCGCGATGAGCACTACAGCGTCGACGA
TGGCGGCTTCGAGTTCCACCTCACCCGTGAAGGGGGCCATAGCCACCGGCGCATCAT
CCACGCCGCCGACGCTACCGGCGCGGCAATCTTCACCACGCTGCTGGAACAGGCTC

GCCAGCGCCCGAACATCCAGCTGCTGGAGCAGCGGGTGGCGGTCGACCTGATCACT
GAACGCCGCCTGGGCCTGCCCGGCGAACGCTGCCTGGGCGCCTACGTGCTCGACCG
CAACACCGGCGAGGTGGACACCTTCGGCGCGCGCTTCACCGTGCTGGCCACGGGCG
GTGCGGCCAAGGTCTATCTCTACACCAGCAACCCCGATGGTGCCTGCGGCGACGGT
ATCGCCATGGCCTGGCGGGCCGGCTGCCGAGTGGCGAACCTGGAATTCAACCAGTT
CCACCCGACCTGCCTGTATCACCCACAGGCCAAGAGCTTCCTGATCACCGAAGCCCT
GCGCGGCGAGGGCGCCCTGCTGCGCCTGCCCAACGGCGAACGTTTCATGCCACGCTT
CGACCCACGCGAAGAGCTGGCCCCACGGGACATCGTGGCCCGCGCCATCGACCACG
AGATGAAGCGCCTGGGCGTGGACTGCGTATACCTGGACATCACTCACAAGCCTGCA
GATTTCATCAAGAGCCACTTCCCCACCGTGTACGAGCGCTGCCTGGCCTTTGGCATC
GATATCACCCGTCAGCCGATCCCGGTGGTGCCTGCGGCGCATTACACCTGCGGCGGG
GTGATGGTCGACGACTGCGGCCACACCGATGTGCCTGGCTTGTATGCCATCGGCGAA
ACCAGTTTCACCGGCCTGCACGGCGCCAACCGCATGGCCAGCAACTCGCTGCTGGA
ATGTTTTGTGTACGGTCGCGCCGCCGCTGCCGACATCCAGGCGCACCTGGAGCAAGT
GGCCATGCCCAAGGCCTTGCCCGGCTGGGACGCCAGCCAGGTGACCGACTCGGACG
AGGACGTGATCATTGCGCACAACTGGGACGAACTGCGGCGCTTCATGTGGGACTAC
GTCGGCATCGTGCGCACCAGCAAGCGCCTGCAGCGGGCCCAGCACCGCATTCGCCT
GCTGCTGGATGAAATCGACGAGTTCTACAGCAACTACAAGGTCAGCCGTGACCTGA
TCGAGCTGCGCAACCTGGCGCAAGTGGCCGAGCTGATGATCCTGTCAGCCATGCAG
CGCAAGGAAAGCCGAGGGTTGCATTACACACTGGATTATCCAGGGATGCTGGACGA
GGCCAAGGACACCATCCTTAACCCGCTCTGAtctaga

>optimized RIDD with linker sequence

GGTGGCGGTGGTTCTGGCGGTGGCGGTTCTGGTGGCGGCGGTTGCGGTTCTCTGCGT
GAGTGCGAACTGTACGTTCAGAAACACAACATCCAGGCGCTGCTGAAAGATAGCAT
CGTTCAACTGTGTACCGCACGTCCGGAACGTCCGATGGCATTTCTGCGCGAATACTT
CGAACGCCTGGAAAAAGAAGAAGCGAAAGGTGGCGGTGGCTCAGGTGGCGGTGGT
TCAGGTGGTGGTGGTTGTGGT

>optimized RIAD with linker sequence

ccatggaattcGGTGGTGGCGGTTCTGGTGGCGGCGGTTCTGGTGGCGGCGGTTGCGGTCT
GGAACAATACGCGAATCAGCTGGCGGATCAGATTATCAAAGAAGCGACCGAAGGCT
GCGGCGGCGGTGGTTCAGGTGGCGGCGGTTCAGGTGGCGGTGGTTGTGGTggatcc

Supplementary Materials for

Metabolic engineering of *Escherichia coli* for quinolinic acid production by assembling L-aspartate oxidase and quinolinate synthase as an enzyme complex

Fayin Zhu[a,b], Matthew Peña[a], George N. Bennett[a,c]*

a Department of BioSciences, Rice University, Houston, TX, USA, 77005

b present address: Department of Chemical, Biological, and Materials Engineering, University of South Florida, Tampa, FL 33620

c Department of Chemical and Biomolecular Engineering, Rice University, Houston, TX, USA, 77005

* Corresponding author: Department of BioSciences, Rice University, Houston, TX 77005, E-mail address: gbennett@rice.edu

This document includes:

- Figures S1-6
- Tables S1-3

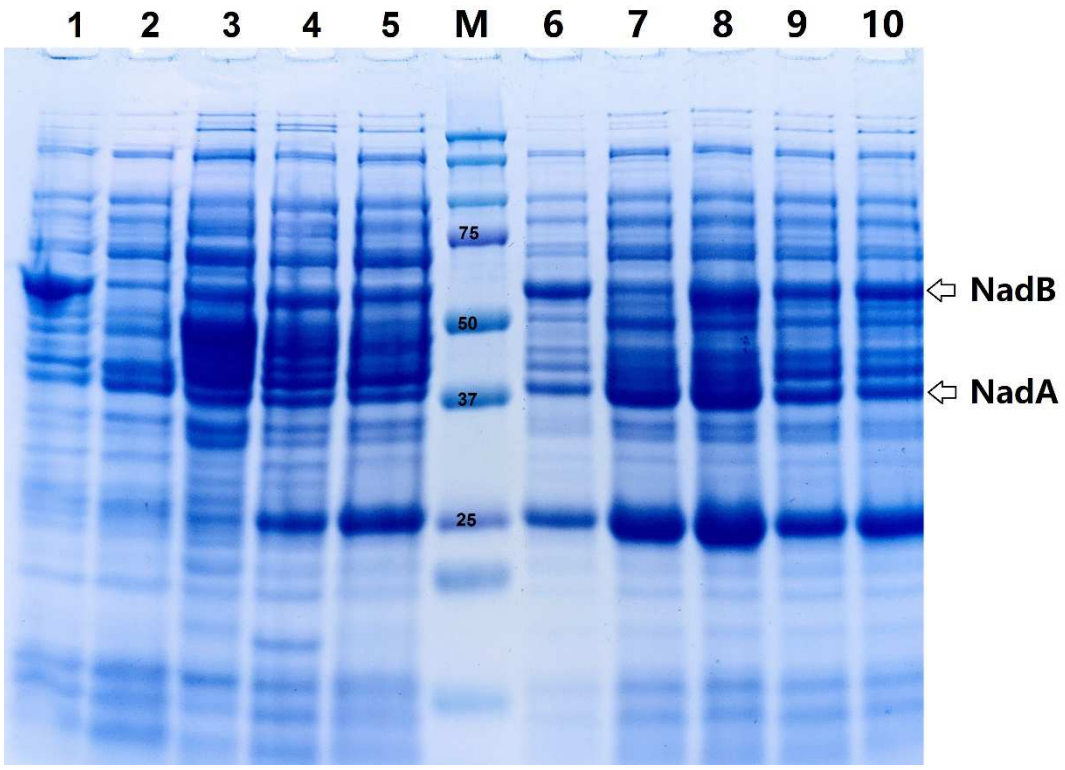

Fig. S1. SDS-PAGE analysis of soluble protein. FZ763 was used as the host strain, 12 μL sample was loaded unless otherwise specified. From left to right: 1, pFZGNB14 [*E. coli* NadB (5 μL)]; 2, pFZGNB34 (*E. coli* NadA); 3, pTrc99a- St*nadB* [*Sulfolobus tokodaii* NadB (StNadB)]; 4, pFZGNB183 [*Pseudomonas putida* KT2440 NadB (PpNadB)]; 5, pFZGNB43[*Bacillus subtilis* NadA (BsNadA)]; M: Bio-Rad dual color standards (5 μL); 6, FZ763/pFZGNB190 (7 μL); 7, FZ763/pFZGNB189; 8, FZ763/pFZGNB193; 9, FZ763/pFZGNB207; 10, FZ763/pFZGNB190. Numbers on the marker indicates the protein molecular weight (kDa)

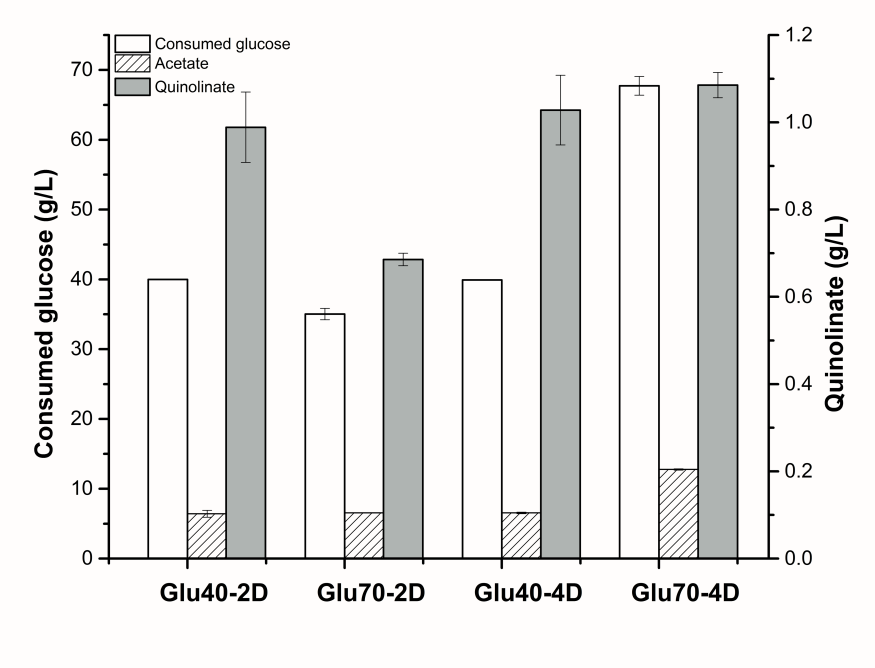

Fig. S2. The effect of glucose concentration on quinolinate production in FZ763/pFZGNB190. Aerobic cultures were performed at 37 ºC, 350 rpm. Values are the average of three replicates with error bars indicating standard deviation. Glu40/70 indicates fermentation with 40 or 70 g/L glucose and the -2D or -4D indicates the culture was incubated for 2 or 4 days.

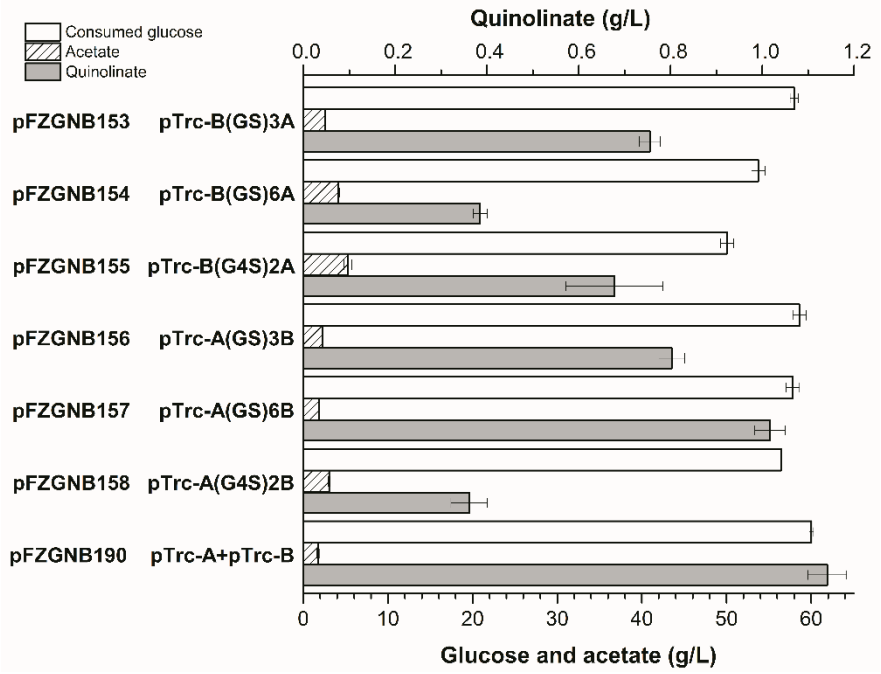

Fig. S3. The effect of NadA-NadB fusion proteins on quinolinic acid production in FZ763. Aerobic cultures were performed at 37 ºC, 350 rpm for 4 days. NadA-NadB fusion protein with different linkers and different orders were over-expressed under the control of pTrc promoter in pFZGNB33. Values are the average of three replicates with error bars indicating standard deviation.

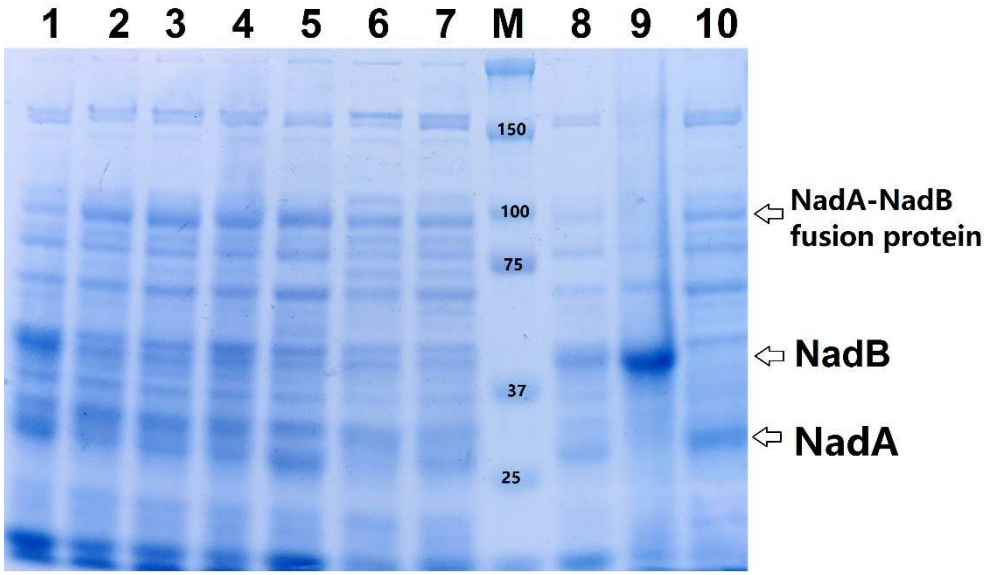

Fig. S4. SDS-PAGE analysis of soluble protein. Non-reducing SDS-PAGE analysis of soluble protein in FZ763 harboring different plasmids. 20 μL sample was loaded otherwise specified. From left to right: 1, pFZGNB190; 2, pFZGNB153; 3, pFZGNB154; 4, pFZGNB155; 5, pFZGNB156; 6, pFZGNB157; 7, pFZGNB158; M: Bio-Rad dual color standards (5 μL); 8, pFZGNB190 (7 μL); 9, pFZGNB14 [*E. coli* NadB (7 μL)]; 10, pFZGNB34 (*E. coli* NadA). Numbers on the marker indicates the protein molecular weight (kDa), the approximate protein location was also labeled based on the protein molecular weight.

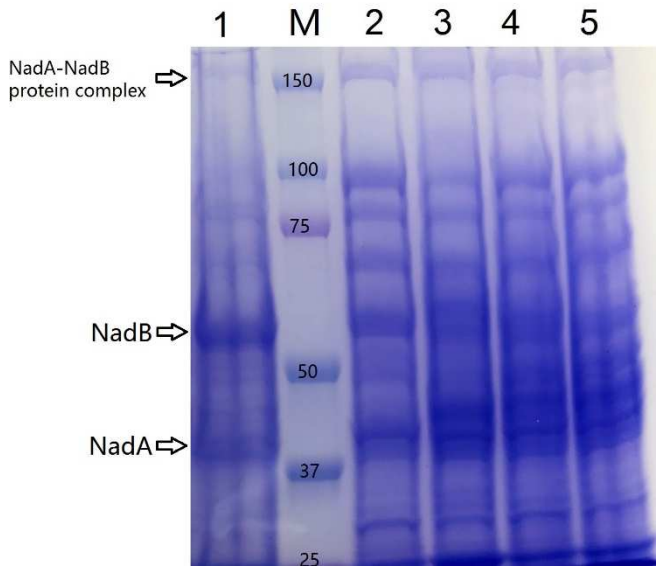

Fig. S5: Non-reducing SDS-PAGE analysis of soluble protein in FZ763 harboring different plasmids. 20 μL sample was loaded otherwise specified. From left to right: 1, pFZGNB190 (7 μL); M: Bio-Rad dual color standards (5 μL); 2, pFZGNB232 (15 μL); 3, pFZGNB233 (25 μL); 4, pFZGNB234 (15 μL); 5, pFZGNB235 (15 μL). Numbers on the marker indicates the protein molecular weight (kDa), the approximate protein location was also labeled based on the protein molecular weight. Non-reducing SDS-PAGE indicates no reductant (Dithiothreitol or 2-mercaptoethanol) was added to the loading buffer.

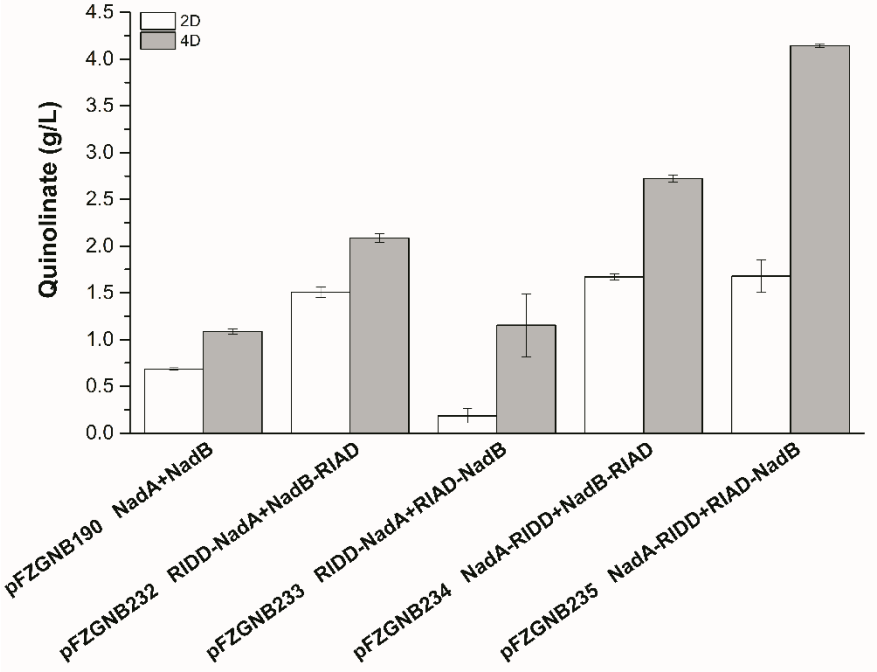

Fig. S6. The effect of NadA-NadB enzyme complex on quinolinic acid production in FZ763 with 70 g/L glucose. Aerobic cultures were performed at 37 ^{o}C, 350 rpm for 4 days. NadA-RIDD and NadB-RIAD fusion proteins were over-expressed under the control of their pTrc promoter in pFZGNB227, NadA-NadB enzyme complex was assembled with the help of peptides, RIAD and RIDD. Values are the average of three replicates with error bars indicating standard deviation.

72 **Table S1. Plasmids and strains used in this study.**

	Description	Source
plasmids		
pHL413K	Amp^R of pTrc99a was replaced with Km^R, and *pycA* gene	(Thakker et al., 2011)
pKK313	S8D mutant *Pepc* from *sorghum*, Amp^R	(Wang et al., 1992)
pFZGNB16	BglII was introduced 193 bp before pTrc promoter of pTrc99a, Amp^R	This study
pFZGNB33	Amp^R of pFZGNB16 was replaced by Km^R from pHL413K, Km^R	This study
pFZGNB34	*nadA* was inserted into pFZGNB33 between EcoRI and BamHI	This study
pFZGNB35	*nadB* was inserted into pFZGNB33 between NcoI and BamHI	This study
pFZGNB36	*aspC* was inserted into pFZGNB33 between EcoRI and BamHI	This study
pFZGNB37	pFZGNB33 with *nadA-nadB-aspC*	This study
pFZGNB38	pFZGNB33 with *nadA-aspC-nadB*	This study
pFZGNB39	pFZGNB33 with *nadB-aspC-nadA*	This study
pFZGNB40	pFZGNB33 with *nadB-nadA-aspC*	This study
pFZGNB41	pFZGNB33 with *aspC-nadA-nadB*	This study
pFZGNB42	pFZGNB33 with *aspC-nadB-nadA*	This study
pFZGNB43	*nadA* from *Bacillus subtilis* with an extra DNA fragment coding an HisTag at C-terminal (Bs*nadA*-HisTag) was cloned into pFZGNB33 between EcoRI and XbaI	This study

pFZGNB44	pTargetT contains N_{20} specific for *ptsG*, Sm^R	This study
pFZGNB46	Upstream and downstream homologous arms of *ptsG* were inserted into pFZGNB44, for *ptsG* deletion, Sm^R	This study
pFZGNB50	pTrc-*pepc* fragment from pKK313 was inserted into pFZGNB46 between homologous arms, for replacement of native *ptsG* with pTrc-*pepc* fragment, Sm^R	This study
pFZGNB63	pTargetT contains N_{20} specific for *tpiA*, upstream and downstream homologous arms of *tpiA*, Sm^R, for *tpiA* deletion	This study
pFZGNB65	pTargetT contains N_{20} specific for *sucA*, upstream and downstream homologous arms of suc*AB*, Sm^R, for *sucAB* deletion	This study
pFZGNB74	pTargetT contains N_{20} specific for *lpd*, upstream and downstream homologous arms of *lpd*, Sm^R, for *lpd* deletion	This study
pFZGNB75	pTargetT contains N_{20} specific for *ackA*, upstream and downstream homologous arms of *ackA*, Sm^R, for *ackA* deletion	This study
pFZGNB76	pTargetT contains N_{20} specific for *ackA*, upstream and downstream homologous arms of *pta-ackA*, Sm^R, for *pta-ackA* deletion	This study
pFZGNB117	pTrc-*pepc* from pKK313 was inserted into pFZGNB75 between homologous arms, for replacement of *ackA* with pTrc-*pepc* fragment, Sm^R	This study

pFZGNB118	pTrc-*pepc* from pKK313 was inserted into pFZGNB76 between homologous arms, for replacement of *pta-ackA* with pTrc-*pepc* fragment, Sm^R	This study
pFZGNB153	Gene encoding NadB-$(GlySer)_3$-NadA under the control of pTrc promoter in pFZGNB33	This study
pFZGNB154	Gene encoding NadB-$(GlySer)_6$-NadA under the control of pTrc promoter in pFZGNB33	This study
pFZGNB155	Gene encoding NadB-$(Gly_4Ser)_2$-NadA under the control of pTrc promoter in pFZGNB33	This study
pFZGNB156	Gene encoding NadA-$(GlySer)_3$-NadB under the control of pTrc promoter in pFZGNB33	This study
pFZGNB157	Gene encoding NadA-$(GlySer)_6$-NadB under the control of pTrc promoter in pFZGNB33	This study
pFZGNB158	Gene encoding NadA-$(Gly_4Ser)_2$-NadB under the control of pTrc promoter in pFZGNB33	This study
pFZGNB183	*nadB* from *Pseudomonas putida* KT2440 (Pp*nadB*) was inserted into pFZGNB33 between BamHI and XbaI	This study
pFZGNB33-staspO	*nadB* (StaspO) from *Sulfolobus tokodaii* (St*nadB*) was inserted into pFZGNB33 between NcoI and BamHI	This study
pFZGNB189	pFZGNB33 with pTrc-*nadA* and pTrc-St*nadB*	This study
pFZGNB190	pFZGNB33 with pTrc-*nadA* and pTrc-*nadB*	This study
pFZGNB193	pFZGNB33 with pTrc-*nadA* and pTrc-Pp*nadB*	This study
pFZGNB204	pFZGNB33 with pTrc-*nadA*, pTrc-*nadB* and pTrc-*aspC*	This study

pFZGNB207	pFZGNB33 with pTrc-Bs*nadA* and pTrc-*nadB*	This study
RIDD	DNA coding RIDD with linker was synthesized and inserted into pUC57	This study
RIAD	DNA coding RIAD with linker was synthesized and inserted into pUC57	This study
pFZGNB227	A SpeI was introduced into pFZGNB33 in front of pTrc promoter, Km^R	This study
pFZGNB228	pFZGNB227 with pTrc-*ridd-nadA*	This study
pFZGNB229	pFZGNB227 with pTrc-*nadB-riad*	This study
pFZGNB230	pFZGNB227 with pTrc-*riad-nadB*	This study
pFZGNB231	pFZGNB227 with pTrc-*nadA-ridd*	This study
pFZGNB232	pFZGNB227 with pTrc-*ridd-nadA* and pTrc-*nadB-riad*	This study
pFZGNB233	pFZGNB227 with pTrc-*ridd-nadA* and pTrc-*riad-nadB*	This study
pFZGNB234	pFZGNB227 with pTrc-*nadA-ridd* and pTrc-*nadB-riad*	This study
pFZGNB235	pFZGNB227 with pTrc-*nadA-ridd* and pTrc-*riad-nadB*	This study
Strains		
MG1655	*E. coli* K12 MG1655, F^- *lambda*$^-$ *ilvG- rfb*-50 *rph*-1	
FZ700	MG1655 Δ*nadC*	This study
FZ703	MG1655 Δ*nadC,* Δ*nadR*	This study
FZ723	MG1655 Δ*nadC,* Δ*nadR,* Δ*ptsG*	This study
FZ734	MG1655 Δ*nadC,* Δ*nadR, ptsG::pTrc-pepc*	This study
FZ738	FZ734 Δ*tpiA*	This study
FZ740	FZ734 Δ*sucAB*	This study

FZ741	FZ734 Δ*poxB*	This study
FZ742	FZ734 Δ*lpd*	This study
FZ756	FZ734 Δ*poxB::pTrc-pepc*	This study
FZ757	FZ734 Δ*poxB*, Δ*ackA*	This study
FZ763	FZ734 Δ*poxB, ackA::pTrc-pepc*	This study

Table S2. Acetate accumulated in engineered strains

	MG1655	FZ700	FZ703	FZ723	FZ734
1 day	18.0 ± 0.3	7.2 ± 0.1	14.1 ± 0.3	4.8 ± 0.5	4.6 ± 0.1
3 day	34.7 ± 0.4	30.4 ± 1.9	29.0 ± 0.5	18.8 ± 0.2	18.4 ± 0.5
5 day	38.8 ± 1.2	34.2 ± 1.1	33.9 ± 0.3	26.1 ± 0.1	25.8 ± .5
7 day	42.2 ± 0.9	36.0 ± .4	37.0 ± 0.4	32.0 ± 0.6	32.5 ± 0.5
nadC	+	-	-	-	-
nadR	+	+	-	-	-
ptsG	+	+	+	-	-
pTrc-pepc	-	-	-	-	+

Plasmid pFZGNB42 (pTrc-*aspC-nadB-nadA*) was introduced into the tested strains to check their performance, aerobic cultures were performed at 37 ºC, 350 rpm. The numbers indicate acetate concentration (g/L, average of three replicates with error bars indicating standard deviation).

Table S3. DNA sequences used in this study

>pFZGNB33 partial sequence

GCGCAACGCAATTAATGTGAGTTAGCGCGAATAGATCTGGTTTGACAGCTTATCATC
GACTGCACGGTGCACCAATGCTTCTGGCGTCAGGCAGCCATCGGAAGCTGTGGTATG

GCTGTGCAGGTCGTAAATCACTGCATAATTCGTGTCGCTCAAGGCGCACTCCCGTTC
TGGATAATGTTTTTTGCGCCGACATCATAACGGTTCTGGCAAATATTCTGAAATGAG
CTGTTGACAATTAATCATCCGGCTCGTATAATGTGTGGAATTGTGAGCGGATAACAA
TTTCACACAGGAAACAGACCATGGAATTCGAGCTCGGTACCCGGGGATCCTCTAGA
GTCGACCTGCAGGCATGCAAGCTTAGCTTGCAGTGGGCTTACATGGCGATAGCTAGA
CTGGGCGGTTTTATGGACAGCAAGCGAACCGGA

The special features are highlighted BglII, pTrc promoter, MCS

>pFZGNB227 partial sequence

GCGCAACGCAATTAATGTGAGTTAGCGCGAATAGATCTGGTTTGACAGCTTATCATC
GACTGCACGGTGCACCAATGCTTCTGGCGTCAGGCAGCCATCGGAAGCTGTGGTATG
GCTGTGCAGGTCGTAAATCACTGCATAATTCGTGTCGCTCAAGGCGCACTCCCGTTC
TGGATAATGTTTTTTGCGCCGACATCATAACGGTTCTGGCAAATATTCTGAAATGAC
TAGTGTTGACAATTAATCATCCGGCTCGTATAATGTGTGGAATTGTGAGCGGATAAC
AATTTCACACAGGAAACAGACCATGGAATTCGAGCTCGGTACCCGGGGATCCTCTA
GAGTCGACCTGCAGGCATGCAAGCTTAGCTTGCAGTGGGCTTACATGGCGATAGCTA
GACTGGGCGGTTTTATGGACAGCAAGCGAACCGGA

The special features are highlighted BglII, SpeI, pTrc promoter, MCS

> BsnadA-HisTag sequence

gaattcATGTCAATTCTTGATGTGATCAAACAATCGAATGATATGATGCCCGAAAGTTA
TAAAGAACTATCGAGAAAGGATATGGAAACGCGCGTTGCCGCCATTAAGAAAAAGT
TCGGCAGCAGGCTCTTTATACCAGGCCATCATTATCAAAAGGATGAAGTGATACAAT
TTGCTGACCAAACAGGCGACTCCCTGCAATTGGCCCAAGTAGCGGAAAAAAACAAA
GAAGCGGATTATATCGTATTTTGCGGCGTTCACTTTATGGCAGAAACCGCCGATATG
CTGACAAGCGAGCAGCAAACGGTCGTCCTGCCAGATATGAGAGCTGGATGTTCTAT
GGCTGACATGGCTGACATGCAGCAGACCAATAGGGCATGGAAGAAGCTTCAGCATA
TATTTGGAGATACGATCATACCTTTAACTTATGTGAACTCCACTGCGGAGATCAAGG
CATTCGTCGGAAAGCATGGCGGAGCAACTGTAACTTCTTCGAATGCGAAAAAAGTG
CTTGAATGGGCGTTTACACAGAAAAAAAGAATTTTATTTTTGCCTGATCAGCATTTA
GGGAGAAATACGGCTTATGATCTGGGCATTGCGCTTGAAGATATGGCTGTGTGGGAT
CCGATGAAAGATGAATTAGTAGCTGAATCCGGGCATACGAATGTGAAAGTGATTTT
GTGGAAAGGGCATTGCTCTGTTCACGAGAAATTCACCACTAAAAATATCCATGATAT
GAGAGAGCGAGACCCCGACATTCAGATCATTGTGCACCCGGAATGTTCACACGAAG
TCGTGACACTAAGCGATGATAACGGATCAACGAAATATATTATCGACACAATCAAC
CAGGCTCCGGCGGGAAGCAAGTGGGCAATCGGGACAGAAATGAATCTTGTTCAGCG
GATCATTCACGAGCATCCAGATAAACAAATCGAATCACTCAACCCTGACATGTGCCC
TTGCCTGACAATGAACCGAATTGATTTGCCGCATTTGTTGTGGTCGCTGGAACAAAT

TGAAAAAGGAGAACCTTCAGGCGTCATCAAGGTGCCAAAAGCCATTCAGGAAGATG
CACTCCTTGCCCTGAATCGAATGCTTTCGATCACGCACCACCACCACCACCactaga

>stnadB sequence

ccatggaaATGATCTATATTATCGGTAGCGGTATTGCAGGTCTGAGTGCCGGTGTTGCAC
TGCGTCGTGCAGGTAAAAAAGTTACCCTGATTAGCAAACGCATTGATGGTGGTAGC
ACCCCGATTGCAAAAGGTGGTGTTGCAGCAAGCGTTGGTAGTGATGATAGTCCGGA
ACTGCATGCACAGGATACCATTCGTGTTGGTGATGGTCTGTGTGATGTTAAAACCGT
TAATTATGTTACCAGCGAGGCCAAAAACGTGATTGAAACCTTTGAAAGCTGGGGCTT
TGAATTTGAAGAAGATCTGCGTCTGGAAGGTGGTCATACCAAACGTCGTGTTCTGCA
TCGTACCGATGAAACCGGTCGTGAAATTTTTAACTTCCTGCTGAAACTGGCACGCGA
AGAAGGTATTCCGATTATTGAAGATCGCCTGGTTGAAATTCGCGTGAAAGATGGTAA
AGTTACCGGTTTTGTGACCGAAAAACGTGGTCTGGTTGAAGATGTTGATAAACTGGT
TCTGGCAACCGGTGGTTATAGCTATCTGTATGAATATAGCAGCACCCAGAGCACCAA
TATCGGTGATGGTATGGCAATTGCATTTAAAGCAGGCACCATTCTGGCCGATATGGA
ATTTGTTCAGTTTCATCCGACCGTTACCAGCCTGGATGGTGAAGTTTTTCTGCTGACC
GAAACCCTGCGTGGTGAAGGTGCACAGATTATTAATGAAAATGGCGAACGCTTTCT
GTTTAACTATGATAAACGTGGTGAACTGGCACCGCGTGATATTCTGAGCCGTGCAAT
TTATATCGAAATGCTGAAAGGCCATAAAGTGTTTATCGACCTGAGCAAAATCGAAG
ATTTCGAACGTAAATTTCCGGTGGTTGCAAAATATCTGGCACGTCATGGCCATAACT
ATAAAGTGAAAATTCCGATTTTTCCGGCAGCCCATTTTGTGGATGGTGGTATTCGTG
TTAATATTCGTGGCGAAAGCAACATTGTGAACCTGTATGCAATTGGTGAAGTTAGCG
ATAGCGGTCTGCATGGTGCAAATCGTCTGGCAAGCAATAGCCTGCTGGAAGGTCTG
GTTTTTGGTATTAATCTGCCTCGTTATGTTGATAGCAGCTGGGAAGGTATTAGCACC
GATGATGGTATTGTTCATAGCGTTCGTATTAGCGGTAATAAAACCCTGAGCCTGAAA
GAAATTCGTCGCATTAATTGGGAAAACGTGGGCATTATTCGCAACGAAGAAAAACT
GGTGAAAGCCATTAACACCTATAGCAGCAGTACCCAGAACGAAGCAATTATTAGCT
ATCTGACCGCACTGGCAGCAGAAATTCGTAAAGAAAGCCGTGGTAATCACTTTCGTG
AGGATTATCCGTATAAAGATCCGAATTGGGAGAAACGCATTTACTTTAAACTGGTGG
TGCTCGAGTAATAAggatcc

>PpnadB sequence

ggatccATGAGCCAACAATTCCAACATGATGTCCTGGTGATCGGCAGCGGTGCCGCCGG
TCTCAGCCTGGCACTTAACCTCCCCAGCCACCTTCGCGTTGCCGTATTGAGCAAGGG
CGACCTGTCCAACGGCTCGACCTTCTGGGCCCAGGGCGGCGTCGCTGCAGTGCTGGA
CAACACCGATACTGTGCAGTCGCATGTCGAGGACACCCTCAATGCCGGCGGCGGGC
TGTGCCATGAAGACGCAGTGCGCTTTACCGTCGAGCACAGCCGCGAAGCGATCCAA
TGGCTGATCGAGCAAGGCGTGCCCTTCACCCGCGATGAGCACTACAGCGTCGACGA
TGGCGGCTTCGAGTTCCACCTCACCCGTGAAGGGGGCCATAGCCACCGGCGCATCAT
CCACGCCGCCGACGCTACCGGCGCGGCAATCTTCACCACGCTGCTGGAACAGGCTC

GCCAGCGCCCGAACATCCAGCTGCTGGAGCAGCGGGTGGCGGTCGACCTGATCACT
GAACGCCGCCTGGGCCTGCCCGGCGAACGCTGCCTGGGCGCCTACGTGCTCGACCG
CAACACCGGCGAGGTGGACACCTTCGGCGCGCGCTTCACCGTGCTGGCCACGGGCG
GTGCGGCCAAGGTCTATCTCTACACCAGCAACCCCGATGGTGCCTGCGGCGACGGT
ATCGCCATGGCCTGGCGGGCCGGCTGCCGAGTGGCGAACCTGGAATTCAACCAGTT
CCACCCGACCTGCCTGTATCACCCACAGGCCAAGAGCTTCCTGATCACCGAAGCCCT
GCGCGGCGAGGGCGCCCTGCTGCGCCTGCCCAACGGCGAACGTTTCATGCCACGCTT
CGACCCACGCGAAGAGCTGGCCCCACGGGACATCGTGGCCCGCGCCATCGACCACG
AGATGAAGCGCCTGGGCGTGGACTGCGTATACCTGGACATCACTCACAAGCCTGCA
GATTTCATCAAGAGCCACTTCCCCACCGTGTACGAGCGCTGCCTGGCCTTTGGCATC
GATATCACCCGTCAGCCGATCCCGGTGGTGCCTGCGGCGCATTACACCTGCGGCGGG
GTGATGGTCGACGACTGCGGCCACACCGATGTGCCTGGCTTGTATGCCATCGGCGAA
ACCAGTTTCACCGGCCTGCACGGCGCCAACCGCATGGCCAGCAACTCGCTGCTGGA
ATGTTTTGTGTACGGTCGCGCCGCCGCTGCCGACATCCAGGCGCACCTGGAGCAAGT
GGCCATGCCCAAGGCCTTGCCCGGCTGGGACGCCAGCCAGGTGACCGACTCGGACG
AGGACGTGATCATTGCGCACAACTGGGACGAACTGCGGCGCTTCATGTGGGACTAC
GTCGGCATCGTGCGCACCAGCAAGCGCCTGCAGCGGGCCCAGCACCGCATTCGCCT
GCTGCTGGATGAAATCGACGAGTTCTACAGCAACTACAAGGTCAGCCGTGACCTGA
TCGAGCTGCGCAACCTGGCGCAAGTGGCCGAGCTGATGATCCTGTCAGCCATGCAG
CGCAAGGAAAGCCGAGGGTTGCATTACACACTGGATTATCCAGGGATGCTGGACGA
GGCCAAGGACACCATCCTTAACCCGCTCTGAtctaga

>optimized RIDD with linker sequence

GGTGGCGGTGGTTCTGGCGGTGGCGGTTCTGGTGGCGGCGGTTGCGGTTCTCTGCGT
GAGTGCGAACTGTACGTTCAGAAACACAACATCCAGGCGCTGCTGAAAGATAGCAT
CGTTCAACTGTGTACCGCACGTCCGGAACGTCCGATGGCATTTCTGCGCGAATACTT
CGAACGCCTGGAAAAAGAAGAAGCGAAAGGTGGCGGTGGCTCAGGTGGCGGTGGT
TCAGGTGGTGGTGGTTGTGGT

>optimized RIAD with linker sequence

ccatggaattcGGTGGTGGCGGTTCTGGTGGCGGCGGTTCTGGTGGCGGCGGTTGCGGTCT
GGAACAATACGCGAATCAGCTGGCGGATCAGATTATCAAAGAAGCGACCGAAGGCT
GCGGCGGCGGTGGTTCAGGTGGCGGCGGTTCAGGTGGCGGTGGTTGTGGTggatcc